UK Atomic Energy Authority

ExCALIBUR

Technical report on Physics model selection

M2.8.2

The report describes work for ExCALIBUR project NEPTUNE at Milestone 2.8.2.

This report provides a digest of the reports produced by the Oxford group regarding the development of a drift kinetic model for plasma in the tokamak edge. There are eight reports to date, five of which concern the development of the model: “Physics in the edge of fusion devices (2047357-TN-03-02)” [1]; “1D drift kinetic models with periodic boundary conditions (2047357-TN-01-02) [2]; “1D drift kinetic models with wall boundary conditions (2047357-TN-05) [3]”; “2D drift kinetic model with wall boundary conditions (2047357-TN-07-01)” [4]; and “2D drift kinetic model with periodic boundary conditions (2047357-TN-09-01)” [5]. The remaining three reports concern the numerical implementation of the model. The five theory reports are appended to this report in their logical reading order: TN-03, TN-01, TN-05, TN-07, TN-09.

This report summarizes the five reports on theory development, discussing the state of the field before this work in Section 1, and the development of the model in Section 2. The work is summarized and future work is discussed in Section 3.

1 Background

The first report [1] describes the important physical regimes in the tokamak edge plasma and reviews the state-of-the-art of edge plasma codes. The report focusses on known problems of fluid models, but emphasises the importance of fluid models and states that research with fluid model should proceed in parallel to research on kinetic models. In particular, one challenge it notes for kinetic modelling is to match to fluid models efficiently, and to determine which spatial regions may be treated using fluid models.

The report contains four topic sections: a discussion of characteristic time and length scales in the edge; an overview of the existing fluid models for the edge; a list physical phenomena that cannot be captured by fluid models (and an explanation of how these phenomena are currently treated by fluid models); and a discussion of the proposed work to develop a complete set of kinetic equations for the edge.

There are two key limitations of using fluid codes to model edge plasma. The first is that the calculated diffusion heat flux is accurate only in a very collisional plasma. This is because the heat flux is predominantly due to energetic particles which are much less collisional than thermal particles. Fluid models overestimate the number of energetic particles present in hot plasmas,

while underestimating the number of energetic particles present in cold plasmas. This results in inaccurate heat fluxes.

The second limitation concerns boundary conditions. At the wall, ions and electron recombine, meaning that near the wall, the distribution function vanishes for velocities corresponding to motion into the wall. Thus the distribution function of charged particles is highly non-Maxwellian near the wall and must be treated kinetically.

Together, these two effects result in an incorrect description of energetic electrons, which in turn yields incorrect heat transport and thus incorrect density and temperature profiles. Such effects have been seen in 1D kinetic simulations [6, 7].

Kinetic models for neutrals have long been used by the community in codes such as EIRENE [8] or DEGAS [9]. However, energetic electrons also mediate important collisional processes in neutral models, like radiation, ionization and recombination, meaning that fluid-plasma simulations of models containing neutrals can be inaccurate, even when kinetic models are used for the neutrals.

The community is also starting to develop edge code that treat charged particles kinetically, such as XGC [10], GKEYLL [11] and COGENT [12]. However, all these models are based on δf gyrokinetics [13, 14], originally developed for the tokamak core, and which assume that turbulence structures are larger than the ion gyroradius, and that density and temperature are slowly varying. These assumption no longer hold at the edge, and it is necessary instead to use "full f" gyrokinetics [15, 16] where the distribution function is no longer taken to be a small perturbation about a Maxwellian. Full f gyrokinetics is more general formulation, and by imposing appropriate additional orderings, one may recover either δf gyrokinetics for the core, or a regime appropriate for describing the edge plasma. The latter is essentially drift kinetics but with corrections due to finite gyroradius effects. These finite gyroradius effects are important in two places. Firstly, damping terms appear in the kinetic equation which stabilize the small wavelength instabilities that appear in drift kinetics. Secondly, a "polarization density" term appears in the field equations (quasineutrality and Ampére's law). This term is often small, but can become important to determine the electromagnetic fields in certain scenarios, such as in shear Alfvén waves.

While implementing the damping terms is relatively straightforward in PIC codes, doing so has not been attempted in full f continuum codes. Moreover, the correction terms in the field equations can lead to significant complications. For example, to include these corrections while also ensuring the scheme conserves energy and momentum would lead to the need to solve a nonlinear equation at every point in velocity space.

In addition to these problems, there are other issues a model must address. There is as yet no gyrokinetic formulation for the wall boundary conditions (only a much less general formulation for ions on magnetic field lines that intersect the wall at a shallow angle [17]). It also remains to develop a model for collisions between charged particles and neutrals, which is challenging in a gyrokinetic framework as gyrophase can be important in the process. Finally, gyrokinetics assumes fluctuations have a characteristic scale of the ion gyroradius. In order to describe Edge Localized Modes – significant disruptions in the plasma at the tokamak edge – it is necessary to extend gyrokinetics to described fluctuations on larger MHD scales.

1.1 Workplan

It is therefore established that accurate modelling of the tokamak edge requires the inclusion of kinetic effects. A tractable model will also use gyroaveraging to remove the fastest timescales from the problem. There is however, no existing systematic derivation containing both of these for plasma in the tokamak edge. Making such a derivation is the main thrust of this work package. The main difficulty is performing the derivation while ensuring that the equations contain all the information required to completely determine the system. One specific problem is that the electrostatic potential must be determined from the quasineutrality condition. However, even small deviations from charge neutrality cause large variations in the electrostatic potential, leading to numerical instabilities. Thus the derived system must be amenable to implicit time stepping, as solving quasineutrality for the potential explicitly strongly limits possible timesteps [18].

The derivation introduces a novel "moment kinetic" approach, which evolves the fluid moments of the distribution function separately from the rest of the distribution function. As well as allowing efficient matching between fluid and kinetic models, this particular decomposition proves vital for the derivation of a tractable system in 2D.

The work plan is to derive this model, first in 1D with periodic and wall boundary conditions appropriate for closed and open field line regions of the edge respectively. The model will then be extended to 3D, but using an axisymmetric helical field. This will provide a model that is improves upon models implemented in existing continuum edge codes. The model is limited by being essentially 2D, and for using a simplified helical field, rather than a realistic tokamak field. Both of these are candidates for future work, as discussed in Section 3.1.

2 Theory development

2.1 1D drift kinetics with periodic boundary conditions

The first report "1D drift kinetic models with periodic boundary conditions (2047357-TN-01-02) [2] develops a proof-of-concept for the moment kinetic approach. It uses a simple 1D drift kinetic model with periodic boundary conditions, appropriate for the edge region inside the separatrix that has closed field lines.

In the standard kinetic approaches, one solves for perturbations about a Maxwellian that has a single global reference density, bulk velocity and thermal velocity. In the moment-kinetic approach, one instead perturbs about a Maxwellian where the density, bulk velocity and thermal velocity are themselves variables to be evolved using self-consistent fluid equations. Thus one replaces a single kinetic equation for the distribution function with a set of a fluid equations and a kinetic equation for a modified distribution function.

The main motivation for this approach is the hope that it would allow the electrostatic potential to be derived through a vorticity equation (using fluid variables) rather than through a field solve (requiring kinetic variables). This simplifies the solution procedure, but requires further theory development. A secondary benefit of splitting out the moments is that it helps the numerics when

dealing with dramatic change in thermal velocity from pedestal to divertor. This approach normalizes the velocity variable in the modified distribution function to the local thermal velocity, meaning no regridding is necessary for different regimes in the plasma. Finally, this approach also allows one to develop an adaptive model which would automatically switch from solving the fluid+modified kinetic equations to only fluid equations when the distribution function was sufficiently close to Maxwellian. This may prove to be a very natural and computationally tight way to couple a fluid model to a kinetic model.

2.2 1D drift kinetics with wall boundary conditions

In the second report [3], the 1+1D drift kinetic model is extended so that it can treat the wall boundary conditions of the open field line region of the edge. The wall is assumed to be perpendicular to the magnetic field lines so that simplified boundary conditions, the logical sheath boundary conditions [19] can be used.

The logical boundary conditions account for a thin sheath of non-neutral plasma of width order Debye length in front of the wall. There is a potential drop across this sheath which repels electrons – otherwise electrons (with their lower mass and higher thermal velocity) would flow into the wall at a greater rate than ions, violating quasineutrality. Requiring current into the sheath to vanish gives a condition for the electrostatic potential on the boundaries. This, in conjunction with the electron parallel momentum equation, can be used to find the electrostatic potential across the whole domain.

As before, the low moments of the distribution function are treated separately so that for ions and neutrals three fluid equations and one kinetic equation for the modified distribution function must be evolved. For electrons, two fluid equations and a kinetic equation must be evolved, with the third fluid equation for parallel momentum being used to determine the electrostatic potential.

2.3 2D drift kinetic model with wall boundary conditions

The third report [4] extends the previous model with wall boundary conditions to a 2D model with an axisymmetric helical magnetic field. While being simpler, the helical field has similarities to the magnetic field in the edge of a tokamak.

As the magnetic field is now not perpendicular to the walls, it is in principle necessary to consider the magnetic presheath [20]. However, the boundary conditions that this would entail in drift kinetics are both complicated and an area of open research [17, 21]. To avoid this, it is assumed that the electron gyroradius is much smaller than the Debye length, in which case boundary conditions similar to the logical boundary conditions [19] can again be applied.

In this configuration, the ion and electron bulk properties only vary along field lines, so as before, the system comprises three fluid equations and a kinetic equations for ions, and two fluid equations and a kinetic equation for electrons. As before, the parallel electron momentum equation is used along with boundary conditions to determine the electrostatic potential. Now however, the distribution functions depend on two spatial and two velocity space coordinates. The velocity coor-

dinates are parallel and perpendicular to the magnetic field, with the third direction, the gyrophase, removed by gyroaveraging.

As neutrals are unaffected by the magnetic field, the problem for neutrals is now essentially in 2+3D. There are thus five fluid equations to solve (for density and thermal velocity, plus three bulk velocity components). The kinetic equation for neutrals now also depends on two spatial directions and three velocity space directions.

2.4 2D drift kinetic model with periodic boundary conditions

The fourth report [5] derives a 2D model with periodic boundary conditions relevant for closed flux surfaces, to complement the wall boundary conditions derived in a previous report. That report described how to obtain the electrostatic potential and the parallel electron bulk velocity with wall boundary conditions. The same prescription with periodic boundary conditions only allows one to find the electron velocity; to obtain the electrostatic potential, higher-order terms must be included in the current conservation equations. The main work of this report is deriving these higher-order corrections, and consequently a final, additional equation (for current conservation at higher order) to solve the electrostatic potential.

The derivation of this additional equation is only possible in the moment-kinetic framework, which evolves the ion and electron densities independently of their normalized distribution functions. With unnormalized distribution functions, the corresponding higher-order current conservation equation is not consistent with the density found in the lower-order kinetic equations.

3 Summary

This body of work has rigorously and systematically derived 2D drift kinetic equations, appropriate for the kinetic treatment of ions, electrons and neutral in the tokamak edge. There is one more report on theory development to be submitted under this grant, “2D drift kinetics in a helical field with a ‘separatrix”’ (which is currently under review) and which combines the 2D drift kinetic models for the open and closed field line regions into a single model. This will complete the theoretical work under the current grant.

The theoretical developments have been accompanied by the numerical implementation of these equations, using a Chebyshev spectral finite element implementation in Julia. The code developments are described in separate reports [22, 23, 24], and the software is publicly available [25]. At present, this code only implements a subset of the models presented here; future reports will discuss the software developments when the code is more mature.

3.1 Future directions

There are a number of directions for future work. The first is to extend the model into 3D with realistic tokamak geometry. The main difficulty here is the inclusion of drifts in the direction perpendicular to the flux surfaces. These lead to finite-width particle orbits which can significantly

alter the physics in quiescent 2D [26] and turbulent 3D [27] plasmas. The rigorous derivation of these drifts requires further work.

The resulting 3D model is also expected to have instabilities on the grid scale. While the model could be stabilized using numerical dissipation on the grid scale, further work is required to properly derive the finite ion gyroradius effects that determine behaviour of fluctuations at this scale. This is particularly important for studying high confinement mode (H-mode) where the stabilization of large-scale turbulence is not well understood. In H-mode, turbulence at the ion gyroscale and smaller is important [27], and so the accurate capture of finite ion gyroradius effects is vital. Including these finite gyroradius effects has the potential to be both theoretically and numerically challenging.

The wall boundary conditions in the model are also simplified conditions which assume the magnetic field is perpendicular to the wall. In the edge, this is often not the case, with magnetic field lines meeting the wall at very shallow angles. The boundary conditions are formally valid in the limit of electron gyroradius being much smaller than the Debye length, but relaxing this condition requires further study. This is currently being pursued by Parra and coworkers outside ExCALIBUR.

Finally, it would be beneficial to extend the model to treat fluctuations in the magnetic field, as well as electric field. While electrostatic models are often a good approximation for edge plasmas, including electromagnetic effects would allow this model to connect with the MHD regime, and so to study large-scale plasma disturbances.

Acknowledgement

The support of the UK Meteorological Office and Strategic Priorities Fund is acknowledged.

References

[1] F. I. Parra, M. Barnes, and M. Hardman. Physics in the edge of fusion devices. Technical Report 2047357-TN-03-02, UKAEA Project Neptune, 2021. https://github.com/ExCALIBUR-NEPTUNE/Documents/blob/main/reports/2047357/TN-03.pdf.

[2] F.I Parra, M. Barnes, and M.R. Hardman. 1D drift kinetic models with periodic boundary conditions. Technical Report 2047357-TN-01-02, UKAEA Project Neptune, 2021. https://github.com/ExCALIBUR-NEPTUNE/Documents/blob/main/reports/2047357/TN-01.pdf.

[3] F. I. Parra, M. Barnes, and M. Hardman. 1D drift kinetic models with wall boundary conditions. Technical Report 2047357-TN-05-01, UKAEA Project Neptune, 2021. https://github.com/ExCALIBUR-NEPTUNE/Documents/blob/main/reports/2047357/TN-05.pdf.

[4] F. I. Parra, M. Barnes, and M. Hardman. 2D drift kinetic models with wall boundary conditions. Technical Report 2047357-TN-07-01, UKAEA Project Neptune, 2021. https://github.com/ExCALIBUR-NEPTUNE/Documents/blob/main/reports/2047357/TN-07.pdf.

[5] F. I. Parra, M. Barnes, and M. Hardman. 2D drift kinetic models with periodic boundary conditions. Technical Report 2047357-TN-09-01, UKAEA Project Neptune, 2021. https://github.com/ExCALIBUR-NEPTUNE/Documents/blob/main/reports/2047357/TN-09.pdf.

[6] D. Tskhakaya, S. Jachmich, T. Eich, W. Fundamenski, and JET EFDA contributors. Interpretation of divertor Langmuir probe measurements during the ELMs at JET. *Journal of Nuclear Materials*, 415(1):S860–S864, 2011.

[7] A. V. Chankin and D. P. Coster. On the locality of parallel transport of heat carrying electrons in the SOL. *Journal of Nuclear Materials*, 463:498–501, 2015.

[8] D. Reiter, M. Baelmans, and P. Boerner. The EIRENE and B2-EIRENE codes. *Fusion Science and Technology*, 47(2):172–186, 2005.

[9] D. Stotler and C. Karney. Neutral gas transport modeling with DEGAS 2. *Contributions to Plasma Physics*, 34(2-3):392–397, 1994.

[10] S. Ku, R. Hager, C.-S. Chang, J. M. Kwon, and S. E. Parker. A new hybrid-Lagrangian numerical scheme for gyrokinetic simulation of tokamak edge plasma. *Journal of Computational Physics*, 315:467–475, 2016.

[11] A. H. Hakim, N. R. Mandell, T. N. Bernard, M. Francisquez, G. W. Hammett, and E. L. Shi. Continuum electromagnetic gyrokinetic simulations of turbulence in the tokamak scrape-off layer and laboratory devices. *Physics of Plasmas*, 27(4):042304, 2020.

[12] M. A. Dorf, M. R. Dorr, J. A. Hittinger, R. H. Cohen, and T. D. Rognlien. Continuum kinetic modeling of the tokamak plasma edge. *Physics of Plasmas*, 23(5):056102, 2016.

[13] P. J. Catto. Linearized gyro-kinetics. *Plasma Physics*, 20(7):719, 1978.

[14] E. A. Frieman and L. Chen. Nonlinear gyrokinetic equations for low-frequency electromagnetic waves in general plasma equilibria. *The Physics of Fluids*, 25(3):502–508, 1982.

[15] F. I. Parra and P. J. Catto. Limitations of gyrokinetics on transport time scales. *Plasma Physics and Controlled Fusion*, 50(6):065014, 2008.

[16] A. J. Brizard and T. S. Hahm. Foundations of nonlinear gyrokinetic theory. *Reviews of modern physics*, 79(2):421–468, 2007.

[17] A. Geraldini, F.I. Parra, and F. Militello. Dependence on ion temperature of shallow-angle magnetic presheaths with adiabatic electrons. *Journal of Plasma Physics*, 85(6), 2019.

[18] W.W. Lee. Gyrokinetic particle simulation model. *Journal of Computational Physics*, 72(1):243–269, 1987.

[19] S. E. Parker, R. J. Procassini, C. K. Birdsall, and B. I. Cohen. A suitable boundary condition for bounded plasma simulation without sheath resolution. *Journal of Computational Physics*, 104(1):41–49, 1993.

[20] R. Chodura. Plasma-wall transition in an oblique magnetic field. *The Physics of Fluids*, 25(9):1628–1633, 1982.

[21] A. Geraldini. Large gyro-orbit model of ion velocity distribution in plasma near a wall in a grazing-angle magnetic field. *Journal of Plasma Physics*, 87(1), 2021.

[22] M. Barnes, F. I. Parra, and M. R. Hardman. Numerical study of 1D drift kinetic models with periodic boundary conditions. Technical Report 2047357-TN-02-02, UKAEA Project Neptune, 2021. `https://github.com/ExCALIBUR-NEPTUNE/Documents/blob/main/reports/2047357/TN-02.pdf`.

[23] M. Barnes, F. I. Parra, M. R. Hardman, and J. Omotani. Numerical study of 1+1D, moment-based drift kinetic models with periodic boundary conditions. Technical Report 2047357-TN-04, UKAEA Project Neptune, 2021. `https://github.com/ExCALIBUR-NEPTUNE/Documents/blob/main/reports/2047357/TN-04.pdf`.

[24] M. Barnes, F. I. Parra, M. R. Hardman, and J. Omotani. Numerical study of 1+1D drift kinetic model with wall boundary conditions. Technical Report 2047357-TN-08, UKAEA Project Neptune, 2021. `https://github.com/ExCALIBUR-NEPTUNE/Documents/blob/main/reports/2047357/TN-08.pdf`.

[25] M. A. Barnes and J. T. Omotani. moment_kinetics GitHub repository. `https://github.com/mabarnes/moment_kinetics`, 2021. Accessed: December 2021.

[26] G. Kagan and P. J. Catto. Arbitrary poloidal gyroradius effects in tokamak pedestals and transport barriers. *Plasma Physics and Controlled Fusion*, 50(8):085010, 2008.

[27] J. F. Parisi, F. I. Parra, C. M. Roach, C. Giroud, W. Dorland, D. R. Hatch, M. Barnes, J. C. Hillesheim, N. Aiba, J. Ball, et al. Toroidal and slab ETG instability dominance in the linear spectrum of JET-ILW pedestals. *Nuclear Fusion*, 60(12):126045, 2020.

UKAEA REFERENCE AND APPROVAL SHEET

	Client Reference:	
	UKAEA Reference:	CD/EXCALIBUR-FMS/0058
	Issue:	1.0
	Date:	9 December 2021
Project Name: ExCALIBUR Fusion Modelling System		

	Name and Department	Signature	Date
Prepared By:	Joseph Parker Wayne Arter BD	N/A N/A	9 December 2021 9 December 2021
Reviewed By:	Rob Akers Advanced Computing Dept. Manager		9 December 2021
Approved By:	Rob Akers Advanced Computing Dept. Manager		9 December 2021

Physics in the edge of fusion devices

Felix I. Parra, Michael Barnes and Michael Hardman
Rudolf Peierls Centre for Theoretical Physics, University of Oxford, Oxford OX1 3PU, UK

(This version is of 23 April 2021)

1. Introduction

We present a brief overview of the current state of fusion device edge modeling. This report is written for ExCALIBUR NEPTUNE contract T/NA085/20. This contract stated mission is the development of kinetic models for the edge. Thus, this report will focus on the known problems of fluid models without making much emphasis on their many successes. This lack of praise for fluid models is not the objective of this report and hence we would like to start by reassuring the reader that we believe current fluid codes have much to offer and need to be pursued in parallel to kinetic modeling. One of the challenges for kinetic modeling is to devise methods to match with fluid simulations efficiently. With this capability, the edge can be split into non-overlapping spatial regions with different levels of kinetic sophistication.

The remainder of this reports is organized as follows. In section 2 we explain what the characteristic time and length scales are in the edge. In section 3, we give an overview of the existing fluid models for the edge. In section 4 we list physical phenomena that cannot be captured by fluid models, and we explain how these phenomena have been addressed so far. Finally, we discuss our proposal to develop a complete set of kinetic equations for the edge in section 5.

2. The edge

In this report, we call the edge the plasma that surrounds the separatrix. The separatrix (represented as a red line in figure 1) is the flux surface that separates the region where magnetic field lines are in contact with the walls of the vessel from the region in which magnetic field lines form nested toroidal flux surfaces. This means that the edge includes both **open field lines** (those who are in contact with walls) and **closed field lines** (those that form nested toroidal flux surfaces).

We need to distinguish the core, where the fusion reactions are supposed to take place, from the edge. In this report, we will use a theoretical criterion to distinguish one from the other: whether the characteristic transit times in the directions parallel and perpendicular to the magnetic field are comparable or not. In the core, both ions and electron closely follow magnetic field lines and can travel around the device many times before collisions, turbulent fluctuations or other effects drive them away from the magnetic field line on which they started. As a result, density and temperature are almost constant along magnetic field lines, and one only worries about small fluctuations around the mostly quiescent profiles of density and temperature. This is, of course, a highly idealized situation that ignores violent events taking place in the core, such as sawteeth (Hastie 1997), but it is a useful one.

In contrast, in the edge, charged particles that were well-confined in the core region cross the separatrix and eventually reach the wall by following magnetic field lines. The displacements of ions and electrons away from the magnetic field line in which they

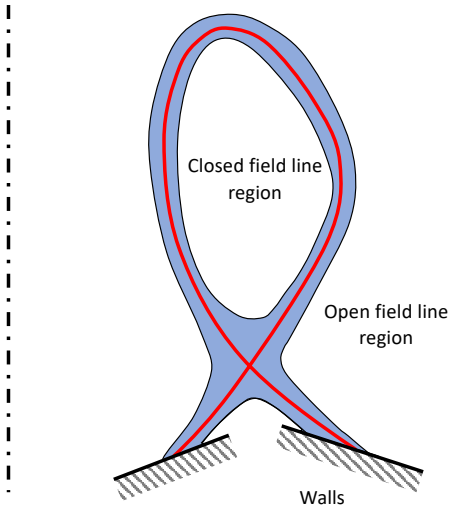

FIGURE 1. Sketch of a tokamak edge on a plane that contains the axis of symmetry (represented here by a dash-dot vertical line). The edge region is in blue, and the separatrix is the red line.

started are still small compared to the size of the device, but they are not small compared with the characteristic lengths of the density and temperature in the edge region. If the characteristic lengths of density and temperature along and across magnetic field lines are $L_\parallel$ and $L_\perp$, the edge is characterized by

$$\frac{|v_\parallel|}{L_\parallel} \sim \frac{|\mathbf{v}_d|}{L_\perp}, \tag{2.1}$$

where $v_\parallel$ is the characteristic parallel velocity of the particles, and $\mathbf{v}_d$ their small drift perpendicular to the magnetic field. Since $|v_\parallel| \gg |\mathbf{v}_d|$, $L_\perp$ is much smaller than $L_\parallel$. In the core, for comparison, we find that $L_\parallel$ and $L_\perp$ are of similar order and comparable to the machine size, giving

$$\frac{|v_\parallel|}{L_\parallel} \gg \frac{|\mathbf{v}_d|}{L_\perp}. \tag{2.2}$$

There is another aspect that makes the edge very different from the core. The temperature of both electrons and ions is kept low near the wall because the wall is a very effective sink of energy (wall materials that prevent slow Hydrogen particles from going back into the plasma are notable exceptions where the temperature of the plasma can be large near the wall; see, for example, Schmitt *et al.* (2015) for liquid Lithium divertors, or Jackson *et al.* (1991) for boronized walls). At low plasma temperatures, the plasma is partially ionized and collisions between the charged particles in the plasma and neutrals become important. In extreme limits, detachment occurs, that is, the plasma temperature decreases sufficiently due to radiation that the plasma recombines and a cushion of neutrals appears in front of the walls protecting them (Krasheninnikov & Kukushkin 2017).

In addition to limiting the temperature, the presence of the wall controls the size of the electric field and the flows in the open field line region. We will discuss these effects in more detail in section 3.

We finish this section by calculating a few characteristic time and length scales. In Militello & Fundamenski (2011), one can find a concise summary of typical values of plasma characteristics in the edge of tokamaks. In current tokamaks, the magnitude of

the magnetic field B is typically 2 T, and the characteristic size of the device is a few meters. The plasma temperature T ranges from 1 keV in the closed magnetic field line part of the edge to 100 eV at the separatrix down to 10 eV near the wall. In detached plasmas, the temperature drops to 1 eV near the wall. The electron density n_e ranges from 10^{19} m^{-3} in the open field line region to 10^{20} m^{-3} in the closed field line region. Neutral density n_n is usually smaller than n_e and it ranges from 10^{15} m^{-3} in the closed field line region to 10^{19} m^{-3} in the open field line region (Colchin *et al.* 2000; Scotti *et al.* 2021). With these quantities, we calculate several characteristic frequencies of interest:

• The gyrofrequencies of both Deuterium and electrons, $\Omega_i := eB/m_D$ and $\Omega_e := eB/m_e$, are the characteristic frequencies of the nearly circular motion of the charged particles around magnetic field lines. Here e is the proton charge, and m_D and m_e are the Deuterium and electron masses.

• The transit frequencies for Deuterium ions and electrons, $v_{tD}/L_\parallel$ and $v_{te}/L_\parallel$, are the inverse of the time that it takes charged particles to move along a magnetic field line from one wall to another in the open field line region, and the inverse of the time that it takes charged particles to sample a flux surface in the closed field line region. Here $v_{tD} := \sqrt{2T/m_D}$ and $v_{te} := \sqrt{2T/m_e}$ are the Deuterium and electron thermal speeds, and $L_\parallel$ is the characteristic length of magnetic field lines in the edge, which we take to be 10 m.

• The transit frequency for Deuterium neutrals, $v_{tD}/L_\perp$, is the inverse of the time that it takes neutral atoms to cross the edge region. The characteristic scale of variation of density and temperature across magnetic field lines, $L_\perp$, is of the order of 5 cm or larger in the closed field line region (Sugihara *et al.* 2000), and of the order of 1 cm or larger in the open field line region (Goldston 2012).

• The collision frequencies

$$\nu_{ii} := \frac{4\sqrt{\pi}}{3}\frac{e^4 n_e \ln\Lambda}{(4\pi\epsilon_0)^2 m_D^{1/2} T^{3/2}} \tag{2.3}$$

and

$$\nu_{ep} := \frac{4\sqrt{2\pi}}{3}\frac{e^4 n_e \ln\Lambda}{(4\pi\epsilon_0)^2 m_e^{1/2} T^{3/2}} \tag{2.4}$$

describe how often Deuterium ions collide with each other or electrons collide with other electrons or Deuterium ions, respectively. Here $\ln\Lambda \approx 15$ is the Coulomb logarithm and ϵ_0 is the vacuum permittivity. The factor of $\sqrt{2}$ difference between ν_{ii} and ν_{ep} is a convention introduced by Braginskii (Braginskii 1958).

• We also need the collision frequencies that describe how often Deuterium ions collide with Deuterium neutral atoms, $\nu_{in} := n_n v_{tD}\sigma_{in}$, and how often Deuterium neutral atoms collide with Deuterium ions, $\nu_{ni} := n_i v_{tD}\sigma_{in}$. Here, the ion-neutral cross section σ_{in} is of order 10^{-18} m^2 (Lindsay & Stebbings 2005). Similarly, we need the collision frequencies that describes how often electrons collide with Deuterium neutral atoms, $\nu_{en} := n_n v_{te}\sigma_{en}$, and how often neutrals are ionized, $\nu_{\rm ion} := n_e v_{te}\sigma_{\rm ion}$. Here, the electron-neutral collision cross section σ_{en} is of order 10^{-19} m^2 (Brackmann *et al.* 1958) and the ionization collision cross section $\sigma_{\rm ion}$ is of order 10^{-20} m^2 (Zel'dovich & Raizer 2013).

All these frequencies are shown in table 1. It is clear that the collision frequencies are the ones that change the most across the edge. For ions and electrons, collisions become very important in the cooler plasma of the open field line region, but are infrequent in the closed field line region. Conversely, for neutrals, collision are more frequent in the closed field line region than in the open field line region.

We also calculate a few length scales of interest:

	Ion freq. [10^4 s^{-1}]				Neutral freq. [10^4 s^{-1}]			Electron freq. [10^6 s^{-1}]			
Region	Ω_i	$v_{tD}/L_\parallel$	ν_{ii}	ν_{in}	$v_{tD}/L_\perp$	ν_{ni}	$\nu_{\rm ion}$	Ω_e	$v_{te}/L_\parallel$	ν_{ep}	ν_{en}
Closed lines	9400	3.1	0.16	0.031	610	3100	1800	320000	1.8	0.13	0.0018
Open lines	9400	0.31	16	31	310	31	18	320000	0.18	13	1.8

TABLE 1. Characteristic frequencies for the closed field line region ($B = 2$ T, $n_e = 10^{20}$ m^{-3}, $n_n = 10^{15}$ m^{-3}, $T = 1$ keV) and the open field line region ($B = 2$ T, $n_e = 10^{19}$ m^{-3}, $n_n = 10^{19}$ m^{-3}, $T = 10$ eV).

	Parallel lengths [1 m]					Perpendicular lengths [1 cm]				
Region	$L_\parallel$	λ_{ii}	λ_{in}	λ_{ep}	λ_{en}	$L_\perp$	ρ_i	ρ_e	λ_{ni}	$\lambda_{\rm ion}$
Closed lines	10	190	1000	140	10000	5	0.33	0.0056	1	1.7
Open lines	10	0.19	0.1	0.14	1	1	0.033	0.00056	10	17

TABLE 2. Characteristic lengths for the closed field line region ($B = 2$ T, $n_e = 10^{20}$ m^{-3}, $n_n = 10^{15}$ m^{-3}, $T = 1$ keV) and the open field line region ($B = 2$ T, $n_e = 10^{19}$ m^{-3}, $n_n = 10^{19}$ m^{-3}, $T = 10$ eV).

- The mean free paths $\lambda_{ii} := v_{tD}/\nu_{ii}$ and $\lambda_{in} := v_{tD}/\nu_{in}$ are the distances that a Deuterium ion can travel before colliding with another Deuterium ion or with a Deuterium atom, respectively. Similarly, the mean free paths $\lambda_{ni} := v_{tD}/\nu_{ni}$ and $\lambda_{\rm ion} := v_{tD}/\nu_{\rm ion}$ are the distances that a Deuterium neutral atom can move before colliding with an ion or getting ionized, respectively, and $\lambda_{ep} := v_{te}/\nu_{ep}$ and $\lambda_{en} := v_{te}/\nu_{en}$ are the distances that an electron can move before colliding with another charged particle or with a neutral, respectively.
- The Deuterium and electron gyroradii, $\rho_i := v_{tD}/\Omega_i$ and $\rho_e := v_{te}/\Omega_e$, are the characteristic size of the gyration of charged particles around magnetic field lines.

All these lengths are given in table 2. Unsurprisingly, we see that the mean free paths, inversely proportional to the collision frequencies, are the characteristic lengths that change the most across the edge. In the direction perpendicular to the magnetic field, we see that the gyroradii are small compared to the characteristic lengths.

3. Drift-ordered fluid models

Due to the large collision frequencies in the open field line region, the bulk of the ion and electron distribution functions is Maxwellian. For this reason, much of the edge modeling has been based on plasma fluid equations derived in the limit of large Coulomb collisions (Braginskii 1958). Since the most readily available fluid equations for magnetized plasmas assume that there are no neutrals, most fluid models ignore neutrals, with some notable exceptions.

The main difference between the fluid equations used in edge models and the usual fluid equations is that diffusivities are anisotropic. As demonstrated by table 1, charged particles gyrate around magnetic field lines many times before having a collision. Thus, particles barely move across magnetic field lines and the diffusivity across magnetic field lines is much smaller than the diffusivity along them. To capture the effect of this anisotropy correctly and efficiently, one has to either use flux coordinates that follow magnetic field lines (Beer *et al.* 1995) or employ appropriate discretizations (Hariri & Ottaviani 2013).

The problem with following magnetic field lines is that it is difficult to find a grid that both aligns with the magnetic field lines and extends to the walls of the vessel. Unfortunately, the wall geometry is important because it determines how far neutrals leaving the wall travel into the plasma (Wiesen *et al.* 2018). Finding grids that adjust to the wall geometry has become a problem of great interest in recent years, and the community has been trying exotic methods to address it (Isoardi *et al.* 2010; Bufferand *et al.* 2019).

An important aspect of the edge fluid models is the size of the flow. The potential difference between the wall and the plasma is controlled by the non-neutral Debye sheath that forms around the walls (Riemann 1991). Typically, the potential drop between the wall and the plasma has to be several times the electron temperature because otherwise a large electron current flows into the wall, breaking the neutrality of the plasma. If one assumes that the wall in contact with the plasma is a conductor and hence the potential is constant across its volume, the potential differences within the plasma are restricted to be of the order of the electron temperature, $\phi \sim T/e$. This gives an electric field $\mathbf{E} = -\nabla\phi$ of the order of $T/eL_\perp$. The perpendicular velocity of the fluid is determined by the balance between the electric and magnetic forces,

$$\mathbf{u}_\perp \times \mathbf{B} \sim \mathbf{E}. \tag{3.1}$$

This equation gives a perpendicular velocity of order

$$\mathbf{u}_\perp \sim \frac{|\mathbf{E}|}{B} \sim \frac{\rho_i}{L_\perp} v_{tD}. \tag{3.2}$$

Thus, according to table 2, $\mathbf{u}_\perp$ is significantly smaller than v_{tD}.

The fluid equations obtained with the ordering (3.2) are known as **drift-ordered** equations because the flow is of the same order as the slow particle drifts – the other possible ordering is the **high flow** ordering that assumes that the perpendicular velocity is sonic. Importantly, for fluid velocities of the size given in equation (3.2), one needs to keep terms that depend on the gradient of the temperature and the pressure in the stress tensor to be completely consistent (Mikhailovskii & Tsypin 1971; Simakov & Catto 2003; Catto & Simakov 2004).

The system of drift-ordered fluid equations is usually comprised of

- one continuity equation per ion species (the electron density need not be calculated because it is determined by quasineutrality),
- one conservation equation for the component of the plasma momentum parallel to the magnetic field,
- a vorticity equation that determines the electrostatic potential,
- in electromagnetic models, Ampére's law, and
- one conservation equation for the energy of all ion species and another one for the energy of the electrons.

Note that there is one single conservation equation for the whole plasma parallel momentum and one single conservation equation for the energy of all the ion species, and not several conservation equations, one per ion species. The reason why all ion species must be considered as one in these fluid equations is that, within the large collision frequency approximation, all ion species have the same temperature and all charged species have the same average flow. The electron temperature can be different from the ion temperature due to the mass difference between the two species. The temperature differences between the different ion species are of the same order as kinetic effects that are neglected. The differences between the parallel flows are calculated and used in the vorticity equation, where they are needed because the electric current enters in the Lorenz force.

As we mentioned at the start, the drift-ordered fluid equations usually implemented

in edge codes (Mikhailovskii & Tsypin 1971; Simakov & Catto 2003; Catto & Simakov 2004) ignore neutrals. There have been attempts to include neutrals in the limit where both ions and neutrals are sufficiently collisional that both species can be treated as fluids (Hazeltine *et al.* 1992; Catto 1994; Helander *et al.* 1994). The advantage of these models is that they account for the effect that ion-neutral collisions have on the diffusivities, but it is generally believed that these models are insufficient because neutrals have long mean free paths in large regions of the edge (see tables 1 and 2). There have been some attempts at simplified kinetic treatments of the neutrals (Wersal & Ricci 2015) and there exist sophisticated Monte-Carlo approaches with a large collection of collisions such as EIRENE (Reiter *et al.* 2005) or DEGAS (Stotler & Karney 1994). Note that these Monte-Carlo treatments are not completely self-consistent because they assume that the ion and electron distribution functions are Maxwellian and, depending on the version of the code, they ignore elastic collisions and they average over the dependence of the differential cross section on the scattering angle. Moreover, these neutral kinetic codes are sensitive to the parameters that determine how particles interact with the wall (Chankin *et al.* 2021), and these parameters are not well known.

There are two types of problems in which the drift-ordered fluid equations are used: 2D profiles and turbulence. The objective of 2D fluid solvers such as SOLPS (Wiesen *et al.* 2015), SolEdge2D (Bufferand *et al.* 2015), UEDGE (Rognlien *et al.* 2007) or EDGE2D (Simonini *et al.* 1994) is to determine the toroidally averaged density and temperature profiles in the edge. These codes cannot model turbulent fluctuation because they are missing the third dimension. For this reason, instead of the collisional perpendicular diffusion coefficients, these codes use enhanced perpendicular diffusion coefficients that are chosen to match the experimental observations. These 2D codes are meant to provide detailed understanding of transport along magnetic field lines and of neutrals, as some of them are coupled to Monte-Carlo neutral codes such as EIRENE (Reiter *et al.* 2005) or DEGAS (Stotler & Karney 1994).

Turbulence codes such as GBS (Halpern *et al.* 2016), TOKAM3X (Tamain *et al.* 2016), Hermes (Dudson & Leddy 2017) or GRILLIX (Stegmeir *et al.* 2018) are 3D fluid codes. Originally, fluid turbulence codes assumed that ions were much colder than electrons and that the turbulent fluctuations were small compared to an almost constant background (Zeiler *et al.* 1996). However, it was soon realized that this treatment is not appropriate for the edge. Ions are not cold and the density and temperature profiles cannot be easily split into a slowly varying piece plus small fluctuations due to the presence of the wall. The same wall boundary conditions that constrain the fluid velocity perpendicular to the magnetic field to be subsonic, as shown in equation (3.2), require that the fluid velocity parallel to the magnetic field be sonic near the wall (Chodura 1982). The pressure drops along magnetic field lines have to be significant to ensure that the parallel flow is accelerated sufficiently. This is incompatible with the assumption that the fluctuations are small. Thus, most current edge turbulence codes have tried to lift the assumption of small fluctuations, and they have done so by differing degrees depending on the code or the version of the code in use.

Overall, fluid codes are maturing, and although there is still work to be done, there is starting to be a consensus on the physics that they must include. The same cannot be said about kinetic effects in the edge.

4. Kinetic effects

Tables 1 and 2 are evidence that kinetic effects must be taken into account: in the closed magnetic field line region and in part of the open field line region, ions and electrons can

travel a distance of the size of the device without suffering a single collision. Moreover, kinetic effects are surprisingly important even in the regions where the collision frequency is high. There are two reasons for this.

- The diffusive heat flux calculated in the fluid limit is only accurate if $\nu_{ep} \gtrsim 100\, v_{te}/L_{\|}$ because the heat flux is dominated by energetic particles that collide much less than the thermal particles (Gurevich & Istomin 1979; Gray & Kilkenny 1980). The fluid solution assumes that there are too many energetic particles in the hot plasma regions, and predicts too few energetic particles in the cooler regions. This is a well known issue, and in 2D fluid simulations, it is resolved by imposing an upper bound for the electron heat flux that is of order $n_e T v_{te}$.
- The other region where kinetic effects are important is near the wall. The ions and electrons that reach the wall recombine and do not come back as charged particles. As a result of this recombination, the charged particle distribution functions vanish for significant parts of the velocity space and cannot be approximated by Maxwellians, as one would need to be the case to be able to use fluid equations. Thus, the treatment of charged particles near the wall has to be kinetic (Loizu *et al.* 2011; Geraldini *et al.* 2018). The combination of these two issues can manifest in a population of energetic electrons that cannot be predicted by fluid models. In turn, these energetic electrons affect the density and temperature by suppressing or enhancing heat transport and by changing the potential difference across the Debye sheaths. Evidence of these effects has been found in direct kinetic simulations of 1D problems (Tskhakaya *et al.* 2011; Chankin & Coster 2015).

The fact that kinetic effects are important has been recognized for neutrals, leading to kinetic codes for them (Reiter *et al.* 2005; Stotler & Karney 1994). However, as we have pointed out before, these codes ignore any possible non-Maxwellian features in the ion and electron distribution functions, are sensitive to the parameters that determine how particles interact with the wall and, depending on the version, do not include many elastic collisions or detailed collision physics. The non-Maxwellian features of the electron distribution function are particularly important as electrons mediate many of the processes considered important in these neutral models: radiation, ionization, recombination, etc.

For ions and electrons, the community is starting to construct edge kinetic codes such as XGC (Ku *et al.* 2016), GKEYLL (Hakim *et al.* 2020) or COGENT (Dorf *et al.* 2016). These codes are broadly based on the same gyroaveraged kinetic models used in δf gyrokinetic codes such as GS2 (Kotschenreuther *et al.* 1995; Dorland *et al.* 2000), GENE (Dannert & Jenko 2005) or stella (Barnes *et al.* 2019), but are very different from them because of the edge particularities, as we proceed to explain. The idea behind gyroaveraged kinetic models is to average over the fast gyrofrequency time scale to avoid a cripplingly small time step. All gyroaveraged kinetic models are based on an asymptotic expansion in $\rho_i/L_{\perp} \ll 1$ (see table 2 for values of ρ_i and $L_{\perp}$). The simplest possible approach is drift kinetics (Hazeltine 1973) that assumes that the size of all turbulent structures is much larger than ρ_i. Unfortunately, in the presence of temperature and density gradients, drift kinetics develops instabilities at the grid scale. These instabilities can be stabilized by numerical dissipation, and in the real word, they are stabilized by finite gyroradius effects that drift kinetics neglects. Gyrokinetics (Catto 1978; Frieman & Chen 1982) was developed to solve this problem in the core of the tokamak. Initially, δf gyrokinetics assumed that turbulent fluctuations had a characteristic size of the order of ρ_i and their amplitude was small by a factor of $\rho_i/L_{\perp} \ll 1$. This ensures that the gradients of the fluctuations are comparable to the background gradient and not larger.

However, as we have explained in section 3, in the edge it is not possible to assume that density and temperature are slowly varying quantities plus small fluctuations. This fact

was part of the justification to develop what is know as full f gyrokinetics, in which the distribution function is not assumed to be composed of a slowly varying piece plus small fluctuations. See Parra & Catto (2008) and Brizard & Hahm (2007) for two different types of derivations of full f gyrokinetics. Overall, full f gyrokinetics can be seen as a mixture of drift kinetics and the original δf gyrokinetics. The distribution function is allowed to have wavelengths that range from $L_\perp$ to ρ_i, but the size of these different Fourier components has to be sufficiently small that the gradient of the distribution function is never larger than $1/L_\perp$. Assuming a core ordering (2.2), one naturally recovers δf gyrokinetics, showing that the distribution function has to be a slowly varying piece plus small fluctuations (Parra & Catto 2010; Calvo & Parra 2012).

In the edge ordering (2.1), full f gyrokinetics fundamentally becomes drift kinetics with some small corrections. These corrections are of two types.

- The electromagnetic fields appear in the kinetic equation averaged over circular gyro-orbits. Thus, electromagnetic fluctuations that have characteristic lengths much smaller than the gyroradius are averaged over and do not drive fluctuations in the distribution function. Since these short wavelength electromagnetic fluctuations can only survive if there are charge and current fluctuations of similar wavelength, which they are not able to drive, they eventually damp and disappear.
- The field equations, quasineutrality and Ampére's law, contain densities and currents that one calculates from the ion and electron distribution functions. As a result of the gyrokinetic expansion, these distribution functions have finite gyroradius corrections that give terms that are small in $\rho_i/L_\perp \ll 1$. One of these small terms in particular, the polarization density in the quasineutrality equation, is important because, despite its small size, it can determine the electric field in different situations. For example, for shear Alfven waves, the polarization density is small, but so are the rest of the contributions to the density, so in the end a balance between the polarization density and another term determines the fluctuating electric field. Another example is the component of the electric field perpendicular to the flux surfaces, which is also determined by a balance between the polarization density and other terms (Parra & Catto 2009).

The small finite gyroradius terms in the full f gyrokinetic equations are important to stabilize the short wavelength instabilities, and some of them (e.g. the polarization density) can also be important for certain aspects of the physics. Keeping the finite gyroradius effects in the kinetic equation is relatively straightforward in PIC codes, although one has to be careful with the accuracy of the average (Guadagni & Cerfon 2017). We are not aware of any full f edge gyrokinetic code that retains finite gyroradius effects in the kinetic equation.

The corrections to the field equations are much more difficult to retain – formulations that explicitly try to conserve energy and momentum exactly require solving nonlinear equations for every element in velocity space, for instance. This has driven the community towards simplifying these terms. As a result of these simplifications, several edge codes solve drift kinetics with some *ad hoc* additions to the field equations, such as a simplified polarization density.

In addition to these fundamental issues, edge drift kinetics and gyrokinetics need to address other problems. As gyrokinetics was devised to model turbulent fluctuations with a spatial size of the order of ρ_i in tokamak cores, most available models do not include features that are important for edge physics.

- There is no gyrokinetic formulation for the wall boundary conditions. Only recently one such formulation was developed for drift kinetic ions in magnetic fields that reach the wall with a grazing angle (Geraldini *et al.* 2018). This work has to be generalized to

electrons, more general angles between the wall and the magnetic field, and eventually to gyrokinetics.

• Gyrokinetics does not usually include collisions with neutrals, and such collisions are important because neutrals break the symmetry introduced by the fast charged particle gyration around magnetic field lines. In other words, the dependence on gyrophase, neglected in gyrokinetics, can become important.

• Gyrokinetics was developed for fluctuations with characteristic scales of the order of the ion gyroradius. At these scales, the magnetic field fluctuations have a very constrained form. For this reason, the extension of gyrokinetics to include MagnetoHydroDynamic (MHD) modes is non-trivial and an active area of research. See Zheng *et al.* (2007) for a theoretical treatment, and Collar *et al.* (2020) for recent numerical work in this area. A gyrokinetic model of the edge should be able to reproduce MHD results, as MHD modes are believed to be the main drive of the eruptions known as Edge Localized Modes (ELMs) (Ham *et al.* 2020).

5. Discussion

A complete edge description requires kinetic effects. Current attempts to model kinetic effects in the edge rely heavily on gyroaveraged kinetic models that average over the very fast gyrofrequency timescale.

In our opinion, there does not exist a systematic procedure to choose the relevant finite gyroradius effects to be kept in the kinetic and field equations. The first objective of a kinetic modeling effort for the edge must be to establish the finite gyroradius effects to be kept in the equations. To do so, for contract T/NA085/20, we have proposed as a first attempt to construct a drift kinetic model. This drift kinetic model will be unstable at grid scales, but hyperviscosity might be enough to stabilize such scales if they do not contribute much to transport (as one would expect due to their small size). For the contract work, we will use the model only in 1D and 2D configurations that cannot develop these grid scale instabilities. We will then determine analytically which finite gyroradius effects must be kept in the equations to determine every part of the problem, and in particular the component of the electric field perpendicular to the flux surfaces.

A well known issue arises when keeping finite gyroradius effects in the field equations. In quasineutrality, the only term that contains the electric potential explicitly is the small finite gyroradius correction. Thus, unless an implicit time stepping algorithm is employed, one needs to solve for the potential by inverting a small term in the equation. This procedure limits the time step size severely (Lee 1987; Barnes *et al.* 2019). Thus, in addition to keeping finite gyroradius effects, we need to make sure that the kinetic equations that we obtain are amenable to implicit time stepping methods.

In addition to studying finite gyroradius effects, we will determine the effect that collisions with neutrals have on the gyrokinetic formalism by introducing charge exchange collisions and ionization collisions.

The final deliverable of contract T/NA085/20 will be a drift kinetic model with neutrals and the finite gyroradius terms that are needed to calculate the component of the electric field that is perpendicular to the flux surfaces. Both of these features will be improvements on the models implemented in existing continuum edge codes.

By the end of the contract, the model will have been tested in 1D and 2D problems, and even though it will have a 3D version, this 3D version will not have been tested in the turbulent regime. Moreover, all the work will have been performed in a helical field and not in a diverted tokamak field because the helical field is the state-of-the-art for continuum edge kinetic codes (only recently, in the 2020 Annual APS DPP meeting, the

two leading continuum codes, GKEYLL and COGENT, have reported the first runs with more complex tokamak geometry). The limitations of the model delivered at the end of contract T/NA085/20 leave two obvious avenues for future work.

• The main theoretical difficulty added by tokamak magnetic fields is the presence of a component of the drifts in the direction perpendicular to the flux surface that does not exist in the case of a helical field. This component of the drifts leads to finite orbit widths and can significantly modify some of the physics of both quiescent 2D plasmas (Kagan & Catto 2008; Landreman *et al.* 2014) and 3D turbulence (Parisi *et al.* 2020). Adding this component of the particle drift to the equations will require extra work.

• As we have explained above, the 3D model is expected to have grid scale instabilities that can be stabilized by hyperviscosity or other numerical methods of dissipation. To properly capture the fluctuations at the ion gyroradius scale, one would have to include more precise finite gyroradius effects. This is an obvious extension of the work in contract T/NA085/20, and it is very important for High confinement mode (H-mode) where the turbulence at scales larger than the ion gyroradius is stabilized for still unclear reasons. In this regime, turbulence at scales of the order of or smaller than the ion gyroradius is important (Hillesheim *et al.* 2016; Hatch *et al.* 2017; Parisi *et al.* 2020), and the finite gyroradius effects become crucial for ions. We foresee that adding more detailed finite gyroradius effects will be theoretically and numerically challenging and will require dedicated work.

Two other aspects of an edge kinetic model are beyond the scope of contract T/NA085/20.

• To test the effect of wall boundary conditions on drift kinetics, we will impose a simplified version of the boundary conditions that are valid in the limit in which the electron gyroradius is much smaller than the Debye length. However, more detailed boundary conditions must be found because usually the electron gyroradius is larger than or comparable to the Debye length. This is work that is being pursued by one of the authors of this report (F.I.P.) with other sources of funding.

• We pointed out above that it would be desirable to be able to recover MHD modes with the edge kinetic model. In the work for contract T/NA085/20, the fluctuations in the magnetic field will be neglected (this is a good approximation for many edge plasmas), and hence it will not be possible to explore connections with MHD. This is an area of research where ExCALIBUR NEPTUNE could benefit from collaboration with the EPSRC Programme Grant 'Turbulent Dynamics of Tokamak Plasmas (TDoTP)'. Several PIs in the ExCALIBUR NEPTUNE project also belong to TDoTP.

REFERENCES

Barnes, M., Parra, F.I. & Landreman, M. 2019 stella: An operator-split, implicit-explicit δf-gyrokinetic code for general magnetic field configurations. *J. Comput. Phys.* **391**, 365.

Beer, M.A., Cowley, S.C. & Hammett, G.W. 1995 Field-aligned coordinates for nonlinear simulations of tokamak turbulence. *Phys. Plasmas* **2**, 2687.

Brackmann, R.T., Fite, W.L. & Neynaber, R.H. 1958 Collisions of Electrons with Hydrogen Atoms. III. Elastic Scattering. *Phys. Rev.* **112**, 1157.

Braginskii, S.I. 1958 Transport phenomena in a completely ionized two-temperature plasma. *Sov. Phys. JETP* **6**, 358.

Brizard, A.J. & Hahm, T.S. 2007 Foundations of nonlinear gyrokinetic theory. *Rev. Mod. Phys.* **79**, 421.

Bufferand, H., Ciraolo, G., Marandet, Y., Bucalossi, J., Ghendrih, Ph., Gunn, J., Mellet, N., Tamain, P., Leybros, R., Fedorczak, N., Schwander, F. & Serre, E. 2015 Numerical modelling for divertor design of the WEST device with a focus on plasmawall interactions. *Nucl. Fusion* **55**, 053025.

Bufferand, H., Tamain, P., Baschetti, S., Bucalossi, J., Ciraolo, G., Fedorczak, N.,

Ghendrih, Ph., Nespoli, F., Schwander, F. & E. Serre and, Y. Marandet 2019 Three-dimensional modelling of edge multi-component plasma taking into account realistic wall geometry. *Nucl. Mat. Energy* **18**, 82.

Calvo, I. & Parra, F.I. 2012 Long-wavelength limit of gyrokinetics in a turbulent tokamak and its intrinsic ambipolarity. *Plasma Phys. Control. Fusion* **54**, 115007.

Catto, P.J. 1978 Linearized gyro-kinetics. *Plasma Phys.* **20**, 719.

Catto, P.J. 1994 A short mean-free path, coupled neutral-ion transport description of a tokamak edge plasma. *Phys. Plasmas* **1**, 1936.

Catto, P.J. & Simakov, A.N. 2004 A drift ordered short mean free path description for magnetized plasma allowing strong spatial anisotropy. *Phys. Plasmas* **11**, 90.

Chankin, A.V., Corrigan, G. & JET Contributors 2021 EDGE2D-EIRENE modeling of the impact of wall materials on core edge, scrape-off layer and divertor parameters. *Plasma Phys. Control. Fusion* **63**, 035010.

Chankin, A.V. & Coster, D.P. 2015 On the locality of parallel transport of heat carrying electrons in the SOL. *J. Nucl. Mater.* **463**, 498.

Chodura, R. 1982 Plasma-wall transition in an oblique magnetic field. *Phys. Fluids* **25**, 1628.

Colchin, R.J., Maingi, R., Fenstermacher, M.E., Carlstrom, T.N., Isler, R.C., Owen, L.W. & Groebner, R.J. 2000 Measurement of neutral density near the X point in the DIII-D tokamak. *Nucl. Fusion* **40**, 175.

Collar, J.P.M., McMillan, B.F., Saarelma, S. & Bottino, A. 2020 Comparing electromagnetic instabilities in global gyrokinetic simulations with local and MHD models. *Plasma Phys. Control. Fusion* **62**, 095005.

Dannert, T. & Jenko, F. 2005 Gyrokinetic simulation of collisionless trapped-electron mode turbulence. *Phys. Plasmas* **12**, 072309.

Dorf, M.A., Dorr, M.R., Hittinger, J.A., Cohen, R.H. & Rognlien, T.D. 2016 Continuum kinetic modeling of the tokamak plasma edge. *Phys. Plasmas* **23**, 056102.

Dorland, W., Jenko, F., Kotschenreuther, M. & Rogers, B.N. 2000 Electron Temperature Gradient Turbulence. *Phys. Rev. Lett.* **85**, 5579.

Dudson, B.D. & Leddy, J. 2017 Hermes: global plasma edge fluid turbulence simulations. *Plasma Phys. Control. Fusion* **59**, 054010.

Frieman, E.A. & Chen, L. 1982 Nonlinear gyrokinetic equations for low-frequency electromagnetic waves in general plasma equilibria. *Phys. Fluids* **25**, 502.

Geraldini, A., Parra, F.I. & Militello, F. 2018 Solution to a collisionless shallow-angle magnetic presheath with kinetic ions. *Plasma Phys. Control. Fusion* **60**, 125002.

Goldston, R.J. 2012 Heuristic drift-based model of the power scrape-off width in low-gas-puff H-mode tokamaks. *Nucl. Fusion* **52**, 013009.

Gray, D.R. & Kilkenny, J.D. 1980 The measurement of ion acoustic turbulence and reduced thermal conductivity caused by a large temperature gradient in a laser heated plasma. *Plasma Phys.* **22**, 81.

Guadagni, J. & Cerfon, A.J. 2017 Fast and spectrally accurate evaluation of gyroaverages in non-periodic gyrokinetic Poisson simulations. *J. Plasma Phys.* **83**, 905830407.

Gurevich, A. & Istomin, Ya.N. 1979 Thermal runaway and convective heat transport by fast electrons in a plasma. *Sov. Phys. JETP* **50**, 470.

Hakim, A.H., Mandell, N.R., T.N. Bernard and, M. Francisquez, Hammett, G.W. & Shi, E. L. 2020 Continuum electromagnetic gyrokinetic simulations of turbulence in the tokamak scrape-off layer and laboratory devices. *Phys. Plasmas* **27**, 042304.

Halpern, F.D., Ricci, P., Jolliet, S., Loizu, J., Morales, J., Mosetto, A., Musil, F., Riva, F., Tran, T.M. & Wersal, C. 2016 The GBS code for tokamak scrape-off layer simulations. *J. Comput. Phys.* **315**, 388.

Ham, C., Kirk, A., Pamela, S. & Wilson, H. 2020 Filamentary plasma eruptions and their control on the route to fusion energy. *Nature Rev. Phys.* **2**, 159.

Hariri, F. & Ottaviani, M. 2013 A flux-coordinate independent field-aligned approach to plasma turbulence simulations. *Comput. Phys. Comm.* **184**, 2419.

Hastie, R.J. 1997 Sawtooth instability in tokamak plasmas. *Astrophys. Space Sci.* **256**, 177.

Hatch, D.R., Kotschenreuther, M., Mahajan, S., Valanju, P. & Liu, X. 2017 A gyrokinetic perspective on the JET-ILW pedestal. *Nucl. Fusion* **57**, 036020.

Hazeltine, R.D. 1973 Recursive derivation of drift-kinetic equation. *Plasma Phys.* **15**, 77–80.

Hazeltine, R.D., Calvin, M.D., Valanju, P.M. & Solano, E.R. 1992 Analytical calculation of neutral transport and its effect on ions. *Nucl. Fusion* **32**, 3.

Helander, P., Krasheninnikov, S.I. & Catto, P.J. 1994 Fluid equations for a partially ionized plasma. *Phys. Plasmas* **1**, 3174.

Hillesheim, J.C., Dickinson, D., Roach, C.M., Saarelma, S., Scannell, R., Kirk, A., Crocker, N.A., Peebles, W.A., Meyer, H. & the MAST Team 2016 Intermediate-k density and magnetic field fluctuations during inter-ELM pedestal evolution in MAST. *Plasma Phys. Control. Fusion* **58**, 014020.

Isoardi, L., Chiavassa, G., Ciraolo, G., Haldenwang, P., Serre, E., Ghendrih, Ph., Sarazin, Y., Schwander, F. & Tamain, P. 2010 Penalization modeling of a limiter in the Tokamak edge plasma. *J. Comput. Phys.* **229**, 2220.

Jackson, G.L., Winter, J., Taylor, T.S., Burrell, K.H., DeBoo, J.C., Greenfield, C.M., Groebner, R.J., Hodapp, T., Holtrop, K., Lazarus, E.A., Lao, L.L., Lippmann, S.I., Osborne, T.H., Petrie, T.W., Phillips, J., James, R., Schissel, D.P., Strait, E.J., Turnbull, A.D., West, W.P. & the DIII-D Team 1991 Regime of very high confinement in the boronized DIII-D tokamak. *Phys. Rev. Lett.* **67**, 3098.

Kagan, G. & Catto, P.J. 2008 Arbitrary poloidal gyroradius effects in tokamak pedestals and transport barriers. *Plasma Phys. Control. Fusion* **50**, 085010.

Kotschenreuther, M., Rewoldt, G. & Tang, W.M. 1995 Comparison of initial value and eigenvalue codes for kinetic toroidal plasma instabilities. *Comput. Phys. Comm.* **88**, 128.

Krasheninnikov, S.I. & Kukushkin, A.S. 2017 Physics of ultimate detachment of a tokamak divertor plasma. *J. Plasma Phys.* **83**, 155830501.

Ku, S., Hager, R., Chang, C.S., Kwon, J.M. & Parker, S.E. 2016 A new hybrid-Lagrangian numerical scheme for gyrokinetic simulation of tokamak edge plasma. *J. Comput. Phys.* **315**, 467.

Landreman, M., Parra, F.I., Catto, P.J., Ernst, D.R. & Pusztai, I. 2014 Radially global δf computation of neoclassical phenomena in a tokamak pedestal. *Plasma Phys. Control. Fusion* **56**, 045005.

Lee, W.W. 1987 Gyrokinetic particle simulation model. *J. Comput. Phys.* **72**, 243.

Lindsay, B.G. & Stebbings, R.F. 2005 Charge transfer cross sections for energetic neutral atom data analysis. *J. Geophys. Res.* **110**, A12213.

Loizu, J., Ricci, P. & Theiler, C. 2011 Existence of subsonic plasma sheaths. *Phys. Rev. E* **83**, 016406.

Mikhailovskii, A.B. & Tsypin, V.S. 1971 Transport equations and gradient instabilities in a high pressure collisional plasma. *Plasma Phys.* **13**, 785.

Militello, F. & Fundamenski, W. 2011 Multi-machine comparison of drift fluid dimensionless parameters. *Plasma Phys. Control. Fusion* **53**, 095002.

Parisi, J.F., Parra, F.I., Roach, C.M., Giroud, C., Dorland, W., Hatch, D.R., Barnes, M., Hillesheim, J.C., Aiba, N. & Ball, J. 2020 Toroidal and slab ETG instability dominance in the linear spectrum of JET-ILW pedestals. *Nucl. Fusion* **60**, 126045.

Parra, F.I. & Catto, P.J. 2008 Limitations of gyrokinetics on transport time scales. *Plasma Phys. Control. Fusion* **50**, 065014.

Parra, F.I. & Catto, P.J. 2009 Vorticity and intrinsic ambipolarity in turbulent tokamaks. *Plasma Phys. Control. Fusion* **51**, 095008.

Parra, F.I. & Catto, P.J. 2010 Turbulent transport of toroidal angular momentum in low flow gyrokinetics. *Plasma Phys. Control. Fusion* **52**, 045004.

Reiter, D., Baelmans, M. & Börner, P. 2005 The EIRENE and B2-EIRENE Codes. *Fusion Sci. Tech.* **47**, 172.

Riemann, K.-U. 1991 The Bohm criterion and sheath formation. *J. Phys. D: Appl. Phys.* **24**, 493.

Rognlien, T.D., Rensink, M.E. & Smith, G.R. 2007 User manual for the UEDGE edge-plasma transport code. *Tech. Rep.* UCRL-ID-137121. Lawrence Livermore National Laboratory.

Schmitt, J.C., Bell, R.E., Boyle, D.P., Esposti, B., Kaita, R., Kozub, T., LeBlanc, B.P., Lucia, M., Maingi, R., Majeski, R., Merino, E., Punjabi-Vinoth, S., Tchilingurian, G., Capece, A., Koel, B., Roszell, J., Biewer, T. M., Gray, T. K., Kubota,

S., Beiersdorfer, P., Widmann, K. & Tritz, K. 2015 High performance discharges in the Lithium Tokamak eXperiment with liquid Lithium walls. *Phys. Plasmas* **22**, 056112.

Scotti, F., Stotler, D.P., Bell, R.E., LeBlanc, B.P., Sabbagh, S.A., Soukhanovskii, V.A., Umansky, M.V. & Zweben, S.J. 2021 Outer midplane neutral density measurements and H-mode fueling studies in NSTX-U. *Nucl. Fusion* **61**, 036002.

Simakov, A.N. & Catto, P.J. 2003 Drift-ordered fluid equations for field-aligned modes in low-β collisional plasma with equilibrium pressure pedestals. *Phys. Plasmas* **10**, 4744.

Simonini, R., Corrigan, G., Radford, G., Spence, J. & Taroni, A. 1994 Models and Numerics in the Multi-Fluid 2-D Edge Plasma Code EDGE2D/U. *Contrib. Plasma Phys.* **34**, 368.

Stegmeir, A., Coster, D., Ross, A., Maj, O., Lackner, K. & Poli, E. 2018 GRILLIX: a 3D turbulence code based on the flux-coordinate independent approach. *Plasma Phys. Control. Fusion* **60**, 035005.

Stotler, D. & Karney, C. 1994 Neutral Gas Transport Modeling with DEGAS 2. *Contrib. Plasma Phys.* **34**, 392.

Sugihara, M., Igitkhanov, Yu., Janeschitz, G., Hubbard, A.E., Kamada, Y., Lingertat, J., Osborne, T.H. & Suttrop, W. 2000 A model for H mode pedestal width scaling using the International Pedestal Database. *Nucl. Fusion* **40**, 1743.

Tamain, P., Bufferand, H., Ciraolo, G., Colin, C., Galassi, D., Ph.Ghendrih, Schwander, F. & Serre, E. 2016 The TOKAM3X code for edge turbulence fluid simulations of tokamak plasmas in versatile magnetic geometries. *J. Comput. Phys.* **321**, 606.

Tskhakaya, D., Jachmich, S., Eich, T., Fundamenski, W. & JET EFDA contributors 2011 Interpretation of divertor Langmuir probe measurements during the ELMs at JET. *J. Nucl. Mater.* **415**, S860.

Wersal, C. & Ricci, P. 2015 A first-principles self-consistent model of plasma turbulence and kinetic neutral dynamics in the tokamak scrape-off layer. *Nucl. Fusion* **55**, 123014.

Wiesen, S., Brezinsek, S., Bonnin, X., Delabie, E., Frassinetti, L., Groth, M., Guillemaut, C., Harrison, J., Harting, D., Henderson, S., Huber, A., Kruezi, U., Pitts, R.A., Wischmeier, M. & JET contributors 2018 On the role of finite grid extent in SOLPS-ITER edge plasma simulations for JET H-mode discharges with metallic wall. *Nucl. Mat. Energy* **17**, 174.

Wiesen, S., Reiter, D., Kotov, V., Baelmans, M., Dekeyser, W., Kukushkin, A.S., Lisgo, S.W., Pitts, R.A., Rozhansky, V., Saibene, G., Veselova, I. & Voskoboynikov, S. 2015 The new SOLPS-ITER code package. *J. Nucl. Mater.* **463**, 480.

Zeiler, A., Biskamp, D., Drake, J.F. & Guzdar, P.N. 1996 Three-dimensional fluid simulations of tokamak edge turbulence. *Phys. Plasmas* **3**, 2951.

Zel'dovich, Ya. B. & Raizer, Yu. P. 2013 *Physics of Shock Waves and High-Temperature Hydrodynamic Phenomena*. Dover Publications.

Zheng, L.J., Kotschenreuther, M.T. & Dam, J.W. Van 2007 Revisiting linear gyrokinetics to recover ideal magnetohydrodynamics and missing finite Larmor radius effects. *Phys. Plasmas* **14**, 072505.

1D drift kinetic models with periodic boundary conditions

Felix I. Parra, Michael Barnes and Michael Hardman
Rudolf Peierls Centre for Theoretical Physics, University of Oxford, Oxford OX1 3PU, UK

(This version is of 22 February 2021)

1. Introduction

In this report, we propose 1D drift kinetic equations to test the possibility of extracting low order moments from the distribution functions for implicit methods. The model that we present here has periodic boundary conditions, adequate for the closed field line region of the edge. We will address wall boundary conditions for open field lines in the reports for milestones M1.3, M2.4 and M2.5.

2. 1D electrostatic drift kinetics

We consider a plasma with one ion species with charge e and mass m_i, electrons with charge $-e$ and mass m_e, and one species of neutrals with mass

$$m_n = m_i. \tag{2.1}$$

The plasma is magnetized by a constant magnetic field $\mathbf{B} = B\hat{\mathbf{z}}$, and we assume that the plasma only varies along magnetic field lines. In this case, the electric field produced by the plasma is electrostatic, $\mathbf{E} = -(\partial\phi/\partial z)\hat{\mathbf{z}}$. The potential $\phi(z,t)$ depends on the position along magnetic field lines z and on time t.

If we assume that the gyroradii are small compared to the length scales of interest, and that the gyrofrequencies are much larger than the frequencies that we want to model (Hazeltine 1973), the distribution functions $f_s(z, v_\parallel, v_\perp, t)$ of the different species $s = i, e, n$ only depend on the component of the velocity parallel to the magnetic field $v_\parallel$ and the magnitude of the velocity perpendicular to the magnetic field $v_\perp$, and are independent of the direction of the velocity perpendicular to the magnetic field. Thus, the distribution functions that in general can depend on three spatial variables $\mathbf{r}$, three components of the velocity $\mathbf{v}$ and the time t depend only on z, $v_\parallel$, $v_\perp$ and t,

$$f_s(\mathbf{r}, \mathbf{v}, t) = f_s(z, v_\parallel, v_\perp, t). \tag{2.2}$$

The equations for the distribution functions of the different species are

$$\frac{\partial f_i}{\partial t} + v_\parallel \frac{\partial f_i}{\partial z} - \frac{e}{m_i}\frac{\partial \phi}{\partial z}\frac{\partial f_i}{\partial v_\parallel} = C_{ii}[f_i] + C_{in}[f_i, f_n], \tag{2.3}$$

$$\frac{\partial f_e}{\partial t} + v_\parallel \frac{\partial f_e}{\partial z} + \frac{e}{m_e}\frac{\partial \phi}{\partial z}\frac{\partial f_e}{\partial v_\parallel} = C_{ee}[f_e] + C_{ei}[f_e, f_i] + C_{en}[f_e, f_n] \tag{2.4}$$

and

$$\frac{\partial f_n}{\partial t} + v_\parallel \frac{\partial f_n}{\partial z} = C_{ni}[f_n, f_i]. \tag{2.5}$$

Here we have included ion-ion and electron-electron collisions, modeled by the Fokker-Planck collision operators $C_{ii}[f_i]$ and $C_{ee}[f_e]$ (Rosenbluth *et al.* 1957), elastic electron-ion

and electron-neutral collisions, modeled by the simplified Fokker-Planck collision operator $C_{ei}[f_e, f_i]$ (Braginskii 1958) and the Boltzmann collision operator $C_{en}[f_e, f_n]$, and charge-exchange collisions, represented by the simplified Boltzmann collision operators

$$C_{in}[f_i, f_n] = -\int R_{in}(|\mathbf{v}-\mathbf{v}'|)\left[f_i(\mathbf{v})f_n(\mathbf{v}') - f_i(\mathbf{v}')f_n(\mathbf{v})\right] \mathrm{d}^3v' \tag{2.6}$$

and

$$C_{ni}[f_n, f_i] = -\int R_{in}(|\mathbf{v}-\mathbf{v}'|)\left[f_n(\mathbf{v})f_i(\mathbf{v}') - f_n(\mathbf{v}')f_i(\mathbf{v})\right] \mathrm{d}^3v', \tag{2.7}$$

To simplify our equations, we assume that the function R_{in} is constant (Connor 1977; Hazeltine *et al.* 1992; Catto 1994), finding

$$C_{in}[f_i, f_n] = -R_{in}\left(n_n f_i - n_i f_n\right) \tag{2.8}$$

and

$$C_{ni}[f_n, f_i] = -R_{in}\left(n_i f_n - n_n f_i\right), \tag{2.9}$$

where the densities are

$$n_s(z,t) := 2\pi \int_{-\infty}^{\infty} \mathrm{d}v_\parallel \int_0^{\infty} \mathrm{d}v_\perp \, v_\perp f_s(z, v_\parallel, v_\perp, t). \tag{2.10}$$

Note that we can neglect the effect of electron collisions on ions and on neutrals due to the smallness of the electron mass (Braginskii 1958). We have also neglected neutral-neutral collisions because, in current fusion devices, the neutral density is sufficiently small that the neutral-neutral collisions are rare.

The kinetic equations will be solved in the interval $z \in [0, L]$, and we will impose periodic boundary conditions at $z = 0$ and $z = L$,

$$f_s(z = 0, v_\parallel, v_\perp, t) = f_s(z = L, v_\parallel, v_\perp, t). \tag{2.11}$$

Finally, the potential $\phi(z,t)$ is determined by the quasineutrality equation

$$n_i = n_e. \tag{2.12}$$

To solve this equation, we need to treat the equations implicitly as the potential enters only via its effect on $\partial f_i/\partial t$ and $\partial f_e/\partial t$. The need to use implicit methods is one of the reasons why we are trying to extract some of the low order moments from the distribution function, notably the density.

Before we treat the complete problem, we will simplify the treatment of electrons to obtain a system of equations that can be solved with an explicit time advance so that we can compare our implicit schemes with an explicit numerical method. Instead of solving for f_e, we will use a Maxwell-Boltzmann response,

$$n_e(z,t) = N_e \exp\left(\frac{e\phi(z,t)}{T_e}\right), \tag{2.13}$$

where N_e and T_e are constants (see Appendix A for a derivation of the Maxwell-Boltzmann response). Moreover, the full Fokker-Planck ion-ion collision operator $C_{ii}[f_i]$ is a complicated integro-differential operator that we will not implement in the first versions of our drift kinetic code, so we do not include it in the equations for now. Thus, the final simplified model for $f_i(z, v_\parallel, v_\perp, t)$, $f_n(z, v_\parallel, v_\perp, t)$ and $\phi(z,t)$ is given by the equations

$$\frac{\partial f_i}{\partial t} + v_\parallel \frac{\partial f_i}{\partial z} - \frac{e}{m_i}\frac{\partial \phi}{\partial z}\frac{\partial f_i}{\partial v_\parallel} = -R_{in}(n_n f_i - n_i f_n), \tag{2.14}$$

$$\frac{\partial f_n}{\partial t} + v_\parallel \frac{\partial f_n}{\partial z} = -R_{in}(n_i f_n - n_n f_i) \tag{2.15}$$

and

$$n_i = N_e \exp\left(\frac{e\phi}{T_e}\right), \tag{2.16}$$

with periodic boundary conditions (2.11). This system of equations can be solved explicitly because the simple electron model allows one to obtain ϕ as a function of n_i.

3. 1D moment drift kinetics

Instead of solving for $f_s(z, v_\parallel, v_\perp, t)$, we solve for

$$F_s(z, w_\parallel, w_\perp, t) := \frac{v_{ts}^3(z,t)}{n_s(z,t)} f_s\Big(z, u_{s\parallel}(z,t) + v_{ts}(z,t)w_\parallel, v_{ts}(z,t)w_\perp, t\Big), \tag{3.1}$$

where we have defined the normalized velocities

$$w_\parallel(z, v_\parallel, t) := \frac{v_\parallel - u_{s\parallel}(z,t)}{v_{ts}(z,t)} \tag{3.2}$$

and

$$w_\perp(z, v_\perp, t) := \frac{v_\perp}{v_{ts}(z,t)}, \tag{3.3}$$

the average parallel velocity

$$u_{s\parallel}(z,t) := \frac{2\pi}{n_s} \int_{-\infty}^{\infty} \mathrm{d}v_\parallel \int_0^\infty \mathrm{d}v_\perp \, v_\perp v_\parallel f_s(z, v_\parallel, v_\perp, t) \tag{3.4}$$

and the thermal speed

$$v_{ts}(z,t) := \sqrt{\frac{4\pi}{3n_s} \int_{-\infty}^{\infty} \mathrm{d}v_\parallel \int_0^\infty \mathrm{d}v_\perp \, v_\perp [(v_\parallel - u_{s\parallel}(z,t))^2 + v_\perp^2] f_s(z, v_\parallel, v_\perp, t)}. \tag{3.5}$$

According to its definition, $F_s(z, w_\parallel, w_\perp, t)$ must satisfy the conditions

$$2\pi \int_{-\infty}^{\infty} \mathrm{d}w_\parallel \int_0^\infty \mathrm{d}w_\perp \, w_\perp F_s(z, w_\parallel, w_\perp, t) = 1, \tag{3.6}$$

$$2\pi \int_{-\infty}^{\infty} \mathrm{d}w_\parallel \int_0^\infty \mathrm{d}w_\perp \, w_\perp w_\parallel F_s(z, w_\parallel, w_\perp, t) = 0 \tag{3.7}$$

and

$$2\pi \int_{-\infty}^{\infty} \mathrm{d}w_\parallel \int_0^\infty \mathrm{d}w_\perp \, w_\perp (w_\parallel^2 + w_\perp^2) F_s(z, w_\parallel, w_\perp, t) = \frac{3}{2} \tag{3.8}$$

at every point z and time t.

The equations for ions become

$$\frac{\partial n_i}{\partial t} + \frac{\partial}{\partial z}\left(n_i u_{i\parallel}\right) = 0, \tag{3.9}$$

$$n_i m_i \left(\frac{\partial u_{i\parallel}}{\partial t} + u_{i\parallel}\frac{\partial u_{i\parallel}}{\partial z}\right) = -\frac{\partial p_{i\parallel}}{\partial z} - e n_i \frac{\partial \phi}{\partial z} + n_i n_n m_i R_{in}(u_{n\parallel} - u_{i\parallel}), \tag{3.10}$$

$$\frac{3}{2}n_i m_i v_{ti}\left(\frac{\partial v_{ti}}{\partial t}+u_{i\parallel}\frac{\partial v_{ti}}{\partial z}\right)=-\frac{\partial q_{i\parallel}}{\partial z}-p_{i\parallel}\frac{\partial u_{i\parallel}}{\partial z}+\frac{3}{4}n_i n_n m_i R_{in}(v_{tn}^2-v_{ti}^2) +\frac{1}{2}n_i n_n m_i R_{in}(u_{n\parallel}-u_{i\parallel})^2 \tag{3.11}$$

and

$$\frac{\partial F_i}{\partial t}+\dot{z}_i\frac{\partial F_i}{\partial z}+\dot{w}_{\parallel i}\frac{\partial F_i}{\partial w_\parallel}+\dot{w}_{\perp i}\frac{\partial F_i}{\partial w_\perp}=\dot{F}_i+\mathcal{C}_{in}. \tag{3.12}$$

Here, we have defined the coefficients

$$\dot{z}_s[F_s](z,w_\parallel,t):=u_{s\parallel}+v_{ts}w_\parallel, \tag{3.13}$$

$$\dot{w}_{\parallel s}[F_s](z,w_\parallel,t):=\frac{1}{n_s m_s v_{ts}}\frac{\partial p_{s\parallel}}{\partial z}+\frac{2w_\parallel}{3n_s m_s v_{ts}^2}\left[\frac{\partial q_{s\parallel}}{\partial z}+\left(p_{s\parallel}-\frac{3}{2}n_s m_s v_{ts}^2\right)\frac{\partial u_{s\parallel}}{\partial z}\right] -w_\parallel^2\frac{\partial v_{ts}}{\partial z}, \tag{3.14}$$

$$\dot{w}_{\perp s}[F_s](z,w_\parallel,w_\perp,t):=\frac{2w_\perp}{3n_s m_s v_{ts}^2}\left(\frac{\partial q_{s\parallel}}{\partial z}+p_{s\parallel}\frac{\partial u_{s\parallel}}{\partial z}\right)-w_\parallel w_\perp\frac{\partial v_{ts}}{\partial z} \tag{3.15}$$

and

$$\dot{F}_s[F_s](z,w_\parallel,w_\perp,t):=\left[w_\parallel\left(3\frac{\partial v_{ts}}{\partial z}-\frac{v_{ts}}{n_s}\frac{\partial n_s}{\partial z}\right) -\frac{2}{n_s m_s v_{ts}^2}\left(\frac{\partial q_{s\parallel}}{\partial z}+\left(p_{s\parallel}-\frac{1}{2}n_s m_s v_{ts}^2\right)\frac{\partial u_{s\parallel}}{\partial z}\right)\right]F_s, \tag{3.16}$$

the parallel pressure

$$p_{s\parallel}[F_s](z,t):=2\pi n_s m_s v_{ts}^2\int_{-\infty}^{\infty}\mathrm{d}w_\parallel\int_0^\infty\mathrm{d}w_\perp\, w_\perp w_\parallel^2 F_s(z,w_\parallel,w_\perp,t) \tag{3.17}$$

the parallel heat flux

$$q_{s\parallel}[F_s](z,t):=\pi n_s m_s v_{ts}^3\int_{-\infty}^{\infty}\mathrm{d}w_\parallel\int_0^\infty\mathrm{d}w_\perp\, w_\perp w_\parallel(w_\parallel^2+w_\perp^2)F_s(z,w_\parallel,w_\perp,t), \tag{3.18}$$

and the modified charge exchange collision operator

$$\begin{aligned}\mathcal{C}_{in}&[F_i,F_n,n_n,u_{i\parallel},u_{n\parallel},v_{ti},v_{tn}](z,w_\parallel,w_\perp,t)\\ &:=-n_n R_{in}\left[F_i-\frac{v_{ti}^3}{v_{tn}^3}F_n\left(z,\frac{u_{i\parallel}-u_{n\parallel}}{v_{tn}}+\frac{v_{ti}}{v_{tn}}w_\parallel,\frac{v_{ti}}{v_{tn}}w_\perp,t\right)\right]\\ &\quad+n_n R_{in}\frac{\partial}{\partial w_\parallel}\left[\left(\frac{u_{n\parallel}-u_{i\parallel}}{v_{ti}}+\frac{w_\parallel}{2}\left(\frac{v_{tn}^2}{v_{ti}^2}-1+\frac{2(u_{n\parallel}-u_{i\parallel})^2}{3v_{ti}^2}\right)\right)F_i\right]\\ &\quad+\frac{n_n R_{in}}{w_\perp}\frac{\partial}{\partial w_\perp}\left[\frac{w_\perp^2}{2}\left(\frac{v_{tn}^2}{v_{ti}^2}-1+\frac{2(u_{n\parallel}-u_{i\parallel})^2}{3v_{ti}^2}\right)F_i\right].\end{aligned} \tag{3.19}$$

Note that the differential terms in this modified collision operator could have been included in the definitions of the coefficients $\dot{w}_{\parallel i}$, $\dot{w}_{\perp i}$ and $\dot{F}_i$, but we have decided to make them part of a modified collision operator instead to separate the effect of collisions clearly. This split should not be taken as a suggestion on how to implement these terms in a code.

The equations for the neutrals are

$$\frac{\partial n_n}{\partial t} + \frac{\partial}{\partial z}\left(n_n u_{n\parallel}\right) = 0, \tag{3.20}$$

$$n_n m_i \left(\frac{\partial u_{n\parallel}}{\partial t} + u_{n\parallel}\frac{\partial u_{n\parallel}}{\partial z}\right) = -\frac{\partial p_{n\parallel}}{\partial z} + n_i n_n m_i R_{in}(u_{i\parallel} - u_{n\parallel}), \tag{3.21}$$

$$\frac{3}{2} n_n m_i v_{tn}\left(\frac{\partial v_{tn}}{\partial t} + u_{n\parallel}\frac{\partial v_{tn}}{\partial z}\right) = -\frac{\partial q_{n\parallel}}{\partial z} - p_{n\parallel}\frac{\partial u_{n\parallel}}{\partial z} + \frac{3}{4} n_n n_i m_i R_{in}(v_{ti}^2 - v_{tn}^2) + \frac{1}{2} n_n n_i m_i R_{in}(u_{n\parallel} - u_{i\parallel})^2 \tag{3.22}$$

and

$$\frac{\partial F_n}{\partial t} + \dot{z}_n \frac{\partial F_n}{\partial z} + \dot{w}_{\parallel n}\frac{\partial F_n}{\partial w_\parallel} + \dot{w}_{\perp n}\frac{\partial F_n}{\partial w_\perp} = \dot{F}_n + \mathcal{C}_{ni}. \tag{3.23}$$

Here, we have defined the modified charge exchange collision operator

$$\begin{aligned}
&\mathcal{C}_{ni}[F_n, F_i, n_i, u_{n\parallel}, u_{i\parallel}, v_{tn}, v_{ti}](z, w_\parallel, w_\perp, t) \\
&\quad := -n_i R_{in}\left[F_n - \frac{v_{tn}^3}{v_{ti}^3} F_i\left(z, \frac{u_{n\parallel} - u_{i\parallel}}{v_{ti}} + \frac{v_{tn}}{v_{ti}} w_\parallel, \frac{v_{tn}}{v_{ti}} w_\perp, t\right)\right] \\
&\qquad + n_i R_{in}\frac{\partial}{\partial w_\parallel}\left[\left(\frac{u_{i\parallel} - u_{n\parallel}}{v_{tn}} + \frac{w_\parallel}{2}\left(\frac{v_{ti}^2}{v_{tn}^2} - 1 + \frac{2(u_{n\parallel} - u_{i\parallel})^2}{3v_{tn}^2}\right)\right) F_n\right] \\
&\qquad + \frac{n_i R_{in}}{w_\perp}\frac{\partial}{\partial w_\perp}\left[\frac{w_\perp^2}{2}\left(\frac{v_{ti}^2}{v_{tn}^2} - 1 + \frac{2(u_{n\parallel} - u_{i\parallel})^2}{3v_{tn}^2}\right) F_n\right].
\end{aligned} \tag{3.24}$$

Equations (3.12) and (3.23) for F_i and F_n are constructed such that conditions (3.6), (3.7) and (3.8) are satisfied at all times if they are satisfied at $t = 0$.

4. Linear test

One possible test for the sets of 1D equations described above is the evolution of small perturbations to a uniform Maxwellian equilibrium. We assume the following form for the ion and neutral distribution functions,

$$f_s(z, v_\parallel, v_\perp, t) = f_{Ms}(v_\parallel, v_\perp) + f_{s1}(v_\parallel, v_\perp)[\exp(\mathrm{i}k_\parallel z - \mathrm{i}\omega t) + \text{complex conjugate}], \tag{4.1}$$

where

$$f_{Ms}(v_\parallel, v_\perp) = n_s\left(\frac{m_i}{2\pi T_h}\right)^{3/2}\exp\left(-\frac{m_i(v_\parallel^2 + v_\perp^2)}{2T_h}\right). \tag{4.2}$$

Note that both species share the same constant temperature T_h. To ensure that the potential is small, we assume $n_i = N_e$.

Since the perturbations $f_{s1}(v_\parallel, v_\perp)$ and ϕ are small, equations (2.14), (2.15) and (2.16) can be linearized to give

$$(k_\parallel v_\parallel - \omega - \mathrm{i}n_n R_{in}) f_{i1} + \mathrm{i}n_i R_{in} f_{n1} = -\frac{e\phi}{T_h} k_\parallel v_\parallel f_{Mi} + \mathrm{i}R_{in}(n_{n1} f_{Mi} - n_{i1} f_{Mn}), \tag{4.3}$$

$$\mathrm{i}n_n R_{in} f_{i1} + (k_\parallel v_\parallel - \omega - \mathrm{i}n_i R_{in}) f_{n1} = \mathrm{i}R_{in}(n_{i1} f_{Mn} - n_{n1} f_{Mi}) \tag{4.4}$$

and

$$\frac{n_{i1}}{n_i} = \frac{e\phi}{T_e}. \tag{4.5}$$

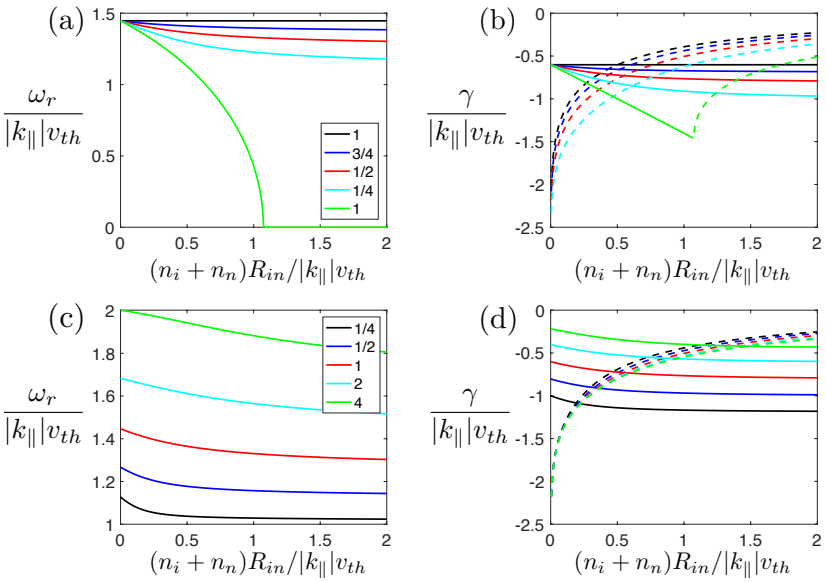

FIGURE 1. Solutions to the dispersion relation (4.7): acoustic waves (solid lines) and non-propagating modes (dashed lines). (a) Real frequency $\omega_r := \mathrm{Re}(\omega)$ and (b) growth rate $\gamma := \mathrm{Im}(\omega)$ as functions of the charge exchange collision frequency $(n_i + n_n)R_{in}$ for $T_e/T_h = 1$ and several values of the parameter $n_i/(n_i + n_n)$. (c) Real frequency ω_r and (d) growth rate γ as functions of the the charge exchange collision frequency $(n_i + n_n)R_{in}$ for $n_i/(n_i + n_n) = 1/2$ and several values of the parameter T_e/T_h.

Here, we have defined the perturbations to the density as

$$n_{s1} = 2\pi \int_{-\infty}^{\infty} \mathrm{d}v_\parallel \int_0^{\infty} \mathrm{d}v_\perp \, v_\perp f_{s1}. \tag{4.6}$$

Solving for the functions f_{i1} and f_{n1} as functions of n_{i1} and n_{n1} and then integrating f_{i1} and f_{n1} over velocity space, we find the equations

$$\begin{pmatrix} A_{ii} & A_{in} \\ A_{ni} & A_{nn} \end{pmatrix} \begin{pmatrix} n_{i1} \\ n_{n1} \end{pmatrix} = \begin{pmatrix} 0 \\ 0 \end{pmatrix}, \tag{4.7}$$

where the elements of the matrix are

$$A_{ii} = 1 + \frac{T_e}{T_h} + \frac{n_i}{n_i+n_n}\frac{T_e}{T_h}\zeta Z(\zeta) + \frac{n_n}{n_i+n_n}\left[\left(1+\frac{T_e}{T_h}\right)\zeta_{in} - \zeta\right] Z(\zeta_{in}) \tag{4.8}$$

$$A_{in} = -\frac{n_i}{n_i+n_n}(\zeta_{in} - \zeta)Z(\zeta_{in}) \tag{4.9}$$

$$A_{ni} = -\frac{n_n}{n_i+n_n}\left\{\left[\left(1+\frac{T_e}{T_h}\right)\zeta_{in} - \zeta\right] Z(\zeta_{in}) - \frac{T_e}{T_h}\zeta Z(\zeta)\right\} \tag{4.10}$$

and

$$A_{nn} = 1 + \frac{n_i}{n_i+n_n}(\zeta_{in} - \zeta)Z(\zeta_{in}). \tag{4.11}$$

Here, we have defined

$$\zeta := \frac{\omega}{|k_\parallel|v_{th}}, \quad \zeta_{in} := \frac{\omega + \mathrm{i}(n_i+n_n)R_{in}}{|k_\parallel|v_{th}}, \tag{4.12}$$

with $v_{th} := \sqrt{2T_h/m_i}$, and we have used the plasma dispersion function (Fried & Conte

1961)

$$Z(\zeta) := \exp(-\zeta^2)\left(\mathrm{i}\sqrt{\pi} - 2\int_0^{\zeta} \exp(y^2)\,\mathrm{d}y\right). \tag{4.13}$$

By setting the determinant of the matrix in equation (4.7) to zero, we can calculate the frequency ω of the modes for an initial $k_\parallel$.

We show two different types of solutions to the dispersion relation in figure 1: acoustic waves that have both real frequency $\omega_r := \mathrm{Re}(\omega)$ and damping rate $\gamma := \mathrm{Im}(\omega)$, and non-propagating modes with $\omega_r = 0$. In the figure, we plot the real frequency and damping rate for the acoustic waves as solid lines, whereas for the non-propagating modes, we only plot the damping rates as dashed lines. We can use these solutions to benchmark the implementation of the equations in our code.

5. Conclusions

We have identified the first set of equations that we will use to test a new approach to drift kinetics that extracts the low order moments from the distribution function. The chosen model can be integrated without employing implicit time-stepping methods. This is a choice that we have made to ensure that we can compare the new model with the well-established drift kinetic model.

We have also developed an analytical benchmark for the equations. The calculation ignores ion-ion collisions and it is hence not relevant to all edge operational regimes, but it allows us to test the implementation of the equations with and without collisions. Similar calculations can be performed including the full ion-ion collision operator and model collision operators.

REFERENCES

Braginskii, S.I. 1958 Transport phenomena in a completely ionized two-temperature plasma. *Sov. Phys. JETP.* **6**, 358.

Catto, P.J. 1994 A short mean-free path, coupled neutral-ion transport description of a tokamak edge plasma. *Phys. Plasmas* **1**, 1936.

Connor, J.W. 1977 An analytic solution for the distribution function of neutral particles in a Maxwellian plasma using the method of singular eignfunctions. *Plasma Phys.* **19**, 853.

Fried, B.D. & Conte, S.D. 1961 *The Plasma Dispersion Function: The Hilbert transform of the Gaussian*. Academic Press.

Hazeltine, R.D. 1973 Recursive derivation of drift-kinetic equation. *Plasma Phys.* **15**, 77–80.

Hazeltine, R.D., Calvin, M.D., Valanju, P.M. & Solano, E.R. 1992 Analytical calculation of neutral transport and its effect on ions. *Nucl. Fusion* **32**, 3.

Rosenbluth, M.N., MacDonald, W.M. & Judd, D.L. 1957 Fokker-Planck Equation for an Inverse-Square Force. *Phys. Rev.* **107**, 1.

Appendix A. The Maxwell-Boltzmann response

The Maxwell-Boltzmann response in equation (2.13) is the solution to electron drift kinetic equation (2.4) in the limit $\sqrt{m_e/m_i} \ll 1$. The expansion in the mass ratio is based on the fact that the species within the plasma tend to thermalize due to collisions, and hence the different species have in general similar average kinetic energies. Thus, the characteristic thermal speeds of the ions and neutrals, v_{ti} and v_{tn}, scale as $m_i^{-1/2}$, whereas the electron thermal speed scales as $m_e^{-1/2}$, giving $v_{te} \gg v_{ti} \sim v_{tn}$.

We assume that the massive ions and neutrals control the dynamics of interest, giving

the estimate

$$\frac{\partial}{\partial t} \sim \frac{v_{ti}}{L}. \tag{A 1}$$

Thus, the time derivative in equation (2.4) is negligible compared to terms like

$$v_\parallel \frac{\partial f_e}{\partial z} \sim f_e \frac{v_{te}}{L}. \tag{A 2}$$

Hence, we can neglect the time derivative to find

$$v_\parallel \frac{\partial f_e}{\partial z} + \frac{e}{m_e}\frac{\partial \phi}{\partial z}\frac{\partial f_e}{\partial v_\parallel} = C_{ee}[f_e] + C_{ei}[f_e, f_i] + C_{en}[f_e, f_n]. \tag{A 3}$$

To solve this equation, we need to use the properties of the collision operators. The electron-electron collision operator satisfies an H-theorem: the entropy production

$$-\int \ln f_e \, C_{ee}[f_e] \, \mathrm{d}^3 v \geqslant 0 \tag{A 4}$$

is always positive and it only vanishes if f_e is a Maxwellian. The elastic collision operators $C_{ei}[f_e, f_i]$ and $C_{en}[f_e, f_n]$ also satisfy H-theorems, but they are much more complicated as in general these theorems involve the ions and the neutrals. Luckily, if we perform the expansion $\sqrt{m_e/m_i} \ll 1$, $C_{ei}[f_e, f_i]$ and $C_{en}[f_e, f_n]$ satisfy simplified versions of their H-theorems, namely, the entropy productions

$$-\int \ln f_e \, C_{ei}[f_e, f_i] \, \mathrm{d}^3 v \geqslant 0 \text{ and } -\int \ln f_e \, C_{en}[f_e, f_n] \, \mathrm{d}^3 v \geqslant 0 \tag{A 5}$$

are always positive, and they only vanish if f_e is isotropic. Note that, in the limit $\sqrt{m_e/m_i} \ll 1$, these operators do not impose conditions on f_i or f_n.

Armed with these properties, we multiply equation (A 3) by $-\ln f_e$ and we integrate over velocity space to obtain

$$\begin{aligned}\frac{\partial}{\partial z}\left[-\int (f_e \ln f_e - f_e)\, v_\parallel \, \mathrm{d}^3 v\right] = &-\int \ln f_e \, C_{ee}[f_e] \, \mathrm{d}^3 v - \int \ln f_e \, C_{ei}[f_e, f_i] \, \mathrm{d}^3 v \\ &- \int \ln f_e \, C_{en}[f_e, f_n] \, \mathrm{d}^3 v.\end{aligned} \tag{A 6}$$

Integrating this equation over z and using the periodic boundary conditions, we finally obtain

$$\begin{aligned}0 = &-\int_0^L \mathrm{d}z \int \ln f_e \, C_{ee}[f_e] \, \mathrm{d}^3 v - \int_0^L \mathrm{d}z \int \ln f_e \, C_{ei}[f_e, f_i] \, \mathrm{d}^3 v \\ &- \int_0^L \mathrm{d}z \int \ln f_e \, C_{en}[f_e, f_n] \, \mathrm{d}^3 v.\end{aligned} \tag{A 7}$$

Since the entropy production of each collision operator is always positive, this equation can only be satisfied if each of the entropy productions vanish at every z. This implies that, at every z, f_e is Maxwellian and isotropic,

$$f_e(z, v_\parallel, v_\perp) = f_{Me}(z, v_\parallel, v_\perp, t) := n_e(z,t)\left(\frac{m_e}{2\pi T_e(z,t)}\right)^{3/2} \exp\left(-\frac{m_e(v_\parallel^2 + v_\perp^2)}{2T_e(z,t)}\right). \tag{A 8}$$

We need to determine the dependence of $n_e(z,t)$ and $T_e(z,t)$ on z. Substituting the

solution $f_{Me}(z, v_\parallel, v_\perp, t)$ on equation (A 3), we find

$$\left[v_\parallel \left(\frac{\partial}{\partial z} \ln n_e - \frac{e}{T_e} \frac{\partial \phi}{\partial z} \right) + v_\parallel \left(\frac{m_e(v_\parallel^2 + v_\perp^2)}{2T_e} - \frac{3}{2} \right) \frac{\partial}{\partial z} \ln T_e \right] f_{Me} = 0. \tag{A 9}$$

Since this equation has to be satisfied for every value of $v_\parallel$ and $v_\perp$, $T_e(t)$ cannot depend on z, and $n_e(z,t) = N_e(t) \exp(e\phi(z,t)/T_e(t))$. Thus, we find equation (2.13) with N_e and T_e being in general functions of t. For simplicity, we choose them to be constants.

1D drift kinetic models with wall boundary conditions

Felix I. Parra, Michael Barnes and Michael Hardman

Rudolf Peierls Centre for Theoretical Physics, University of Oxford, Oxford OX1 3PU, UK

(This version is of 27 August 2021)

1. Introduction

In previous reports, we proposed 1D drift kinetic equations with periodic boundary conditions, adequate for the closed field line region of the edge. In this report, we discuss a minimal 1D drift kinetic model with wall boundary conditions that represents open field lines. The basic drift kinetic model is presented in section 2, and the wall boundary conditions are discussed in section 3. We then proceed to determine the novel moment drift kinetic equations for ions and neutrals in section 4, and for electrons in section 5. The electrons have to be treated differently so that we can exploit the expansion in the electron-ion mass ratio. We finish with a discussion in section 6. Some of the details of the collision operators in the moment drift kinetic formulation are relegated to appendices to make the main text easier to read.

2. 1D electrostatic drift kinetics

We consider a plasma with one ion species with charge e and mass m_i, electrons with charge $-e$ and mass m_e, and one species of neutrals with mass

$$m_n = m_i. \tag{2.1}$$

The plasma is magnetized by a constant magnetic field $\mathbf{B} = B\hat{\mathbf{z}}$, and we assume that the plasma only varies along magnetic field lines. In this case, the electric field produced by the plasma is electrostatic, $\mathbf{E} = -(\partial\phi/\partial z)\hat{\mathbf{z}}$. The potential $\phi(z,t)$ depends on the position along magnetic field lines z and on time t.

If we assume that the gyroradii are small compared to the length scales of interest, and that the gyrofrequencies are much larger than the frequencies that we want to model (Hazeltine 1973), the distribution functions $f_s(z, v_\parallel, v_\perp, t)$ of the different species $s = i, e, n$ only depend on the component of the velocity parallel to the magnetic field $v_\parallel$ and the magnitude of the velocity perpendicular to the magnetic field $v_\perp$, and are independent of the direction of the velocity perpendicular to the magnetic field. Thus, the distribution functions that in general can depend on three spatial variables $\mathbf{r}$, three components of the velocity $\mathbf{v}$ and the time t depend only on z, $v_\parallel$, $v_\perp$ and t,

$$f_s(\mathbf{r}, \mathbf{v}, t) = f_s(z, v_\parallel, v_\perp, t). \tag{2.2}$$

The equations for the distribution functions of the different species are

$$\frac{\partial f_i}{\partial t} + v_\parallel \frac{\partial f_i}{\partial z} - \frac{e}{m_i}\frac{\partial \phi}{\partial z}\frac{\partial f_i}{\partial v_\parallel} = C_{ii}[f_i] + C_{in}[f_i, f_n] + C_{i,\mathrm{ion}}[f_e, f_n] + C_{ie}[f_i, f_e] + S_i, \tag{2.3}$$

$$\frac{\partial f_e}{\partial t}+v_\parallel\frac{\partial f_e}{\partial z}+\frac{e}{m_e}\frac{\partial\phi}{\partial z}\frac{\partial f_e}{\partial v_\parallel}=C_{ee}[f_e]+C_{ei}[f_e,f_i]\left[1+O\left(\frac{m_e}{m_i}\right)\right]$$
$$+C_{en}[f_e,f_n]\left[1+O\left(\frac{m_e}{m_i}\right)\right]+C_{e,\mathrm{ion}}[f_e,f_n]+S_e \tag{2.4}$$

and

$$\frac{\partial f_n}{\partial t}+v_\parallel\frac{\partial f_n}{\partial z}=C_{ni}[f_n,f_i]+C_{ne}[f_n,f_e]+C_{n,\mathrm{ion}}[f_n,f_e]+S_n. \tag{2.5}$$

The sources $S_s(z,w_\parallel,w_\perp,t)$ with $s=i,e,n$ represent heating, fueling and the effect of transport perpendicular to the magnetic field line.

We have included the following collisions.

• Ion-ion and electron-electron collisions are modeled by the Fokker-Planck collision operators $C_{ii}[f_i]$ and $C_{ee}[f_e]$ (Rosenbluth *et al.* 1957),

$$C_{ss}[f_s]:=\frac{2\pi e^4\ln\Lambda}{(4\pi\epsilon_0)^2m_s^2}\nabla_v\cdot\left(\mathbf{D}[f_s]\cdot\nabla_v f_s+\mathbf{P}[f_s]f_s\right), \tag{2.6}$$

where the matrix $\mathbf{D}$ is

$$\mathbf{D}[f_s]:=\int\frac{|\mathbf{v}-\mathbf{v}'|^2\mathbf{I}-(\mathbf{v}-\mathbf{v}')(\mathbf{v}-\mathbf{v}')}{|\mathbf{v}-\mathbf{v}'|^3}f_s(\mathbf{v}')\,\mathrm{d}^3v' \tag{2.7}$$

and the vector $\mathbf{P}$ is

$$\mathbf{P}[f_s]:=-2\int\frac{\mathbf{v}-\mathbf{v}'}{|\mathbf{v}-\mathbf{v}'|^3}f_s(\mathbf{v}')\,\mathrm{d}^3v'. \tag{2.8}$$

Here, $\mathbf{I}$ is the 3D unit matrix, ϵ_0 the vacuum permittivity and $\ln\Lambda\approx 15$ the Coulomb logarithm.

• The effect of electron-ion and elastic electron-neutral collisions on the electron distribution function can be simplified in the limit of small electron-ion mass ratio, $m_e/m_i\ll 1$. With this expansion, we find the simplified Fokker-Planck collision operator

$$C_{ei}[f_e,f_i]:=\frac{2\pi e^4n_i\ln\Lambda}{(4\pi\epsilon_0)^2m_e^2}\nabla_v\cdot\left[\frac{|\mathbf{v}-\mathbf{u}_i|^2\mathbf{I}-(\mathbf{v}-\mathbf{u}_i)(\mathbf{v}-\mathbf{u}_i)}{|\mathbf{v}-\mathbf{u}_i|^3}\cdot\nabla_v f_e\right] \tag{2.9}$$

for electron-ion collisions (Braginskii 1958), and the simplified Boltzmann collision operator

$$C_{en}[f_e,f_n]:=\frac{n_n}{4\pi}\int_0^\pi\mathrm{d}\chi\int_0^{2\pi}\mathrm{d}\varphi\,\sin\chi R_{en}(|\mathbf{v}-\mathbf{u}_n|,\chi)\left[f_e(\overline{\mathbf{v}}(\mathbf{v},\chi,\varphi,\mathbf{u}_n))-f_e(\mathbf{v})\right] \tag{2.10}$$

for electron-neutral collisions. Here

$$n_s(z,t):=2\pi\int_{-\infty}^{\infty}\mathrm{d}v_\parallel\int_0^\infty\mathrm{d}v_\perp\,v_\perp f_s(z,v_\parallel,v_\perp,t). \tag{2.11}$$

is the density of species s, $\mathbf{u}_s:=n_s^{-1}\int\mathbf{v}f_s\,\mathrm{d}^3v$ is the average velocity of species s,

$$\overline{\mathbf{v}}(\mathbf{v},\chi,\varphi,\mathbf{u}_n):=\mathbf{u}_n+\cos\chi(\mathbf{v}-\mathbf{u}_n)+|\mathbf{v}-\mathbf{u}_n|\sin\chi(\cos\varphi\,\hat{\mathbf{e}}_1+\sin\varphi\,\hat{\mathbf{e}}_2) \tag{2.12}$$

is a rotation of the vector $\mathbf{v}$ centered around $\mathbf{u}_n$, $R_{en}(|\mathbf{v}-\mathbf{u}_n|,\chi)$ is a function determined by the physics of the electron-neutral collisions, and the unit vectors $\hat{\mathbf{e}}_1$ and $\hat{\mathbf{e}}_2$ are chosen to form an orthonormal basis with the vector $(\mathbf{v}-\mathbf{u}_n)/|\mathbf{v}-\mathbf{u}_n|$. In equation (2.4), we have indicated that both C_{ei} and C_{en} are missing pieces small in m_e/m_i. These pieces can become important because they represent collisional energy exchange and collisional heating, but they are cumbersome. The moment method that we propose in

this document will allow us to keep these important effects even with the simplified collision operators (2.9) and (2.10).

• The expansion in electron-ion mass ratio also implies electron-ion collisions and electron-neutral collisions have a very small effect on f_i and f_n – the terms C_{ie} and C_{ne} in equations (2.3) and (2.5) are small compared with C_{ii} and C_{ni} by a factor of $\sqrt{m_e/m_i} \ll 1$,

$$C_{ie} \sim \sqrt{\frac{m_e}{m_i}} C_{ii}, \quad C_{ne} \sim \sqrt{\frac{m_e}{m_i}} C_{ni}. \tag{2.13}$$

Like the mass ratio corrections to C_{ei} and C_{en}, these terms can become important because they contain the collisional energy exchange between electrons and the heavier species. We will keep these effects in a simplified form in our moment formulation.

• Charge-exchange collisions are represented by the simplified Boltzmann collision operators

$$C_{in}[f_i, f_n] := -\int R_{in}(|\mathbf{v} - \mathbf{v}'|) \left[f_i(\mathbf{v}) f_n(\mathbf{v}') - f_i(\mathbf{v}') f_n(\mathbf{v}) \right] \mathrm{d}^3 v' \tag{2.14}$$

and

$$C_{ni}[f_n, f_i] := -\int R_{in}(|\mathbf{v} - \mathbf{v}'|) \left[f_n(\mathbf{v}) f_i(\mathbf{v}') - f_n(\mathbf{v}') f_i(\mathbf{v}) \right] \mathrm{d}^3 v'. \tag{2.15}$$

• To model ionization, we use the collision operators

$$C_{i,\mathrm{ion}}[f_e, f_n] := f_n \int R_{\mathrm{ion}}(v') f_e(\mathbf{v}') \, \mathrm{d}^3 v' \tag{2.16}$$

and

$$C_{n,\mathrm{ion}}[f_e, f_n] := -f_n \int R_{\mathrm{ion}}(v') f_e(\mathbf{v}') \, \mathrm{d}^3 v'. \tag{2.17}$$

We also need to include a collision operator $C_{e,\mathrm{ion}}$ in the electron equation to model the increase in the number of electrons and the energy loss due to ionization. This operator is complicated because it involves three particles (the resulting ion and two electrons), but we will be able to avoid giving it a definite form. Instead, we will use the expansion in $m_e/m_i \ll 1$ and the fact that

$$C_{e,\mathrm{ion}}[f_e, f_n] \sim n_n R_{\mathrm{ion}} f_e. \tag{2.18}$$

• We have neglected neutral-neutral collisions because, in current fusion devices, the neutral density is sufficiently small that the neutral-neutral collisions are rare. It is possible that the higher densities expected in fusion reactors will make neutral-neutral collisions more relevant. To include neutral-neutral collisions, a Boltzmann collision operator is in principle required, but using a simplified collision may be possible if the exact shape of the neutral distribution function is not important for the physics of interest.

To simplify our equations, we assume that the functions R_{en}, R_{in} and R_{ion} are constant (Connor 1977; Hazeltine *et al.* 1992; Catto 1994), finding

$$C_{en}[f_e, f_n] = n_n R_{en} \left[\frac{1}{2} \int_0^\pi f_e(z, u_{n\parallel} + |\mathbf{v} - \mathbf{u}_n| \cos\chi, |\mathbf{v} - \mathbf{u}_n| \sin\chi, t) \sin\chi \, \mathrm{d}\chi \right.$$
$$\left. - f_e(z, v_\parallel, v_\perp, t) \right], \tag{2.19}$$

with $|\mathbf{v}-\mathbf{u}_n| = \sqrt{(v_\parallel - u_{n\parallel})^2 + v_\perp^2}$,

$$C_{in}[f_i, f_n] = -R_{in}\left(n_n f_i - n_i f_n\right), \tag{2.20}$$

$$C_{ni}[f_n, f_i] = -R_{in}\left(n_i f_n - n_n f_i\right), \tag{2.21}$$

$$C_{i,\mathrm{ion}}[f_e, f_n] = f_n n_e R_{\mathrm{ion}} \tag{2.22}$$

and

$$C_{n,\mathrm{ion}}[f_e, f_n] = -f_n n_e R_{\mathrm{ion}}. \tag{2.23}$$

The potential $\phi(z,t)$ is determined by the quasineutrality equation

$$n_i = n_e. \tag{2.24}$$

To solve this equation, we need to treat the equations implicitly as the potential enters only via its effect on $\partial f_i/\partial t$ and $\partial f_e/\partial t$. The need to use implicit methods is one of the reasons why we are trying to extract some of the low order moments from the distribution function.

3. Wall boundary conditions

The kinetic equations will be solved in the interval $z \in [0, L]$, and we will impose wall boundary conditions at $z = 0$ and $z = L$. We assume the wall to be exactly perpendicular to the magnetic field lines to be able to impose a set of simplified boundary conditions: the logical sheath boundary conditions of Parker *et al.* (1993). When the magnetic field is at an angle to the wall, one needs to consider a thin boundary layer with a width of the order of the ion gyroradius that forms on the wall and is known as the magnetic presheath (Chodura 1982). The complicated boundary conditions that this layer imposes on drift kinetic models are an active area of research (Geraldini *et al.* 2017, 2018, 2019; Geraldini 2021). These works indicate that the magnetic presheath and the Debye sheath must be solved in conjunction with the quasineutral plasma, but this is not necessarily computationally expensive as the presheath and sheath models are 1D or at most 2D, and hence cheaper than the 5D drift kinetic models that one needs for edge turbulence. The technique proposed by Geraldini *et al.* (2018), for example, solves the magnetic presheath in a single processor in seconds, and this technique can be parallelized.

Logical sheath boundary conditions make use of the fact that a thin sheath of non-neutral plasma with a width of the order of the Debye length forms on walls to ensure quasineutrality. The potential drop across this sheath repels electrons away from the wall because otherwise electrons would flow to the wall at much greater rate than ions due to their lower mass and higher thermal speed. In our model, $\phi(0,t)$ and $\phi(L,t)$ are not the potential of the wall, but the potential at the entrance of the sheath. In this report, we choose the potential of the wall at $z = 0$ to be 0 without loss of generality. We denote the potential of the wall at $z = L$ as ϕ_w. Then, for the sheaths to repel electrons, $\phi(0,t)$ must be larger than 0 and $\phi(L,t)$ must be larger than ϕ_w.

The value of the potential at $z = 0$ and $z = L$ is determined by requiring that the current towards the wall at both $z = 0$ and $z = L$ vanishes. We consider the sheath at $z = L$ first, and we will then apply the results that we obtain to the sheath at $z = 0$. Since the thin sheath at $z = L$ imposes a large electric field perpendicular to the wall, which in this case is along the magnetic field $\mathbf{B} = B\hat{\mathbf{z}}$, the sheath only modifies the parallel velocity of electrons. Within the sheath, the parallel energy $\mathcal{E}_\parallel := m_e v_\parallel^2/2 - e\phi$ is conserved, and as a result an electron that has velocity $v_\parallel$ at the entrance of the sheath

is slowed down to a parallel velocity $\sqrt{v_\parallel^2 - 2e(\phi(L,t)-\phi_w)/m_e}$ when it reaches the wall. Thus, electrons with parallel velocity larger than $\sqrt{2e(\phi(L,t)-\phi_w)/m_e}$ reach the wall, where they recombine with ions, whereas electrons with parallel velocity smaller than $\sqrt{2e(\phi(L,t)-\phi_w)/m_e}$ are repelled back into the quasineutral plasma. Thus, the boundary condition on the electron distribution function at $z = L$ is

$$f_e(L, v_\parallel < 0, v_\perp, t) = \begin{cases} f_e(L, -v_\parallel, v_\perp, t) & \text{for } v_\parallel \geqslant -\sqrt{2e(\phi(L,t)-\phi_w)/m_e}, \\ 0 & \text{for } v_\parallel < -\sqrt{2e(\phi(L,t)-\phi_w)/m_e}, \end{cases} \tag{3.1}$$

i.e. the electron distribution is mirrored with respect to $v_\parallel = 0$ and a cut-off is imposed for sufficiently negative parallel velocities. Note that no boundary condition is needed for $v_\parallel > 0$ at $z = L$ because of the direction of the characteristics of the kinetic equation. Expression (3.1) also gives the electron current density towards the wall at the entrance of the sheath at $z = L$,

$$J_{e\parallel}(L,t) = -2\pi e \int_{\sqrt{2e(\phi(L,t)-\phi_w)/m_e}}^{\infty} \mathrm{d}v_\parallel \int_0^\infty \mathrm{d}v_\perp \, v_\perp v_\parallel f_e(L, v_\parallel, v_\perp, t). \tag{3.2}$$

This is the electron current density at the wall because electron flow is conserved across the sheath. Imposing that the electron current cancels the ion current gives us a nonlinear equation for the potential difference $\phi(L,t) - \phi_w$,

$$\begin{aligned} 2\pi \int_{\sqrt{2e(\phi(L,t)-\phi_w)/m_e}}^{\infty} \mathrm{d}v_\parallel \int_0^\infty \mathrm{d}v_\perp \, v_\perp v_\parallel f_e(L, v_\parallel, v_\perp, t) \\ = 2\pi \int_0^\infty \mathrm{d}v_\parallel \int_0^\infty \mathrm{d}v_\perp \, v_\perp v_\parallel f_i(L, v_\parallel, v_\perp, t). \end{aligned} \tag{3.3}$$

To obtain the ion current, we have used the fact that the sheath attracts ions and hence no ions can have negative parallel velocity at the entrance of the sheath at $z = L$.

The conditions at $z = 0$ for the electron distribution and the potential are similar to those for $z = L$. For the electron distribution function, we find

$$f_e(0, v_\parallel > 0, v_\perp, t) = \begin{cases} f_e(0, -v_\parallel, v_\perp, t) & \text{for } v_\parallel \leqslant \sqrt{2e\phi(0,t)/m_e}, \\ 0 & \text{for } v_\parallel > \sqrt{2e\phi(0,t)/m_e}, \end{cases} \tag{3.4}$$

and for the potential we obtain

$$\begin{aligned} 2\pi \int_{-\infty}^{-\sqrt{2e\phi(0,t)/m_e}} \mathrm{d}v_\parallel \int_0^\infty \mathrm{d}v_\perp \, v_\perp v_\parallel f_e(0, v_\parallel, v_\perp, t) \\ = 2\pi \int_{-\infty}^{0} \mathrm{d}v_\parallel \int_0^\infty \mathrm{d}v_\perp \, v_\perp v_\parallel f_i(0, v_\parallel, v_\perp, t), \end{aligned} \tag{3.5}$$

Note that conditions (3.3) and (3.5) imply that no net electrical current is leaving the system. Thus, the total source of charge in the magnetic field line of interest must be zero,

$$\int_0^L \mathrm{d}z \int S_i \, \mathrm{d}^3 v = \int_0^L \mathrm{d}z \int S_e \, \mathrm{d}^3 v. \tag{3.6}$$

We still need boundary conditions for the ion and neutral distribution functions. Ions recombine when they hit the wall, so no ions come back, giving

$$f_i(0, v_\parallel > 0, v_\perp, t) = 0, \quad f_i(L, v_\parallel < 0, v_\perp, t) = 0. \tag{3.7}$$

The neutrals hit the wall and thermalize at the temperature of the wall T_w, while also

receiving back the ions that have recombined at the wall,

$$f_n(0, v_\parallel > 0, v_\perp, t) = \Gamma_0 f_{Kw}(v_\parallel, v_\perp), \quad f_n(L, v_\parallel < 0, v_\perp, t) = \Gamma_L f_{Kw}(v_\parallel, v_\perp), \tag{3.8}$$

where

$$\Gamma_0 := \sum_{s=i,n} 2\pi \int_{-\infty}^{0} \mathrm{d}v_\parallel \int_0^\infty \mathrm{d}v_\perp \, v_\perp |v_\parallel| f_s(0, v_\parallel, v_\perp, t) \tag{3.9}$$

and

$$\Gamma_L := \sum_{s=i,n} 2\pi \int_{0}^{\infty} \mathrm{d}v_\parallel \int_0^\infty \mathrm{d}v_\perp \, v_\perp v_\parallel f_s(L, v_\parallel, v_\perp, t) \tag{3.10}$$

are the fluxes of neutrals and ions towards the walls at $z = 0$ and $z = L$. Here,

$$f_{Kw}(v_\parallel, v_\perp) := \frac{3}{4\pi} \left(\frac{m_i}{T_w}\right)^2 \frac{|v_\parallel|}{\sqrt{v_\parallel^2 + v_\perp^2}} \exp\left(-\frac{m_i(v_\parallel^2 + v_\perp^2)}{2T_w}\right) \tag{3.11}$$

is the Knudsen cosine distribution (Knudsen 1916) that assumes that the particles have entered the wall lattice, have reached thermodynamic equilibrium with it, and have then left the wall. Knudsen showed that this distribution function fits experimental measurements well.

4. 1D moment drift kinetics for ions and neutrals

Instead of solving for $f_s(z, v_\parallel, v_\perp, t)$ with $s = i, n$, we solve for

$$F_s(z, w_\parallel, w_\perp, t) := \frac{v_{ts}^3(z,t)}{n_s(z,t)} f_s\Big(z, u_{s\parallel}(z,t) + v_{ts}(z,t)w_\parallel, v_{ts}(z,t)w_\perp, t\Big), \tag{4.1}$$

where we have defined the normalized velocities

$$w_\parallel(z, v_\parallel, t) := \frac{v_\parallel - u_{s\parallel}(z,t)}{v_{ts}(z,t)} \tag{4.2}$$

and

$$w_\perp(z, v_\perp, t) := \frac{v_\perp}{v_{ts}(z,t)}, \tag{4.3}$$

the average parallel velocity

$$u_{s\parallel}(z,t) := \frac{2\pi}{n_s} \int_{-\infty}^{\infty} \mathrm{d}v_\parallel \int_0^\infty \mathrm{d}v_\perp \, v_\perp v_\parallel f_s(z, v_\parallel, v_\perp, t) \tag{4.4}$$

and the thermal speed

$$v_{ts}(z,t) := \sqrt{\frac{2T_s(z,t)}{m_s}}, \tag{4.5}$$

with

$$T_s(z,t) := \frac{2\pi}{n_s} \int_{-\infty}^{\infty} \mathrm{d}v_\parallel \int_0^\infty \mathrm{d}v_\perp \, v_\perp \frac{m_s[(v_\parallel - u_{s\parallel}(z,t))^2 + v_\perp^2]}{3} f_s(z, v_\parallel, v_\perp, t) \tag{4.6}$$

the temperature of species s. According to its definition, $F_s(z, w_\parallel, w_\perp, t)$ must satisfy the conditions

$$2\pi \int_{-\infty}^{\infty} \mathrm{d}w_\parallel \int_0^\infty \mathrm{d}w_\perp \, w_\perp F_s(z, w_\parallel, w_\perp, t) = 1, \tag{4.7}$$

$$2\pi \int_{-\infty}^{\infty} \mathrm{d}w_\parallel \int_0^{\infty} \mathrm{d}w_\perp \, w_\perp w_\parallel F_s(z, w_\parallel, w_\perp, t) = 0 \tag{4.8}$$

and

$$2\pi \int_{-\infty}^{\infty} \mathrm{d}w_\parallel \int_0^{\infty} \mathrm{d}w_\perp \, w_\perp (w_\parallel^2 + w_\perp^2) F_s(z, w_\parallel, w_\perp, t) = \frac{3}{2} \tag{4.9}$$

at every point z and time t.

4.1. *Ion equations*

The equations for n_i, $u_{i\parallel}$ and T_i are

$$\frac{\partial n_i}{\partial t} + \frac{\partial}{\partial z}\left(n_i u_{i\parallel}\right) = n_n n_e R_{\mathrm{ion}} + \int S_i \, \mathrm{d}^3 v, \tag{4.10}$$

$$n_i m_i \left(\frac{\partial u_{i\parallel}}{\partial t} + u_{i\parallel}\frac{\partial u_{i\parallel}}{\partial z}\right) = -\frac{\partial p_{i\parallel}}{\partial z} - e n_i \frac{\partial \phi}{\partial z} + n_i m_i (n_n R_{in} + n_e R_{\mathrm{ion}})(u_{n\parallel} - u_{i\parallel}) + \int m_i (v_\parallel - u_{i\parallel}) S_i \, \mathrm{d}^3 v \tag{4.11}$$

and

$$\frac{3}{2} n_i \left(\frac{\partial T_i}{\partial t} + u_{i\parallel}\frac{\partial T_i}{\partial z}\right) = -\frac{\partial q_{i\parallel}}{\partial z} - p_{i\parallel}\frac{\partial u_{i\parallel}}{\partial z} + \frac{3}{2} n_i (n_n R_{in} + n_e R_{\mathrm{ion}})(T_n - T_i) + \frac{1}{2} n_i m_i (n_n R_{in} + n_e R_{\mathrm{ion}})(u_{n\parallel} - u_{i\parallel})^2 + \int \frac{1}{2} m_i |\mathbf{v} - u_{i\parallel}\hat{\mathbf{z}}|^2 C_{ie} \, \mathrm{d}^3 v + \int \left(\frac{1}{2} m_i |\mathbf{v} - u_{i\parallel}\hat{\mathbf{z}}|^2 - \frac{3}{2} T_i\right) S_i \, \mathrm{d}^3 v. \tag{4.12}$$

Here, we have defined the parallel pressure

$$p_{s\parallel}[F_s, n_s, v_{ts}](z,t) := 2\pi n_s m_s v_{ts}^2 \int_{-\infty}^{\infty} \mathrm{d}w_\parallel \int_0^{\infty} \mathrm{d}w_\perp \, w_\perp w_\parallel^2 F_s(z, w_\parallel, w_\perp, t) \tag{4.13}$$

and the parallel heat flux

$$q_{s\parallel}[F_s, n_s, v_{ts}](z,t) := \pi n_s m_s v_{ts}^3 \int_{-\infty}^{\infty} \mathrm{d}w_\parallel \int_0^{\infty} \mathrm{d}w_\perp \, w_\perp w_\parallel (w_\parallel^2 + w_\perp^2) F_s(z, w_\parallel, w_\perp, t). \tag{4.14}$$

We have also included the term $(1/2)\int m_i |\mathbf{v} - u_{i\parallel}\hat{\mathbf{z}}|^2 C_{ie} \, \mathrm{d}^3 v$ due to collisions with electrons. Collisions with electrons are negligible to lowest order in $\sqrt{m_e/m_i}$ in the ion kinetic equation and thus cannot determine the lowest order distribution function F_i, but when collisions are sufficiently frequent that $\nu_{ii} L/v_{ti} \gtrsim \sqrt{m_i/m_e} \gg 1$, the term $(1/2)\int m_i |\mathbf{v} - u_{i\parallel}\hat{\mathbf{z}}|^2 C_{ie} \, \mathrm{d}^3 v$ becomes comparable to the other terms in the energy equation. Here,

$$\nu_{ii} := \frac{8\sqrt{2\pi}}{3} \frac{e^4 n_i \ln \Lambda}{(4\pi\epsilon_0)^2 m_i^2 v_{ti}^3} \tag{4.15}$$

is the ion-ion collision frequency as defined by Braginskii (Braginskii 1958). At the large collision frequencies required for the term $(1/2)\int m_i |\mathbf{v} - u_{i\parallel}\hat{\mathbf{z}}|^2 C_{ie} \, \mathrm{d}^3 v$ to be relevant, the ion and electron distribution functions become close to a Maxwellian,

$$f_s \simeq f_{Ms} := \frac{n_s}{\pi^{3/2} v_{ts}^3} \exp\left(-\frac{(v_\parallel - u_{s\parallel})^2 + v_\perp^2}{v_{ts}^2}\right). \tag{4.16}$$

Thus, we can use the approximation

$$\int \frac{1}{2} m_i |\mathbf{v} - u_{i\parallel}\hat{\mathbf{z}}|^2 C_{ie}[f_i, f_e]\,\mathrm{d}^3 v \simeq \int \frac{1}{2} m_i |\mathbf{v} - u_{i\parallel}\hat{\mathbf{z}}|^2 C_{ie}[f_{Mi}, f_{Me}]\,\mathrm{d}^3 v \simeq \frac{3 n_e m_e \nu_{ei}}{m_i}(T_e - T_i), \tag{4.17}$$

where

$$\nu_{ei} := \frac{16\sqrt{\pi}}{3} \frac{e^4 n_i \ln\Lambda}{(4\pi\epsilon_0)^2 m_e^2 v_{te}^3} \tag{4.18}$$

is the electron-ion collision frequency as defined by Braginskii (Braginskii 1958). Note that Braginskii's definitions of ν_{ii} and ν_{ei} differ by a factor of $\sqrt{2}$.

The ion kinetic equation is

$$\frac{\partial F_i}{\partial t} + \dot{z}_i \frac{\partial F_i}{\partial z} + \dot{w}_{\parallel i} \frac{\partial F_i}{\partial w_\parallel} + \dot{w}_{\perp i} \frac{\partial F_i}{\partial w_\perp} = \dot{F}_i + \mathcal{C}_{ii} + \mathcal{C}_{in} + \mathcal{C}_{i,\mathrm{ion}} + \mathcal{S}_i. \tag{4.19}$$

Here, we have defined the coefficients

$$\dot{z}_s[F_s, u_{s\parallel}, v_{ts}](z, w_\parallel, t) := u_{s\parallel} + v_{ts} w_\parallel, \tag{4.20}$$

$$\dot{w}_{\parallel s}[F_s, n_s, u_{s\parallel}, v_{ts}](z, w_\parallel, t) := \frac{1}{n_s m_s v_{ts}} \frac{\partial p_{s\parallel}}{\partial z} + \frac{2 w_\parallel}{3 n_s m_s v_{ts}^2} \left[\frac{\partial q_{s\parallel}}{\partial z} + \left(p_{s\parallel} - \frac{3}{2} n_s m_s v_{ts}^2 \right) \frac{\partial u_{s\parallel}}{\partial z} \right] - w_\parallel^2 \frac{\partial v_{ts}}{\partial z}, \tag{4.21}$$

$$\dot{w}_{\perp s}[F_s, n_s, u_{s\parallel}, v_{ts}](z, w_\parallel, w_\perp, t) := \frac{2 w_\perp}{3 n_s m_s v_{ts}^2} \left(\frac{\partial q_{s\parallel}}{\partial z} + p_{s\parallel} \frac{\partial u_{s\parallel}}{\partial z} \right) - w_\parallel w_\perp \frac{\partial v_{ts}}{\partial z} \tag{4.22}$$

and

$$\dot{F}_s[F_s, n_s, u_{s\parallel}, v_{ts}](z, w_\parallel, w_\perp, t) := \left[w_\parallel \left(3 \frac{\partial v_{ts}}{\partial z} - \frac{v_{ts}}{n_s} \frac{\partial n_s}{\partial z} \right) - \frac{2}{n_s m_s v_{ts}^2} \left(\frac{\partial q_{s\parallel}}{\partial z} + \left(p_{s\parallel} - \frac{1}{2} n_s m_s v_{ts}^2 \right) \frac{\partial u_{s\parallel}}{\partial z} \right) \right] F_s. \tag{4.23}$$

We have also defined a modified source $\mathcal{S}_i$ and several modified collision operators. The modified source is given by

$$\begin{aligned} &\mathcal{S}_s[S_s, F_s, n_s, u_{s\parallel}, v_{ts}](z, w_\parallel, w_\perp, t) \\ &:= -\left[\frac{F_s}{n_s} \int S_s\,\mathrm{d}^3 v - \frac{v_{ts}^3}{n_s} S_s(z, u_{s\parallel} + v_{ts} w_\parallel, v_{ts} w_\perp, t) \right] \\ &\quad + \frac{\partial}{\partial w_\parallel} \left[F_s \left(\frac{1}{n_s v_{ts}} \int (v_\parallel - u_{s\parallel}) S_s\,\mathrm{d}^3 v + \frac{w_\parallel}{3 n_s v_{ts}^2} \int \left(|\mathbf{v} - u_{s\parallel}\hat{\mathbf{z}}|^2 - \frac{3}{2} v_{ts}^2 \right) S_s\,\mathrm{d}^3 v \right) \right] \\ &\quad + \frac{1}{w_\perp} \frac{\partial}{\partial w_\perp} \left[\frac{w_\perp^2 F_s}{3 n_s v_{ts}^2} \int \left(|\mathbf{v} - u_{s\parallel}\hat{\mathbf{z}}|^2 - \frac{3}{2} v_{ts}^2 \right) S_s\,\mathrm{d}^3 v \right]. \end{aligned} \tag{4.24}$$

Note that the differential terms in this modified source could have been included in the definitions of the coefficients $\dot{w}_{\parallel i}$, $\dot{w}_{\perp i}$ and $\dot{F}_i$, but we have decided to make them part of a modified source instead to separate the effect of the source clearly. We will do the same for collisions. This split should not be taken as a suggestion on how to implement these terms in a code. The modified collisions operators are described in Appendix A.

4.2. *Neutral equations*

The fluid equations for the neutrals are

$$\frac{\partial n_n}{\partial t} + \frac{\partial}{\partial z}\left(n_n u_{n\parallel}\right) = -n_n n_e R_{\rm ion} + \int S_n \,\mathrm{d}^3 v, \tag{4.25}$$

$$n_n m_i \left(\frac{\partial u_{n\parallel}}{\partial t} + u_{n\parallel}\frac{\partial u_{n\parallel}}{\partial z}\right) = -\frac{\partial p_{n\parallel}}{\partial z} + n_n m_i n_i R_{in}(u_{i\parallel} - u_{n\parallel}) + \int m_i (v_\parallel - u_{n\parallel}) S_n \,\mathrm{d}^3 v \tag{4.26}$$

and

$$\frac{3}{2} n_n \left(\frac{\partial T_n}{\partial t} + u_{n\parallel}\frac{\partial T_n}{\partial z}\right) = -\frac{\partial q_{n\parallel}}{\partial z} - p_{n\parallel}\frac{\partial u_{n\parallel}}{\partial z} + \frac{3}{2} n_n n_i R_{in}(T_i - T_n) + \frac{1}{2} n_n m_i n_i R_{in}(u_{n\parallel} - u_{i\parallel})^2 + \int \frac{1}{2} m_i |\mathbf{v} - u_{n\parallel}\hat{\mathbf{z}}|^2 C_{ne} \,\mathrm{d}^3 v + \int \left(\frac{1}{2} m_i |\mathbf{v} - u_{n\parallel}\hat{\mathbf{z}}|^2 - \frac{3}{2} T_n\right) S_n \,\mathrm{d}^3 v. \tag{4.27}$$

As with electron-ion collisions, the term $(1/2)\int m_i |\mathbf{v} - u_{n\parallel}\hat{\mathbf{z}}|^2 C_{ne} \,\mathrm{d}^3 v$ only becomes important when the collisions are sufficiently frequent that the distribution functions are close to Maxwellians, giving

$$\int \frac{1}{2} m_i |\mathbf{v} - u_{n\parallel}\hat{\mathbf{z}}|^2 C_{ne}[f_n, f_e] \,\mathrm{d}^3 v \simeq \int \frac{1}{2} m_i |\mathbf{v} - u_{n\parallel}\hat{\mathbf{z}}|^2 C_{ne}[f_{Mn}, f_{Me}] \,\mathrm{d}^3 v \simeq \frac{3 n_e m_e n_n R_{en}}{m_i}(T_e - T_n), \tag{4.28}$$

The neutral kinetic equation is

$$\frac{\partial F_n}{\partial t} + \dot{z}_n \frac{\partial F_n}{\partial z} + \dot{w}_{\parallel n}\frac{\partial F_n}{\partial w_\parallel} + \dot{w}_{\perp n}\frac{\partial F_n}{\partial w_\perp} = \dot{F}_n + \mathcal{C}_{ni} + \mathcal{S}_n. \tag{4.29}$$

The modified charge exchange collision operator $\mathcal{C}_{ni}$ is described in Appendix B.

Equations (4.19) and (4.29) for F_i and F_n are constructed such that conditions (4.7), (4.8) and (4.9) are satisfied at all times if they are satisfied at $t = 0$. In practice, this property has to be enforced in the numerical method. We have found an algorithm that works well and we have discussed it in report 2047357-TN-04-02 M2.2.

4.3. *Boundary conditions*

These equations for ions and neutrals have to be solved with the boundary conditions in equations (3.7) and (3.8). For n_s, $u_{s\parallel}$, v_{ts} and F_s known at time t, we can construct f_s at $z = 0$ and $z = L$, and we can apply boundary conditions (3.7) and (3.8). We can then use the resulting f_s to obtain n_s, $u_{s\parallel}$, v_{ts} and F_s, and to calculate $p_{s\parallel}$ and $q_{s\parallel}$, closing the system of equations.

We note that this is the only place where the full distribution function f_s is needed. Depending on the numerical method chosen to solve these equations, reconstructing f_s could be expensive. This is one of the problems that needs to be addressed in the proxy apps.

5. 1D moment drift kinetics for electrons

The equation for F_e can be significantly simplified using the expansion in $\sqrt{m_e/m_i}$. The electron source S_e is usually of order

$$S_e \sim \frac{v_{ti} f_e}{L} \tag{5.1}$$

because the ions control the dynamics due to their large mass, and the electrons adapt to the ions because of collisions and quasineutrality. Thus, S_e is a small term in equation (2.4) by a factor of $v_{ti}/v_{te} \sim \sqrt{m_e/m_i} \ll 1$. Moreover, the electron parallel flow $u_{e\parallel}$ is of the order of the ion parallel flow because boundary conditions (3.3) and (3.5) impose that these two velocities be equal at $z = 0$ and $z = L$, and quasineutrality keeps the difference of the order of v_{ti}. As a result, $u_{e\parallel} \sim u_{i\parallel} \sim v_{ti} \ll v_{te}$ and we can neglect $u_{e\parallel}$ to lowest order in most terms in equation (2.4) – the two exceptions in which $u_{e\parallel}$ cannot be neglected are given in Appendix C. Finally, the effect of ionization, modeled by $C_{e,\mathrm{ion}} \sim n_n R_{\mathrm{ion}} f_e$ is, according to equation (4.10), of the order of $f_e v_{ti}/L$ and thus also small.

5.1. *Electron kinetic equation*

Employing the expansion in $\sqrt{m_e/m_i} \ll 1$, the kinetic equation for electrons becomes

$$\dot{z}_e \frac{\partial F_e}{\partial z} + \dot{w}_{\parallel e} \frac{\partial F_e}{\partial w_\parallel} + \dot{w}_{\perp e} \frac{\partial F_e}{\partial w_\perp} = \dot{F}_e + \mathcal{C}_{ee} + \mathcal{C}_{ei} + \mathcal{C}_{en}, \tag{5.2}$$

where

$$\dot{z}_e[F_e, v_{te}](z, w_\parallel, t) := v_{te} w_\parallel, \tag{5.3}$$

$$\dot{w}_{\parallel e}[F_e, u_{e\parallel}, v_{te}](z, w_\parallel, t) := \frac{1}{n_e m_e v_{te}} \frac{\partial p_{e\parallel}}{\partial z} + \frac{2 w_\parallel}{3 n_e m_e v_{te}^2} \frac{\partial q_{e\parallel}}{\partial z} - w_\parallel^2 \frac{\partial v_{te}}{\partial z}, \tag{5.4}$$

$$\dot{w}_{\perp e}[F_e, u_{e\parallel}, v_{te}](z, w_\parallel, w_\perp, t) := \frac{2 w_\perp}{3 n_e m_e v_{te}^2} \frac{\partial q_{e\parallel}}{\partial z} - w_\parallel w_\perp \frac{\partial v_{te}}{\partial z} \tag{5.5}$$

and

$$\dot{F}_e[F_e, u_{e\parallel}, v_{te}](z, w_\parallel, w_\perp, t) := \left[w_\parallel \left(3 \frac{\partial v_{te}}{\partial z} - \frac{v_{te}}{n_e} \frac{\partial n_e}{\partial z} \right) - \frac{2}{n_e m_e v_{te}^2} \frac{\partial q_{e\parallel}}{\partial z} \right] F_e. \tag{5.6}$$

The modified collision operators $\mathcal{C}_{ee}$, $\mathcal{C}_{ei}$ and $\mathcal{C}_{en}$ are described in Appendix C. Note that, in equations (C 1) and (C 6), we have kept small terms that scale with $(u_{s\parallel} - u_{e\parallel})/v_{te} \sim \sqrt{m_e/m_i} \ll 1$, where $s = i, n$. These terms are kept to ensure that we recover the Braginskii equations in the appropriate limit (see subsection 5.4).

We have ensured that equation (5.2) is compatible with conditions (4.7), (4.8) and (4.9) by keeping terms that are second order in $u_{e\parallel}$ in the collision operators in Appendix C. Indeed, multiplying equation (5.2) by 1, $w_\parallel$ and $w_\parallel^2 + w_\perp^2$ and integrating over velocities gives $0 = 0$. Despite the fact that we do not keep all possible terms that are second order in $\sqrt{m_e/m_i}$ in the collision operator, we will see in subsection 5.4 that proposed model recovers the regimes of interest.

Conditions (4.7), (4.8) and (4.9) have to be imposed on F_e when solving the kinetic equation (5.2). One possible way to impose these conditions is to include the term $\partial F_e/\partial t$ in equation (5.2) so that we can evolve F_e to a steady state solution. With this approach, if F_e satisfies conditions (4.7), (4.8) and (4.9) at $t = 0$, it will satisfy them at all times.

5.2. *Electron fluid equations*

Once we know F_e, we can calculate the fluid equations for electrons.

- The electron continuity equation is

$$\frac{\partial n_e}{\partial t} + \frac{\partial}{\partial z}\left(n_e u_{e\parallel}\right) = -n_e n_n R_{\rm ion} + \int S_e \,\mathrm{d}^3 v. \tag{5.7}$$

Subtracting this equation from equation (4.10) and using quasineutrality, we obtain the current conservation equation

$$\frac{\partial}{\partial z}\left[n_e\left(u_{i\parallel} - u_{e\parallel}\right)\right] = \int S_i \,\mathrm{d}^3 v - \int S_e \,\mathrm{d}^3 v. \tag{5.8}$$

This equation can be used to calculate $u_{e\parallel}$.

- The electron parallel momentum equation simplifies to

$$0 = -\frac{\partial p_{e\parallel}}{\partial z} + e n_e \frac{\partial \phi}{\partial z} + F_{ei\parallel} + n_e m_e n_n R_{en}(u_{n\parallel} - u_{e\parallel}), \tag{5.9}$$

where

$$\begin{aligned} &F_{ei\parallel}[F_e, n_e, n_i, u_{e\parallel}, u_{e\parallel}, v_{te}, v_{ti}](z,t) \\ &\quad := -\frac{8\pi^2 e^4 n_e n_i \ln\Lambda}{(4\pi\epsilon_0)^2 m_e v_{te}^2} \int_{-\infty}^{\infty} \mathrm{d}w_\parallel \int_0^{\infty} \mathrm{d}w_\perp \, \frac{w_\perp (w_\parallel - (u_{i\parallel} - u_{e\parallel})/v_{te}) F_e}{[(w_\parallel - (u_{i\parallel} - u_{e\parallel})/v_{te})^2 + w_\perp^2]^{3/2}} \end{aligned} \tag{5.10}$$

is the friction force between electrons and ions. Equation (5.9) can be used to calculate the potential ϕ. Since the potential at $\phi(0,t)$ is determined by equation (3.5), we can start integrating ϕ at $z = 0$. With the potential $\phi(L,t)$ that we obtain from this integration and condition (3.3), we can calculate the potential difference between the two walls, ϕ_w.

- The electron energy equation is

$$\begin{aligned} \frac{3}{2} n_e \left(\frac{\partial T_e}{\partial t} + u_{e\parallel}\frac{\partial T_e}{\partial z}\right) = &-\frac{\partial q_{e\parallel}}{\partial z} - p_{e\parallel}\frac{\partial u_{e\parallel}}{\partial z} + \int \frac{1}{2} m_e |\mathbf{v} - u_{e\parallel}\hat{\mathbf{z}}|^2 C_{e,\rm ion} \,\mathrm{d}^3 v \\ &+ \int \frac{1}{2} m_e |\mathbf{v} - u_{e\parallel}\hat{\mathbf{z}}|^2 C_{ei} \left[1 + O\left(\frac{m_e}{m_i}\right)\right] \mathrm{d}^3 v \\ &+ \int \frac{1}{2} m_e |\mathbf{v} - u_{e\parallel}\hat{\mathbf{z}}|^2 C_{en} \left[1 + O\left(\frac{m_e}{m_i}\right)\right] \mathrm{d}^3 v \\ &+ \int \left(\frac{1}{2} m_e |\mathbf{v} - u_{e\parallel}\hat{\mathbf{z}}|^2 - \frac{3}{2} T_e\right) S_e \,\mathrm{d}^3 v. \end{aligned} \tag{5.11}$$

For the integral over the ionization collision operator, we use the model

$$\int \frac{1}{2} m_e |\mathbf{v} - u_{e\parallel}\hat{\mathbf{z}}|^2 C_{e,\rm ion} \,\mathrm{d}^3 v = -n_e n_n R_{\rm ion} E_{\rm ion}, \tag{5.12}$$

where $E_{\rm ion}$ is the ionization energy cost that includes in it radiation from excited states. The integrals over C_{ei} and C_{en} are only sufficiently large when collisions are large. In this limit, all the species are Maxwellian and we can easily calculate the integrals over C_{ei} and C_{en} to higher order in the mass ratio expansion, finding

$$\begin{aligned} \int \frac{1}{2} m_e |\mathbf{v} - u_{e\parallel}\hat{\mathbf{z}}|^2 C_{ei}[f_e, f_i] \left[1 + O\left(\frac{m_e}{m_i}\right)\right] \mathrm{d}^3 v \simeq &\frac{3 n_e m_e \nu_{ei}}{m_i}(T_i - T_e) \\ &+ F_{ei\parallel}(u_{i\parallel} - u_{e\parallel}) \end{aligned} \tag{5.13}$$

and

$$\int \frac{1}{2} m_e |\mathbf{v} - u_{e\parallel}\hat{\mathbf{z}}|^2 C_{en}[f_e, f_n] \left[1 + O\left(\frac{m_e}{m_i}\right)\right] \mathrm{d}^3 v \simeq \frac{3 n_e m_e n_n R_{en}}{m_i}(T_n - T_e) + n_e m_e n_n R_{en}(u_{n\parallel} - u_{e\parallel})^2. \quad (5.14)$$

5.3. *Boundary conditions*

These equations for electrons have to be solved with the boundary conditions in equations (3.1) and (3.4). As for ions and neutrals, the best way to impose these boundary conditions is to transform back to f_e, apply the boundary conditions and then calculate F_e, n_e, m_e, v_{te}, $p_{e\parallel}$ and $q_{e\parallel}$ from f_e.

5.4. *Some limits of interest*

We finish by showing that these equations recover the desired result in the two limits of interest: a modified Braginskii limit with neutrals, and a collisionless limit.

5.4.1. *Braginskii-like equations*

For the Braginskii-like limit, we use the orderings suggested in (Catto 1994; Helander *et al.* 1994): we assume that the ion-ion, ion-neutral, electron-electron, electron-ion and electron-neutral collisions are so frequent that their collision frequencies $\nu_{ss'}$ satisfy

$$\frac{\nu_{ss'} L}{v_{ts}} \sim \sqrt{\frac{m_i}{m_e}} \gg 1, \quad (5.15)$$

whereas the ionization frequencies $n_e R_{\mathrm{ion}}$ and $n_n R_{\mathrm{ion}}$ are of order v_{ti}/L.

In this limit, the charge exchange collisional terms dominate in the ion and neutral momentum and energy equations, forcing $u_{i\parallel} = u_{n\parallel}$ and $T_i = T_n$. We use $u_{h\parallel}$ and T_h to denote the average flow and temperature of the heavy species. By summing the ion and neutral momentum equations (4.11) and (4.26), we find the equation for $u_{h\parallel}$,

$$(n_i + n_n) m_i \left(\frac{\partial u_{h\parallel}}{\partial t} + u_{h\parallel}\frac{\partial u_{h\parallel}}{\partial z}\right) = -\frac{\partial}{\partial z}(p_{i\parallel} + p_{n\parallel}) - e n_i \frac{\partial \phi}{\partial z} + \int m_i (v_\parallel - u_{h\parallel})(S_i + S_n)\, \mathrm{d}^3 v. \quad (5.16)$$

By summing the ion and neutral energy equations (4.12) and (4.27), we find the equation for T_h,

$$\frac{3}{2}(n_i + n_n)\left(\frac{\partial T_h}{\partial t} + u_{h\parallel}\frac{\partial T_h}{\partial z}\right) = -\frac{\partial}{\partial z}(q_{i\parallel} + q_{n\parallel}) - (p_{i\parallel} + p_{n\parallel})\frac{\partial u_{h\parallel}}{\partial z} + \frac{3 n_e m_e (\nu_{ei} + n_n R_{en})}{m_i}(T_e - T_h) + \int \left(\frac{1}{2} m_i |\mathbf{v} - u_{h\parallel}\hat{\mathbf{z}}|^2 - \frac{3}{2} T_h\right)(S_i + S_n)\, \mathrm{d}^3 v. \quad (5.17)$$

Note that in this energy equation, the terms due to electron-ion and electron-neutral collisions are of the same order as the other terms.

In the electron fluid equations, the collisional friction terms in the electron momentum equation (5.9) are comparable to the pressure and electric field terms. The electron heat flux term and the terms related to the electron-ion and electron-neutral collisions in the electron energy equation (5.11) are also comparable to the rest of the terms.

In the kinetic equations, the collisions dominate and lead to distribution functions that are Maxwellian to lowest order. We can use the kinetic equations to find the corrections

to the Maxwellian. For ions and neutrals, the corrections to the Maxwellian do not give large contributions to either the parallel pressure or the heat flux. For the electrons, however, the correction gives important contributions to the friction force in the momentum equation (5.9) and to the electron heat flux in the energy equation (5.11). If we write $F_e = F_M + F_{e1} + \ldots$, with $F_M := \pi^{-3/2}\exp(-w_\parallel^2 - w_\perp^2)$, we can find the equation for F_{e1} (Braginskii 1958),

$$\begin{aligned}\mathcal{C}_{ee}^{(\ell)}[F_{e1}] + \mathcal{C}_{ei}^{(\ell)}\left[F_{e1} - \frac{2(u_{h\parallel}-u_{e\parallel})w_\parallel}{v_{te}}F_M\right] + \mathcal{C}_{en}^{(\ell)}\left[F_{e1} - \frac{2(u_{h\parallel}-u_{e\parallel})w_\parallel}{v_{te}}F_M\right] \\ + \frac{16\pi^2 e^4 n_i \ln\Lambda}{(4\pi\epsilon_0)^2 m_e^2 v_{te}^3} w_\parallel F_M \int_{-\infty}^{\infty}\mathrm{d}w'_\parallel \int_0^\infty \mathrm{d}w'_\perp \frac{w'_\perp w'_\parallel F_{e1}(z,w'_\parallel,w'_\perp,t)}{(w'^2_\parallel + w'^2_\perp)^{3/2}} \\ = \left[v_{te}w_\parallel\left(w_\parallel^2 + w_\perp^2 - \frac{5}{2}\right)\frac{\partial}{\partial z}\ln T_e + \frac{32\sqrt{\pi}e^4 n_i \ln\Lambda (u_{h\parallel}-u_{e\parallel})w_\parallel}{3(4\pi\epsilon_0)^2 m_e^2 v_{te}^4}\right. \\ \left. + \frac{2n_n R_{en}(u_{h\parallel}-u_{e\parallel})w_\parallel}{v_{te}}\right]F_M. \quad (5.18)\end{aligned}$$

Here we have neglected the electron heat flux $q_{e\parallel}$ because it is proportional to F_{e1}. The collision operators $\mathcal{C}_{ee}^{(\ell)}$, $\mathcal{C}_{ei}^{(\ell)}$ and $\mathcal{C}_{en}^{(\ell)}$ are the linearized collision operators, given in Appendix D. Note that the terms proportional to $u_{h\parallel} - u_{e\parallel}$, needed to recover the friction force and electron heat flux in Braginskii (1958) (see subsection 5.4), come from the electron-ion and electron-electron collision operators in equations (C 1) and (C 6).

We finish by pointing out that F_e satisfies conditions (4.7), (4.8) and (4.9) to the order that we have calculated it. Since F_M satisfies these conditions, the conditions for F_{e1} become

$$2\pi\int_{-\infty}^{\infty}\mathrm{d}w_\parallel\int_0^\infty \mathrm{d}w_\perp\, w_\perp F_{e1}(z,w_\parallel,w_\perp,t) = 0, \quad (5.19)$$

$$2\pi\int_{-\infty}^{\infty}\mathrm{d}w_\parallel\int_0^\infty \mathrm{d}w_\perp\, w_\perp w_\parallel F_{e1}(z,w_\parallel,w_\perp,t) = 0 \quad (5.20)$$

and

$$2\pi\int_{-\infty}^{\infty}\mathrm{d}w_\parallel\int_0^\infty \mathrm{d}w_\perp\, w_\perp (w_\parallel^2 + w_\perp^2) F_{e1}(z,w_\parallel,w_\perp,t) = 0. \quad (5.21)$$

These conditions determine the pieces of F_{e1} that are in the kernel of the operators in the left side of equation (5.18).

5.4.2. *Collisionless electron equations*

We call this limit collisionless in contraposition to the collisional Braginsikii-like limit discussed above, but we still keep collisions. We assume that ion-ion, ion-neutral, electron-electron, electron-ion, electron-neutral and ion-neutral collisions satisfy

$$\frac{\nu_{ss'}L}{v_{ts}} \sim 1. \quad (5.22)$$

The ionization frequencies $n_e R_{\mathrm{ion}}$ and $n_n R_{\mathrm{ion}}$ are still assumed to be of order v_{ti}/L.

In this limit, we can neglect the collisional coupling between the heavy species (ions and neutrals) and electrons in the fluid equations. In the electron energy equation (5.11), the dominant term is $\partial q_{e\parallel}/\partial z$, giving

$$\frac{\partial q_{e\parallel}}{\partial z} \simeq 0 \quad (5.23)$$

In the electron momentum equation (5.9), the friction forces are negligible, giving

$$\frac{\partial p_{e\parallel}}{\partial z} \simeq e n_e \frac{\partial \phi}{\partial z}. \tag{5.24}$$

Using these results in the electron kinetic equation (5.2) and neglecting $u_{i\parallel} - u_{e\parallel}$ and $u_{n\parallel} - u_{e\parallel}$ in the collision operators in equation (C 1) and (C 6), we find

$$\left[v_{te} w_\parallel \frac{\partial}{\partial z} + \left(\frac{e}{m_e v_{te}} \frac{\partial \phi}{\partial z} - w_\parallel^2 \frac{\partial v_{te}}{\partial z} \right) \frac{\partial}{\partial w_\parallel} - w_\parallel w_\perp \frac{\partial v_{te}}{\partial z} \frac{\partial}{\partial w_\perp} \right] \left(\frac{n_e F_e}{v_{te}^3} \right) = \frac{n_e}{v_{te}^3} \left(\mathcal{C}_{ee} + \mathcal{C}_{ei}^{(\ell)} + \mathcal{C}_{en}^{(\ell)} \right). \tag{5.25}$$

The collision operators $\mathcal{C}_{ei}^{(\ell)}$ and $\mathcal{C}_{en}^{(\ell)}$ are defined in Appendix D.

We can use entropy production of the electron-electron, electron-ion and electron-neutral collision operators to solve equation (5.25). We multiply equation (5.25) by $-\ln(n_e F_e / v_{te}^3)$ to find

$$\left[v_{te} w_\parallel \frac{\partial}{\partial z} + \left(\frac{e}{m_e v_{te}} \frac{\partial \phi}{\partial z} - w_\parallel^2 \frac{\partial v_{te}}{\partial z} \right) \frac{\partial}{\partial w_\parallel} - w_\parallel w_\perp \frac{\partial v_{te}}{\partial z} \frac{\partial}{\partial w_\perp} \right] \left[\frac{n_e F_e}{v_{te}^3} \left(1 - \ln \left(\frac{n_e F_e}{v_{te}^3} \right) \right) \right] = -\frac{n_e}{v_{te}^3} \ln \left(\frac{n_e F_e}{v_{te}^3} \right) \left(\mathcal{C}_{ee} + \mathcal{C}_{ei}^{(\ell)} + \mathcal{C}_{en}^{(\ell)} \right). \tag{5.26}$$

Multiplying by v_{te}^3 and integrating over velocity space, we obtain

$$\frac{\partial}{\partial z} \left[n_e v_{te} \int \left(1 - \ln \left(\frac{n_e F_e}{v_{te}^3} \right) \right) F_e w_\parallel w_\perp \, \mathrm{d}w_\parallel \, \mathrm{d}w_\perp \right] = -n_e \int \ln \left(\frac{n_e F_e}{v_{te}^3} \right) \left(\mathcal{C}_{ee} + \mathcal{C}_{ei}^{(\ell)} + \mathcal{C}_{en}^{(\ell)} \right) w_\perp \, \mathrm{d}w_\parallel \, \mathrm{d}w_\perp. \tag{5.27}$$

Integrating equation (5.27) over z gives

$$\left[n_e v_{te} \int \left(1 - \ln \left(\frac{n_e F_e}{v_{te}^3} \right) \right) F_e w_\parallel w_\perp \, \mathrm{d}w_\parallel \, \mathrm{d}w_\perp \right]_{z=0}^{z=L} = -n_e \int_0^L \mathrm{d}z \int \ln \left(\frac{n_e F_e}{v_{te}^3} \right) \left(\mathcal{C}_{ee} + \mathcal{C}_{ei}^{(\ell)} + \mathcal{C}_{en}^{(\ell)} \right) w_\perp \, \mathrm{d}w_\parallel \, \mathrm{d}w_\perp. \tag{5.28}$$

Conditions (3.3) and (3.5) impose that only a few electrons leave the system towards the wall. The number of electrons that leave is small by a factor of $\sqrt{m_e/m_i} \ll 1$ and thus, the left side of equation (5.28) can be neglected, finally giving

$$-\int_0^L \mathrm{d}z \int \ln \left(\frac{n_e F_e}{v_{te}^3} \right) \left(\mathcal{C}_{ee} + \mathcal{C}_{ei}^{(\ell)} + \mathcal{C}_{en}^{(\ell)} \right) w_\perp \, \mathrm{d}w_\parallel \, \mathrm{d}w_\perp \simeq 0. \tag{5.29}$$

The integrand under the integral over z is the entropy production, and it is positive unless the distribution function F_e is the Maxwellian F_M. Hence, F_e is a Maxwellian to lowest order in the expansion in $\sqrt{m_e/m_i}$.

Substituting the Maxwellian into equation (5.25), we find that the right side of the equation vanishes. For the left side of the equation to be zero for all $w_\parallel$ and $w_\perp$, we need $\partial v_{te}/\partial z = 0$ and

$$n_e(z,t) = N_e(t) \exp \left(\frac{e\phi(z,t)}{T_e(t)} \right). \tag{5.30}$$

The value of $N_e(t)$ is calculated from quasineutrality,

$$N_e(t)\int_0^L \exp\left(\frac{e\phi(z,t)}{T_e(t)}\right)\,\mathrm{d}z = \int_0^L n_i(z,t)\,\mathrm{d}z. \tag{5.31}$$

The value of $T_e(t)$ is obtained from the electron energy equation. Integrating the energy equation (5.11) over z, we find

$$\begin{aligned}\frac{3}{2}\frac{\mathrm{d}}{\mathrm{d}t}\left[N_eT_e\int_0^L \exp\left(\frac{e\phi}{T_e}\right)\,\mathrm{d}z\right] &= -\left[\frac{5}{2}n_eu_{e\parallel}T_e + q_{e\parallel}\right]_{z=0}^{z=L}\\ &+\int_0^L\left(en_e\frac{\partial\phi}{\partial z} - n_en_nR_{\mathrm{ion}}E_{\mathrm{ion}} + \int\frac{1}{2}m_ev^2S_e\,\mathrm{d}^3v\right)\mathrm{d}z.\end{aligned} \tag{5.32}$$

It might seem that the heat flux should vanish here because the distribution function is a Maxwellian to lowest order. In reality, the real F_e is sufficiently far from a Maxwellian at large velocities to induce a significant heat flux. Indeed, to satisfy boundary conditions (3.1) and (3.4), the distribution function must vanish exactly in certain regions of phase space. Since these regions are at large velocities, the techniques used to calculate the collisional losses into the loss cones of mirror machines can be used (Pastukhov 1974).

6. Discussion

The model that we propose is comprised of:

- the three fluid equations (4.10), (4.11) and (4.12) for ions that have to be solved in conjunction with the ion kinetic equation (4.19);
- the three fluid equations (4.25), (4.26) and (4.27) for neutrals that have to be solved in conjunction with the neutral kinetic equation (4.29);
- the two fluid equations (5.8) and (5.11) for electrons that have to be solved in conjunction with the electron kinetic equation (5.2) with the modified coefficients (5.3), (5.4), (5.5) and (5.6); and
- the electron parallel momentum equation (5.9) for the potential.

The boundary conditions for this system of equations are described in section 3.

To test the model proposed in this report, we will first extend the existing code based on adiabatic electrons, which we prove to a be a good approximation for collisionless plasmas in section 5.4, to wall boundary conditions. We will then explore the effect of adding electrons. For most physics of interest, it is sufficient to use simplified ion-ion and electron-electron collision operators, and for this reason we do not expect to implement a full Fokker-Planck collision operator.

Appendix A. Modified collision operators for the ion kinetic equation

The modified Fokker-Planck like-particle collision operator is

$$\begin{aligned}&\mathcal{C}_{ss}[F_s,n_s,v_{ts}](z,w_\parallel,w_\perp,t)\\ &:=\frac{2\pi e^4n_s\ln\Lambda}{(4\pi\epsilon_0)^2m_s^2v_{ts}^3}\left\{\frac{\partial}{\partial w_\parallel}\left(\mathcal{D}_{\parallel\parallel}[F_s]\frac{\partial F_s}{\partial w_\parallel}+\mathcal{D}_{\parallel\perp}[F_s]\frac{\partial F_s}{\partial w_\perp}+\mathcal{P}_\parallel[F_s]F_s\right)\right.\\ &\left.+\frac{1}{w_\perp}\frac{\partial}{\partial w_\perp}\left[w_\perp\left(\mathcal{D}_{\parallel\perp}[F_s]\frac{\partial F_s}{\partial w_\parallel}+\mathcal{D}_{\perp\perp}[F_s]\frac{\partial F_s}{\partial w_\perp}+\mathcal{P}_\perp[F_s]F_s\right)\right]\right\}.\end{aligned} \tag{A 1}$$

The coefficients needed for this collision operator are

$$\mathcal{D}_{\parallel\parallel}[F_s](z,w_\parallel,w_\perp,t) := 4\int_{-\infty}^{\infty}\mathrm{d}w'_\parallel\int_0^\infty \mathrm{d}w'_\perp \frac{w'_\perp}{\sqrt{(w_\parallel-w'_\parallel)^2+(w_\perp+w'_\perp)^2}} \times\left(K(\kappa)-\frac{(w_\parallel-w'_\parallel)^2E(\kappa)}{(w_\parallel-w'_\parallel)^2+(w_\perp-w'_\perp)^2}\right)F_s(z,w'_\parallel,w'_\perp,t), \tag{A 2}$$

$$\mathcal{D}_{\parallel\perp}[F_s](z,w_\parallel,w_\perp,t) := 2\int_{-\infty}^{\infty}\mathrm{d}w'_\parallel\int_0^\infty \mathrm{d}w'_\perp \frac{w'_\perp(w_\parallel-w'_\parallel)}{w_\perp\sqrt{(w_\parallel-w'_\parallel)^2+(w_\perp+w'_\perp)^2}} \times\left(\frac{[(w_\parallel-w'_\parallel)^2-w_\perp^2+w'^2_\perp]E(\kappa)}{(w_\parallel-w'_\parallel)^2+(w_\perp-w'_\perp)^2}-K(\kappa)\right)F_s(z,w'_\parallel,w'_\perp,t), \tag{A 3}$$

$$\mathcal{D}_{\perp\perp}[F_s](z,w_\parallel,w_\perp,t) := 2\int_{-\infty}^{\infty}\mathrm{d}w'_\parallel\int_0^\infty \mathrm{d}w'_\perp \frac{w'_\perp}{w_\perp^2\sqrt{(w_\parallel-w'_\parallel)^2+(w_\perp+w'_\perp)^2}} \times\left\{2w_\perp\left[\frac{w_\perp(w_\parallel-w'_\parallel)^2}{(w_\parallel-w'_\parallel)^2+(w_\perp-w_\perp)^2}-w'_\perp\right]E(\kappa) +[(w_\parallel-w'_\parallel)^2+w_\perp^2+w'^2_\perp][K(\kappa)-E(\kappa)]\right\}F_s(z,w'_\parallel,w'_\perp,t), \tag{A 4}$$

$$\mathcal{P}_{\parallel}[F_s](z,w_\parallel,w_\perp,t) := 8\int_{-\infty}^{\infty}\mathrm{d}w'_\parallel\int_0^\infty \mathrm{d}w'_\perp \frac{w'_\perp(w_\parallel-w'_\parallel)}{\sqrt{(w_\parallel-w'_\parallel)^2+(w_\perp+w'_\perp)^2}} \times\left(\frac{K(\kappa)-E(\kappa)}{(w_\parallel-w'_\parallel)^2+(w_\perp+w'_\perp)^2}-\frac{E(\kappa)}{(w_\parallel-w'_\parallel)^2+(w_\perp-w'_\perp)^2}\right)F_s(z,w'_\parallel,w'_\perp,t) \tag{A 5}$$

and

$$\mathcal{P}_{\perp}[F_s](z,w_\parallel,w_\perp,t) := 4\int_{-\infty}^{\infty}\mathrm{d}w'_\parallel\int_0^\infty \mathrm{d}w'_\perp \frac{w'_\perp}{w_\perp\sqrt{(w_\parallel-w'_\parallel)^2+(w_\perp+w'_\perp)^2}} \times\left(\frac{[(w_\parallel-w'_\parallel)^2-w_\perp^2+w'^2_\perp]E(\kappa)}{(w_\parallel-w'_\parallel)^2+(w_\perp-w'_\perp)^2}-K(\kappa)\right)F_s(z,w'_\parallel,w'_\perp,t). \tag{A 6}$$

Here, $K(\kappa) := \int_0^{\pi/2}(1-\kappa^2\sin^2\alpha)^{-1/2}\,\mathrm{d}\alpha$ and $E(\kappa) := \int_0^{\pi/2}(1-\kappa^2\sin^2\alpha)^{1/2}\,\mathrm{d}\alpha$ are the elliptic integrals, and the function κ is

$$\kappa(w_\parallel,w_\perp,w'_\parallel,w'_\perp) := \sqrt{\frac{4w_\perp w'_\perp}{(w_\parallel-w'_\parallel)^2+(w_\perp+w'_\perp)^2}}. \tag{A 7}$$

The modified charge exchange collision operator for the ion kinetic equation is

$$\begin{aligned}
&\mathcal{C}_{in}[F_i, F_n, n_n, u_{i\parallel}, u_{n\parallel}, v_{ti}, v_{tn}](z, w_\parallel, w_\perp, t) \\
&\quad := -n_n R_{in}\left[F_i - \frac{v_{ti}^3}{v_{tn}^3} F_n\left(z, \frac{u_{i\parallel}-u_{n\parallel}}{v_{tn}} + \frac{v_{ti}}{v_{tn}} w_\parallel, \frac{v_{ti}}{v_{tn}} w_\perp, t\right)\right] \\
&\qquad + n_n R_{in}\frac{\partial}{\partial w_\parallel}\left[\left(\frac{u_{n\parallel}-u_{i\parallel}}{v_{ti}} + \frac{w_\parallel}{2}\left(\frac{v_{tn}^2}{v_{ti}^2} - 1 + \frac{2(u_{n\parallel}-u_{i\parallel})^2}{3v_{ti}^2}\right)\right) F_i\right] \\
&\qquad + \frac{n_n R_{in}}{w_\perp}\frac{\partial}{\partial w_\perp}\left[\frac{w_\perp^2}{2}\left(\frac{v_{tn}^2}{v_{ti}^2} - 1 + \frac{2(u_{n\parallel}-u_{i\parallel})^2}{3v_{ti}^2}\right) F_i\right].
\end{aligned} \tag{A 8}$$

Finally, the modified ionization collision operator for the ion kinetic equation is

$$\begin{aligned}
&\mathcal{C}_{i,\mathrm{ion}}[F_n, n_e, u_{i\parallel}, u_{n\parallel}, v_{ti}, v_{tn}](z, w_\parallel, w_\perp, t) \\
&\quad := -n_e R_{\mathrm{ion}}\left[F_i - \frac{v_{ti}^3}{v_{tn}^3} F_n\left(z, \frac{u_{i\parallel}-u_{n\parallel}}{v_{tn}} + \frac{v_{ti}}{v_{tn}} w_\parallel, \frac{v_{ti}}{v_{tn}} w_\perp, t\right)\right] \\
&\qquad + n_e R_{\mathrm{ion}}\frac{\partial}{\partial w_\parallel}\left[\left(\frac{u_{n\parallel}-u_{i\parallel}}{v_{ti}} + \frac{w_\parallel}{2}\left(\frac{v_{tn}^2}{v_{ti}^2} - 1 + \frac{2(u_{n\parallel}-u_{i\parallel})^2}{3v_{ti}^2}\right)\right) F_i\right] \\
&\qquad + \frac{n_e R_{\mathrm{ion}}}{w_\perp}\frac{\partial}{\partial w_\perp}\left[\frac{w_\perp^2}{2}\left(\frac{v_{tn}^2}{v_{ti}^2} - 1 + \frac{2(u_{n\parallel}-u_{i\parallel})^2}{3v_{ti}^2}\right) F_i\right].
\end{aligned} \tag{A 9}$$

Appendix B. Modified collision operators for the neutral kinetic equation

The modified charge exchange collision operator for the neutral kinetic equation is

$$\begin{aligned}
&\mathcal{C}_{ni}[F_n, F_i, n_i, u_{n\parallel}, u_{i\parallel}, v_{tn}, v_{ti}](z, w_\parallel, w_\perp, t) \\
&\quad := -n_i R_{in}\left[F_n - \frac{v_{tn}^3}{v_{ti}^3} F_i\left(z, \frac{u_{n\parallel}-u_{i\parallel}}{v_{ti}} + \frac{v_{tn}}{v_{ti}} w_\parallel, \frac{v_{tn}}{v_{ti}} w_\perp, t\right)\right] \\
&\qquad + n_i R_{in}\frac{\partial}{\partial w_\parallel}\left[\left(\frac{u_{i\parallel}-u_{n\parallel}}{v_{tn}} + \frac{w_\parallel}{2}\left(\frac{v_{ti}^2}{v_{tn}^2} - 1 + \frac{2(u_{n\parallel}-u_{i\parallel})^2}{3v_{tn}^2}\right)\right) F_n\right] \\
&\qquad + \frac{n_i R_{in}}{w_\perp}\frac{\partial}{\partial w_\perp}\left[\frac{w_\perp^2}{2}\left(\frac{v_{ti}^2}{v_{tn}^2} - 1 + \frac{2(u_{n\parallel}-u_{i\parallel})^2}{3v_{tn}^2}\right) F_n\right].
\end{aligned} \tag{B 1}$$

Appendix C. Modified collision operators for the electron kinetic equation

The electron-electron collision operator is described in equation (A 1).
The modified ion-electron collision operator is

$$\begin{aligned}
&\mathcal{C}_{ei}[F_e, n_i, u_{i\parallel}, u_{e\parallel}, v_{te}](z, w_\parallel, w_\perp, t) \\
&\quad := \frac{2\pi e^4 n_i \ln\Lambda}{(4\pi\epsilon_0)^2 m_e^2 v_{te}^3}\left\{\frac{\partial}{\partial w_\parallel}\left[\mathcal{M}_{\parallel\parallel}\frac{\partial F_e}{\partial w_\parallel} + \mathcal{M}_{\parallel\perp}\frac{\partial F_e}{\partial w_\perp} + \left(1 + \frac{2(u_{i\parallel}-u_{e\parallel})w_\parallel}{3v_{te}}\right)\mathcal{F}_\parallel F_e\right]\right. \\
&\qquad \left. + \frac{1}{w_\perp}\frac{\partial}{\partial w_\perp}\left[w_\perp\left(\mathcal{M}_{\parallel\perp}\frac{\partial F_e}{\partial w_\parallel} + \mathcal{M}_{\perp\perp}\frac{\partial F_e}{\partial w_\perp} + \frac{2(u_{i\parallel}-u_{e\parallel})w_\perp}{3v_{te}}\mathcal{F}_\parallel F_e\right)\right]\right\},
\end{aligned} \tag{C 1}$$

where

$$\mathcal{M}_{\parallel\parallel}[u_{e\parallel},v_{te},u_{i\parallel}](z,w_\parallel,w_\perp,t) := \frac{w_\perp^2}{[(w_\parallel-(u_{i\parallel}-u_{e\parallel})/v_{te})^2+w_\perp^2]^{3/2}}, \tag{C 2}$$

$$\mathcal{M}_{\parallel\perp}[u_{e\parallel},v_{te},u_{i\parallel}](z,w_\parallel,w_\perp,t) := -\frac{(w_\parallel-(u_{i\parallel}-u_{e\parallel})/v_{te})^2 w_\perp}{[(w_\parallel-(u_{i\parallel}-u_{e\parallel})/v_{te})^2+w_\perp^2]^{3/2}}, \tag{C 3}$$

$$\mathcal{M}_{\perp\perp}[u_{e\parallel},v_{te},u_{i\parallel}](z,w_\parallel,w_\perp,t) := \frac{(w_\parallel-(u_{i\parallel}-u_{e\parallel})/v_{te})^2}{[(w_\parallel-(u_{i\parallel}-u_{e\parallel})/v_{te})^2+w_\perp^2]^{3/2}} \tag{C 4}$$

and

$$\begin{aligned}&\mathcal{F}_\parallel[F_e,u_{e\parallel},v_{te},u_{i\parallel}](z,t)\\ &\quad := -4\pi\int_{-\infty}^{\infty}\mathrm{d}w_\parallel\int_0^\infty \mathrm{d}w_\perp\,\frac{w_\perp[w_\parallel-(u_{i\parallel}-u_{e\parallel})/v_{te}]F_e(z,w_\parallel,w_\perp,t)}{[(w_\parallel-(u_{i\parallel}-u_{e\parallel})/v_{te})^2+w_\perp^2]^{3/2}}.\end{aligned} \tag{C 5}$$

The modified electron-neutral collision operator is

$$\begin{aligned}\mathcal{C}_{en}[F_e,n_n,u_{n\parallel},u_{e\parallel},v_{te}](z,w_\parallel,w_\perp,t) :=& -n_nR_{en}\left[F_e-\frac{1}{2}\int_0^\pi \sin\chi F_e(z,\overline{w}_\parallel,\overline{w}_\perp,t)\,\mathrm{d}\chi\right]\\ &+\frac{n_nR_{en}(u_{n\parallel}-u_{e\parallel})}{v_{te}}\frac{\partial}{\partial w_\parallel}\left[\left(1+\frac{2(u_{n\parallel}-u_{e\parallel})w_\parallel}{3v_{te}}\right)F_e\right]\\ &+\frac{2n_nR_{en}(u_{n\parallel}-u_{e\parallel})^2}{3v_{te}^2w_\perp}\frac{\partial}{\partial w_\perp}\left(w_\perp^2F_e\right),\end{aligned} \tag{C 6}$$

where

$$\overline{w}_\parallel[u_{e\parallel},v_{te},u_{n\parallel}](\chi,z,w_\parallel,w_\perp,t) := \frac{u_{n\parallel}-u_{e\parallel}}{v_{te}}+\cos\chi\sqrt{\left(w_\parallel-\frac{u_{n\parallel}-u_{e\parallel}}{v_{te}}\right)^2+w_\perp^2} \tag{C 7}$$

and

$$\overline{w}_\perp[u_{e\parallel},v_{te},u_{n\parallel}](\chi,z,w_\parallel,w_\perp,t) := \sin\chi\sqrt{\left(w_\parallel-\frac{u_{n\parallel}-u_{e\parallel}}{v_{te}}\right)^2+w_\perp^2}. \tag{C 8}$$

Appendix D. Linearized collision operators for electrons

The linearized electron-electron collision operator is given by

$$\begin{aligned}&\mathcal{C}_{ee}^{(\ell)}[F_{e1},n_e,v_{te}](z,w_\parallel,w_\perp,t)\\ &:=\frac{2\pi e^4n_e\ln\Lambda}{(4\pi\epsilon_0)^2m_e^2v_{te}^3}\left\{\frac{\partial}{\partial w_\parallel}\left(\mathcal{D}_{\parallel\parallel}[F_M]\frac{\partial F_{e1}}{\partial w_\parallel}+\mathcal{D}_{\parallel\perp}[F_M]\frac{\partial F_{e1}}{\partial w_\perp}+\mathcal{P}_\parallel[F_M]F_{e1}\right.\right.\\ &\quad\left.-2w_\parallel\mathcal{D}_{\parallel\parallel}[F_{e1}]F_M-2w_\perp\mathcal{D}_{\parallel\perp}[F_{e1}]F_M+\mathcal{P}_\parallel[F_{e1}]F_M\right)\\ &\quad+\frac{1}{w_\perp}\frac{\partial}{\partial w_\perp}\left[w_\perp\left(\mathcal{D}_{\parallel\perp}[F_M]\frac{\partial F_{e1}}{\partial w_\parallel}+\mathcal{D}_{\perp\perp}[F_M]\frac{\partial F_{e1}}{\partial w_\perp}+\mathcal{P}_\perp[F_M]F_{e1}\right.\right.\\ &\quad\left.\left.\left.-2w_\parallel\mathcal{D}_{\parallel\perp}[F_{e1}]F_M-2w_\perp\mathcal{D}_{\perp\perp}[F_{e1}]F_M+\mathcal{P}_\perp[F_{e1}]F_M\right)\right]\right\}.\end{aligned} \tag{D 1}$$

The coefficients are defined in Appendix A.

The linearized electron-ion collision operator is

$$\begin{aligned}\mathcal{C}_{ei}^{(\ell)}&[F_{e1}, n_i, v_{te}](z, w_\parallel, w_\perp, t)\\ &:= \frac{2\pi e^4 n_i \ln\Lambda}{(4\pi\epsilon_0)^2 m_e^2 v_{te}^3}\left\{\frac{\partial}{\partial w_\parallel}\left[\frac{w_\perp^2}{(w_\parallel^2+w_\perp^2)^{3/2}}\frac{\partial F_{e1}}{\partial w_\parallel} - \frac{w_\parallel w_\perp}{(w_\parallel^2+w_\perp^2)^{3/2}}\frac{\partial F_{e1}}{\partial w_\perp}\right]\right.\\ &\left. + \frac{1}{w_\perp}\frac{\partial}{\partial w_\perp}\left[w_\perp\left(-\frac{w_\parallel w_\perp}{(w_\parallel^2+w_\perp^2)^{3/2}}\frac{\partial F_{e1}}{\partial w_\parallel} + \frac{w_\parallel^2}{(w_\parallel^2+w_\perp^2)^{3/2}}\frac{\partial F_{e1}}{\partial w_\perp}\right)\right]\right\}. \qquad \text{(D 2)}\end{aligned}$$

Finally, the linearized electron-neutral collision operator is

$$\begin{aligned}\mathcal{C}_{en}^{(\ell)}&[F_{e1}, n_n, v_{te}](z, w_\parallel, w_\perp, t) := -n_n R_{en}\left[F_{e1}\right.\\ &\left. - \frac{1}{2}\int_0^\pi \sin\chi F_{e1}\left(z, \cos\chi\sqrt{w_\parallel^2+w_\perp^2}, \sin\chi\sqrt{w_\parallel^2+w_\perp^2}, t\right)\,\mathrm{d}\chi\right]. \qquad \text{(D 3)}\end{aligned}$$

REFERENCES

Braginskii, S.I. 1958 Transport phenomena in a completely ionized two-temperature plasma. *Sov. Phys. JETP* **6**, 358.

Catto, P.J. 1994 A short mean-free path, coupled neutral-ion transport description of a tokamak edge plasma. *Phys. Plasmas* **1**, 1936.

Chodura, R. 1982 Plasma-wall transition in an oblique magnetic field. *Phys. Fluids* **25**, 1628.

Connor, J.W. 1977 An analytic solution for the distribution function of neutral particles in a Maxwellian plasma using the method of singular eigenfunctions. *Plasma Phys.* **19**, 853.

Geraldini, A. 2021 Large gyro-orbit model of ion velocity distribution in plasma near a wall in a grazing-angle magnetic field. *J. Plasma Phys.* **87**, 905870113.

Geraldini, A., Parra, F.I. & Militello, F. 2017 Gyrokinetic treatment of a grazing angle magnetic presheath. *Plasma Phys. Control. Fusion* **59**, 025015.

Geraldini, A., Parra, F.I. & Militello, F. 2018 Solution to a collisionless shallow-angle magnetic presheath with kinetic ions. *Plasma Phys. Control. Fusion* **60**, 125002.

Geraldini, A., Parra, F.I. & Militello, F. 2019 Dependence on ion temperature of shallow-angle magnetic presheaths with adiabatic electrons. *J. Plasma Phys.* **85**, 795850601.

Hazeltine, R.D. 1973 Recursive derivation of drift-kinetic equation. *Plasma Phys.* **15**, 77–80.

Hazeltine, R.D., Calvin, M.D., Valanju, P.M. & Solano, E.R. 1992 Analytical calculation of neutral transport and its effect on ions. *Nucl. Fusion* **32**, 3.

Helander, P., Krasheninnikov, S.I. & Catto, P.J. 1994 Fluid equations for a partially ionized plasma. *Phys. Plasmas* **1**, 3174.

Knudsen, M. 1916 Das Cosinusgesetz in der kinetischen Gastheorie. *Annal. Phys.* **353**, 1113.

Parker, S.E., Procassini, R.J. & Birdsall, C.K. 1993 A Suitable Boundary Condition for Bounded Plasma Simulation without Sheath Resolution. *J. Comput. Phys.* **104**, 41.

Pastukhov, V.P. 1974 Collisional losses of electrons from an adiabatic trap in a plasma with a positive potential. *Nucl. Fusion* **14**, 3.

Rosenbluth, M.N., MacDonald, W.M. & Judd, D.L. 1957 Fokker-Planck Equation for an Inverse-Square Force. *Phys. Rev.* **107**, 1.

2D drift kinetic model with wall boundary conditions

Felix I. Parra, Michael Barnes and Michael Hardman

Rudolf Peierls Centre for Theoretical Physics, University of Oxford, Oxford OX1 3PU, UK

(This version is of 31 July 2021)

1. Introduction

In previous reports, we proposed 1D drift kinetic equations with periodic boundary conditions, adequate for the closed field line region of the edge, and wall boundary conditions. In this report, we build a 2D drift kinetic model for a helical magnetic field. The helical magnetic field has similarities with the magnetic field in the tokamak edge.

2. Helical magnetic field

To describe the geometry of the magnetic field, we use the cylindrical coordinates $\{r, z, \zeta\}$ (see figure 1). In this coordinates, the helical field is

$$\mathbf{B}(r,\zeta) := B_z(r)\hat{\mathbf{z}} + B_\zeta(r)\hat{\boldsymbol{\zeta}}(\zeta), \tag{2.1}$$

where $\hat{\mathbf{z}}$ and $\hat{\boldsymbol{\zeta}}$ are the unit vectors in the direction of ∇z and $\nabla\zeta$. Note that the components B_z and B_ζ only depend on the radial position r.

In principle, one can use any $B_z(r)$ and $B_\zeta(r)$. There is a particular choice that is more physical. In the edge, the magnetic field is determined by currents running through the core plasma or through external magnets. Thus, according to Ampére's law, the magnetic field in the edge should satisfy $\nabla\times\mathbf{B}\simeq 0$. This condition imposes that B_z be a constant and that B_ζ decay as $1/r$,

$$B_\zeta(r) = \frac{I}{r}, \tag{2.2}$$

where I is a constant determined by the vertical current through the core plasma.

3. Geometry and orderings

We consider a magnetized plasma with one ion species with charge e and mass m_i, electrons with charge $-e$ and mass m_e, and one species of neutrals with mass

$$m_n = m_i. \tag{3.1}$$

The plasma is magnetized by a helical magnetic field like the one described in the previous section, and we assume that the plasma only varies in r and z. We assume that the electric field produced by the plasma is electrostatic, $\mathbf{E} = -(\partial\phi/\partial r)\hat{\mathbf{r}} - (\partial\phi/\partial z)\hat{\mathbf{z}}$, where $\hat{\mathbf{r}}$ is the unit vector in the direction ∇r. The potential $\phi(r,z,t)$ depends on the coordinates r and z and on time t.

There are two conducting walls at $z=0$ and $z=L_z$. In the radial direction, we consider the interval between $r=r_0$ and $r=r_0+L_r$. The length L_r is determined by a balance between the fast parallel velocity of the particles along magnetic field lines

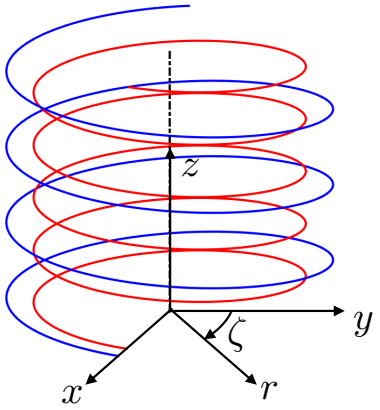

FIGURE 1. Two magnetic field lines (in blue and red) of the helical magnetic field. Note that the direction of the angle ζ is opposite to the direction usually chosen in cylindrical coordinates.

and their slow drift across them. The characteristic length between the two walls along a magnetic field line is of order

$$L_\parallel \sim \frac{B}{B_z} L_z. \tag{3.2}$$

Thus, the typical time that it takes an ion to move from wall to wall is $L_\parallel / v_{ti} \sim (B/B_z)(L_z/v_{ti})$, where $v_{ti} := \sqrt{2T_i/m_i}$ is the ion thermal speed and T_i is the ion temperature. For a potential ϕ of the order of T_i/e, where e is the proton charge, the radial $\mathbf{E}\times\mathbf{B}$ drift is

$$v_{Er} := -\frac{B_\zeta}{B^2}\frac{\partial \phi}{\partial z} \sim \frac{\rho_i}{L_z} v_{ti}, \tag{3.3}$$

where $\rho_i := v_{ti}/\Omega_i$ is the characteristic ion gyroradius and $\Omega_i := eB/m_i$ is the ion gyrofrequency. Thus, the time it takes for an ion to cross the domain in the radial direction is $L_r/v_{Er} \sim L_r L_z/\rho_i v_{ti}$. By making this time of the same order as $L_\parallel/v_{ti}$, we solve for L_r to find

$$L_r \sim \frac{B}{B_z}\rho_i \tag{3.4}$$

To simplify the problem to a tractable drift kinetic form, we assume that ρ_i is much smaller than L_r. This implies that

$$\frac{\rho_i}{L_r} \sim \frac{B_z}{B} \sim \frac{B_z}{B_\zeta} \ll 1, \tag{3.5}$$

that is, we will limit our model to magnetic fields that are mostly azimuthal and have a very small vertical component. This is an approximation that is consistent with magnetic field geometry in conventional tokamaks and also in the edge of many shots in spherical tokamaks.

We also assume that $r_0 \sim L_z \gg L_r$. Since r_0 is the characteristic length of variation of the magnetic field $\mathbf{B}$, the magnetic field barely changes across the domain $[r_0, r_0 + L_r]$. Thus, within our ordering, we assume $\mathbf{B}$ to be uniform in the domain of interest.

Our orderings above rest on the assumption $\phi \sim T_i/e$. This ordering is a result of the wall boundary conditions that impose $\phi \sim T_e/e$ (see section 5) and the fact that $T_i \sim T_e$ due to collisional temperature equilibration.

4. 2D electrostatic drift kinetics

We assume that the gyroradii are small compared to the length scales of interest, and that the gyrofrequencies are much larger than the frequencies that we want to model. Thus, the distribution functions $f_s(r, z, v_\parallel, v_\perp, t)$ of the charged species $s = i, e$ only depend on the component of the velocity parallel to the magnetic field $v_\parallel$ and the magnitude of the velocity perpendicular to the magnetic field $v_\perp$, and are independent of the direction of the velocity perpendicular to the magnetic field (Hazeltine 1973). The distribution functions of ions and electrons ($s = i, e$) that in general can depend on three spatial variables $\mathbf{r}$, three components of the velocity $\mathbf{v}$ and the time t depend only on r, z, $v_\parallel$, $v_\perp$ and t,

$$f_s(\mathbf{r}, \mathbf{v}, t) = f_s(r, z, v_\parallel, v_\perp, t). \tag{4.1}$$

The neutral distribution function depends in general on the three velocity components,

$$f_n(\mathbf{r}, \mathbf{v}, t) = f_n(r, z, v_r, v_z, v_\zeta, t). \tag{4.2}$$

We remind the reader that the model is 2D because we have assumed that the plasma parameters do not depend on the angle ζ.

The equations for the distribution functions of the different species are

$$\begin{aligned}\frac{\partial f_i}{\partial t} - \frac{1}{B}\frac{\partial \phi}{\partial z}\frac{\partial f_i}{\partial r} + \left(\frac{v_\parallel B_z}{B} + \frac{1}{B}\frac{\partial \phi}{\partial r}\right)\frac{\partial f_i}{\partial z} - \frac{eB_z}{m_i B}\frac{\partial \phi}{\partial z}\frac{\partial f_i}{\partial v_\parallel} \\ = C_{ii}[f_i] + \langle C_{in}[f_i, f_n]\rangle + \langle C_{i,\mathrm{ion}}[f_e, f_n]\rangle + C_{ie}[f_i, f_e] + S_i,\end{aligned} \tag{4.3}$$

$$\begin{aligned}\frac{\partial f_e}{\partial t} - \frac{1}{B}\frac{\partial \phi}{\partial z}\frac{\partial f_e}{\partial r} + \left(\frac{v_\parallel B_z}{B} + \frac{1}{B}\frac{\partial \phi}{\partial r}\right)\frac{\partial f_e}{\partial z} + \frac{eB_z}{m_e B}\frac{\partial \phi}{\partial z}\frac{\partial f_e}{\partial v_\parallel} = C_{ee}[f_e] \\ + C_{ei}[f_e, f_i]\left[1 + O\left(\frac{m_e}{m_i}\right)\right] + \left\langle C_{en}[f_e, f_n]\left[1 + O\left(\frac{m_e}{m_i}\right)\right]\right\rangle + \langle C_{e,\mathrm{ion}}[f_e, f_n]\rangle + S_e\end{aligned} \tag{4.4}$$

and

$$\frac{\partial f_n}{\partial t} + v_r\frac{\partial f_n}{\partial r} + v_z\frac{\partial f_n}{\partial z} = C_{ni}[f_n, f_i] + C_{ne}[f_n, f_e] + C_{n,\mathrm{ion}}[f_n, f_e] + S_n. \tag{4.5}$$

The triangular brackets on a function $G(r, z, v_r, v_z, v_\zeta, t)$ indicate gyroaverage,

$$\langle G\rangle(r, z, v_\parallel, v_\perp, t) := \frac{1}{2\pi}\int_0^{2\pi} G\left(r, z, v_\perp\cos\varphi, v_\perp\sin\varphi, v_\parallel, t\right)\,\mathrm{d}\varphi. \tag{4.6}$$

The sources $S_s(r, z, \mathbf{v}, t)$ with $s = i, e, n$ represent heating, fueling and the effect of turbulence. The ion and electron particle sources satisfy

$$\int S_i\,\mathrm{d}^3v = \int S_e\,\mathrm{d}^3v. \tag{4.7}$$

Note that we have neglected the curvature and ∇B drifts in equations (4.3) and (4.4). These drifts point in the z- and ζ-direction. The ζ-direction is unimportant because it is a direction of symmetry, whereas in the z-direction, the magnetic drifts can be neglected compared to the much larger terms due to the parallel velocity, $v_\parallel B_z/B$, and the z-component of the $\mathbf{E}\times\mathbf{B}$ drift, $v_{Ez} \simeq B^{-1}(\partial\phi/\partial r)$.

We have included the following collisions.

- Ion-ion and electron-electron collisions are modeled by the Fokker-Planck collision

operators $C_{ii}[f_i]$ and $C_{ee}[f_e]$ (Rosenbluth *et al.* 1957),

$$C_{ss}[f_s] := \frac{2\pi e^4 \ln\Lambda}{(4\pi\epsilon_0)^2 m_s^2}\nabla_v\cdot\left(\mathbf{D}[f_s]\cdot\nabla_v f_s + \mathbf{P}[f_s]f_s\right), \tag{4.8}$$

where the matrix $\mathbf{D}$ is

$$\mathbf{D}[f_s] := \int \frac{|\mathbf{v}-\mathbf{v}'|^2\mathbf{I} - (\mathbf{v}-\mathbf{v}')(\mathbf{v}-\mathbf{v}')}{|\mathbf{v}-\mathbf{v}'|^3} f_s(\mathbf{v}')\,\mathrm{d}^3v' \tag{4.9}$$

and the vector $\mathbf{P}$ is

$$\mathbf{P}[f_s] := -2\int \frac{\mathbf{v}-\mathbf{v}'}{|\mathbf{v}-\mathbf{v}'|^3} f_s(\mathbf{v}')\,\mathrm{d}^3v'. \tag{4.10}$$

Here, $\mathbf{I}$ is the 3D unit matrix, ϵ_0 the vacuum permittivity and $\ln\Lambda \approx 15$ the Coulomb logarithm.

• The effect of electron-ion and elastic electron-neutral collisions on the electron distribution function can be simplified in the limit of small electron-ion mass ratio, $m_e/m_i \ll 1$. With this expansion, we find the simplified Fokker-Planck collision operator

$$C_{ei}[f_e, f_i] := \frac{2\pi e^4 n_i \ln\Lambda}{(4\pi\epsilon_0)^2 m_e^2}\nabla_v\cdot\left[\frac{|\mathbf{v}-\mathbf{u}_i|^2\mathbf{I} - (\mathbf{v}-\mathbf{u}_i)(\mathbf{v}-\mathbf{u}_i)}{|\mathbf{v}-\mathbf{u}_i|^3}\cdot\nabla_v f_e\right] \tag{4.11}$$

for electron-ion collisions (Braginskii 1958), and the simplified Boltzmann collision operator

$$C_{en}[f_e, f_n] := \frac{n_n}{4\pi}\int_0^\pi \mathrm{d}\chi \int_0^{2\pi}\mathrm{d}\varphi\,\sin\chi R_{en}(|\mathbf{v}-\mathbf{u}_n|,\chi)\left[f_e(\overline{\mathbf{v}}(\mathbf{v},\chi,\varphi,\mathbf{u}_n)) - f_e(\mathbf{v})\right] \tag{4.12}$$

for electron-neutral collisions. Here

$$n_s(r,z,t) := \int f_s(r,z,\mathbf{v},t)\,\mathrm{d}^3v. \tag{4.13}$$

is the density of species s,

$$\mathbf{u}_s(r,z,t) := \frac{1}{n_s}\int \mathbf{v} f_s(r,z,\mathbf{v},t)\,\mathrm{d}^3v \tag{4.14}$$

is the average velocity of species s,

$$\overline{\mathbf{v}}(\mathbf{v},\chi,\varphi,\mathbf{u}_n) := \mathbf{u}_n + \cos\chi(\mathbf{v}-\mathbf{u}_n) + |\mathbf{v}-\mathbf{u}_n|\sin\chi(\cos\varphi\,\hat{\mathbf{e}}_1 + \sin\varphi\,\hat{\mathbf{e}}_2) \tag{4.15}$$

is a rotation of the vector $\mathbf{v}$ centered around $\mathbf{u}_n$, $R_{en}(|\mathbf{v}-\mathbf{u}_n|,\chi)$ is a function determined by the physics of the electron-neutral collisions, and the unit vectors $\hat{\mathbf{e}}_1$ and $\hat{\mathbf{e}}_2$ are chosen to form an orthonormal basis with the vector $(\mathbf{v}-\mathbf{u}_n)/|\mathbf{v}-\mathbf{u}_n|$. In equation (4.4), we have indicated that both C_{ei} and C_{en} are missing pieces small in m_e/m_i. These pieces can become important because they represent collisional energy exchange and collisional heating, but they are cumbersome. We showed in report 2047357-TN-05-01 M1.3 that the moment method that we use allows us to keep these important effects in the moment equations even with the simplified collision operators (4.11) and (4.12).

• The expansion in electron-ion mass ratio also implies electron-ion collisions and electron-neutral collisions have a very small effect on f_i and f_n – the terms C_{ie} and C_{ne} in equations (4.3) and (4.5) are small compared with C_{ii} and C_{ni} by a factor of $\sqrt{m_e/m_i} \ll 1$,

$$C_{ie} \sim \sqrt{\frac{m_e}{m_i}}C_{ii}, \quad C_{ne} \sim \sqrt{\frac{m_e}{m_i}}C_{ni}. \tag{4.16}$$

Like the mass ratio corrections to C_{ei} and C_{en}, these terms can become important because they contain the collisional energy exchange between electrons and the heavier species. We will keep these effects in a simplified form in our moment formulation.

• Charge-exchange collisions are represented by the simplified Boltzmann collision operators

$$C_{in}[f_i, f_n] := -\int R_{in}(|\mathbf{v}-\mathbf{v}'|)\left[f_i(\mathbf{v})f_n(\mathbf{v}') - f_i(\mathbf{v}')f_n(\mathbf{v})\right] \mathrm{d}^3v' \tag{4.17}$$

and

$$C_{ni}[f_n, f_i] := -\int R_{in}(|\mathbf{v}-\mathbf{v}'|)\left[f_n(\mathbf{v})f_i(\mathbf{v}') - f_n(\mathbf{v}')f_i(\mathbf{v})\right] \mathrm{d}^3v'. \tag{4.18}$$

• To model ionization, we use the collision operators

$$C_{i,\mathrm{ion}}[f_e, f_n] := f_n \int R_{\mathrm{ion}}(v')f_e(\mathbf{v}')\,\mathrm{d}^3v' \tag{4.19}$$

and

$$C_{n,\mathrm{ion}}[f_e, f_n] := -f_n \int R_{\mathrm{ion}}(v')f_e(\mathbf{v}')\,\mathrm{d}^3v'. \tag{4.20}$$

We also need to include a collision operator $C_{e,\mathrm{ion}}$ in the electron equation to model the increase in the number of electrons and the energy loss due to ionization. This operator is complicated because it involves three particles (the resulting ion and two electrons), but we will be able to avoid giving it a definite form. Instead, we will use the expansion in $m_e/m_i \ll 1$ and the fact that

$$C_{e,\mathrm{ion}}[f_e, f_n] \sim n_n R_{\mathrm{ion}} f_e. \tag{4.21}$$

See report 2047357-TN-05-01 M1.3 for more details.

• We have neglected neutral-neutral collisions because, in current fusion devices, the neutral density is sufficiently small that the neutral-neutral collisions are rare.

To simplify our equations, we assume that the functions R_{en}, R_{in} and R_{ion} are constant (Connor 1977; Hazeltine *et al.* 1992; Catto 1994), finding

$$\begin{aligned}\langle C_{en}[f_e, f_n]\rangle = &- n_n R_{en}\Bigg[f_e(r, z, v_\parallel, v_\perp, t) \\ &- \frac{1}{8\pi^2}\int_0^\pi \mathrm{d}\chi \int_0^{2\pi}\mathrm{d}\varphi \int_0^{2\pi}\mathrm{d}\varphi' \,\sin\chi f_e\left(r, z, \overline{v}_\parallel, \overline{v}_\perp, t\right)\Bigg],\end{aligned} \tag{4.22}$$

with

$$\overline{v}_\parallel(v_\parallel, v_\perp, \chi, \varphi', \mathbf{u}_n) := u_{n\parallel} + \overline{v}_{en}\cos\chi, \tag{4.23}$$

$$\overline{v}_\perp(v_\parallel, v_\perp, \chi, \varphi, \varphi', \mathbf{u}_n) := \sqrt{u_{n\perp}^2 + \overline{v}_{en}^2\sin^2\chi - 2u_{n\perp}\overline{v}_{en}\sin\chi\cos\varphi} \tag{4.24}$$

and

$$\overline{v}_{en}(v_\parallel, v_\perp, \varphi', \mathbf{u}_n) := \sqrt{(v_\parallel - u_{n\parallel})^2 + v_\perp^2 + u_{n\perp}^2 - 2v_\perp u_{n\perp}\cos\varphi'}, \tag{4.25}$$

$$\langle C_{in}[f_i, f_n]\rangle = -R_{in}\left(n_n f_i - n_i\langle f_n\rangle\right), \tag{4.26}$$

$$C_{ni}[f_n, f_i] = -R_{in}\left(n_i f_n - n_n f_i\right), \tag{4.27}$$

$$\langle C_{i,\mathrm{ion}}[f_e, f_n]\rangle = \langle f_n\rangle n_e R_{\mathrm{ion}} \tag{4.28}$$

and

$$C_{n,\mathrm{ion}}[f_e, f_n] = -f_n n_e R_{\mathrm{ion}}. \tag{4.29}$$

The potential $\phi(r,z,t)$ is determined by the quasineutrality equation

$$n_i = n_e. \tag{4.30}$$

To solve this equation, we need to treat the equations implicitly as the potential enters only via its effect on $\partial f_i/\partial t$ and $\partial f_e/\partial t$. The need to use implicit methods is one of the reasons why we are trying to extract some of the low order moments from the distribution function.

5. Wall boundary conditions

We impose wall boundary conditions at $z = 0$ and $z = L_z$. In principle, we need to consider the effect of the magnetic presheath (Chodura 1982) because the magnetic field is not perpendicular to the wall. However, the complicated boundary conditions that the magnetic presheath imposes on drift kinetic models are an active area of research (Geraldini *et al.* 2017, 2018, 2019; Geraldini 2021). To avoid this complication, we assume that the electron gyroradius is much smaller than the Debye length, thus ensuring that electrons are magnetized even within the thin sheath of non-neutral plasma with a width of the order of the Debye length that forms on walls to ensure quasineutrality. With this assumption, we can impose boundary conditions similar to those proposed by Parker *et al.* (1993).

The boundary conditions that we propose make use of the fact that the potential drop across the magnetic presheath and the Debye sheath repels electrons away from the wall because otherwise electrons would flow to the wall at much greater rate than ions due to their lower mass and higher thermal speed. In our model, $\phi(r,0,t)$ and $\phi(r,L_z,t)$ are not the potential of the wall, but the potential at the entrance of the magnetic presheath. In this report, we choose the potential of the wall at $z = 0$ to be 0 without loss of generality. We denote the potential of the wall at $z = L_z$ as ϕ_w. Then, for the magnetic presheaths and Debye sheaths to repel electrons, $\phi(r,0,t)$ must be larger than 0 and $\phi(r,L_z,t)$ must be larger than ϕ_w.

The value of the potential at $z = 0$ and $z = L_z$ is determined by the relationship between the current crossing the magnetic presheath and the Debye sheath and the total potential drop across these layers. We consider the magnetic presheath and the Debye sheath at $z = L_z$ first, and we will then apply the results that we obtain to the magnetic presheath and the Debye sheath at $z = 0$. Ions recombine when they hit the wall, so no ions come back. The velocity of the ions perpendicular to the wall is a combination of parallel velocity and $\mathbf{E}\times\mathbf{B}$ drift, $v_\parallel B_z/B + B^{-1}(\partial\phi/\partial r)$. Thus, the ions that would come back from the wall must satisfy $v_\parallel < -B_z^{-1}(\partial\phi/\partial r)$, giving

$$f_i(r,L_z,v_\parallel < -B_z^{-1}(\partial\phi/\partial r), v_\perp, t) = 0. \tag{5.1}$$

Since the electrons are magnetized, the potential drop across the magnetic presheath and the Debye sheath only modifies the parallel velocity of electrons. Within these layers, the parallel energy $\mathcal{E}_\parallel := m_e v_\parallel^2/2 - e\phi$ is conserved, and as a result an electron that has velocity $v_\parallel$ at the entrance of the sheath is slowed down to a parallel velocity $[v_\parallel^2 - 2e(\phi(r,L_z,t)-\phi_w)/m_e]^{1/2}$ when it reaches the wall. Thus, electrons with a parallel velocity larger than $\sqrt{2e(\phi(r,L_z,t)-\phi_w)/m_e}$ reach the wall, where they recombine with ions, whereas electrons with parallel velocity smaller than $\sqrt{2e(\phi(r,L_z,t)-\phi_w)/m_e}$ are repelled back into the quasineutral plasma. Thus, the boundary condition on the electron

distribution function at $z = L_z$ is

$$f_e(r, L_z, v_\parallel < 0, v_\perp, t) = \begin{cases} f_e(r, L_z, -v_\parallel, v_\perp, t) & \text{for } v_\parallel \geqslant -\sqrt{2e(\phi(r, L_z, t) - \phi_w)/m_e}, \\ 0 & \text{for } v_\parallel < -\sqrt{2e(\phi(r, L_z, t) - \phi_w)/m_e}. \end{cases} \tag{5.2}$$

Here we can neglect the $\mathbf{E} \times \mathbf{B}$ drift because it is small compared to the typical electron thermal speed by a factor of $\sqrt{m_e/m_i} \ll 1$. Expressions (5.1) and (5.2) give the parallel ion and electron current density towards the wall at the entrance of the sheath at $z = L_z$,

$$J_{i\parallel}(r, L_z, t) = 2\pi e \int_{-B_z^{-1}(\partial\phi/\partial r)}^{\infty} \mathrm{d}v_\parallel \int_0^\infty \mathrm{d}v_\perp \, v_\perp v_\parallel f_i(r, L_z, v_\parallel, v_\perp, t) \tag{5.3}$$

and

$$J_{e\parallel}(r, L_z, t) = -2\pi e \int_{\sqrt{2e(\phi(r,L_z,t)-\phi_w)/m_e}}^{\infty} \mathrm{d}v_\parallel \int_0^\infty \mathrm{d}v_\perp \, v_\perp v_\parallel f_e(r, L_z, v_\parallel, v_\perp, t). \tag{5.4}$$

Hence, the total parallel current density at $z = L_z$ is the following function of $\phi(r, L_z, t) - \phi_w$ and the radial derivative of $\phi(r, L_z, t) - \phi_w$,

$$\begin{aligned} J_\parallel(r, L_z, t) = {} & 2\pi e \int_{-B_z^{-1}(\partial\phi/\partial r)}^{\infty} \mathrm{d}v_\parallel \int_0^\infty \mathrm{d}v_\perp \, v_\perp v_\parallel f_i(r, L_z, v_\parallel, v_\perp, t) \\ & -2\pi e \int_{\sqrt{2e(\phi(r,L_z,t)-\phi_w)/m_e}}^{\infty} \mathrm{d}v_\parallel \int_0^\infty \mathrm{d}v_\perp \, v_\perp v_\parallel f_e(r, L_z, v_\parallel, v_\perp, t). \end{aligned} \tag{5.5}$$

We assume that the potential ϕ_w does not depend on r and hence the radial derivative of $\phi(r, L_z, t) - \phi_w$ is simply the radial derivative of $\phi(r, L_z, t)$.

The conditions at $z = 0$ for the ion and electron distribution functions and the potential are similar to those for $z = L_z$. For the ion and electron distribution functions, we find

$$f_i(r, 0, v_\parallel > -B_z^{-1}(\partial\phi/\partial r), v_\perp, t) = 0 \tag{5.6}$$

and

$$f_e(r, 0, v_\parallel > 0, v_\perp, t) = \begin{cases} f_e(r, 0, -v_\parallel, v_\perp, t) & \text{for } v_\parallel \leqslant \sqrt{2e\phi(r, 0, t)/m_e}, \\ 0 & \text{for } v_\parallel > \sqrt{2e\phi(r, 0, t)/m_e}, \end{cases} \tag{5.7}$$

The relationship between the parallel current and the potential at the magnetic presheath entrance is

$$\begin{aligned} J_\parallel(r, 0, t) = {} & -2\pi e \int_{-\infty}^{-B_z^{-1}(\partial\phi/\partial r)} \mathrm{d}v_\parallel \int_0^\infty \mathrm{d}v_\perp \, v_\perp v_\parallel f_i(r, 0, v_\parallel, v_\perp, t) \\ & +2\pi e \int_{-\infty}^{-\sqrt{2e\phi(r,0,t)/m_e}} \mathrm{d}v_\parallel \int_0^\infty \mathrm{d}v_\perp \, v_\perp v_\parallel f_e(r, 0, v_\parallel, v_\perp, t). \end{aligned} \tag{5.8}$$

We still need boundary conditions for the neutral distribution function. The neutrals hit the wall and thermalize at the temperature of the wall T_w, while also receiving back the ions that have recombined at the wall, that is,

$$f_n(r, 0, v_r, v_z > 0, v_\zeta, t) = \Gamma_0 f_{Kw}\left(v_z, \sqrt{v_r^2 + v_\zeta^2}\right) \tag{5.9}$$

and

$$f_n(r, L_z, v_r, v_z < 0, v_\zeta, t) = \Gamma_L f_{Kw}\left(v_z, \sqrt{v_r^2 + v_\zeta^2}\right), \tag{5.10}$$

where

$$f_{Kw}(v_n, v_t) := \frac{3}{4\pi}\left(\frac{m_i}{T_w}\right)^2 \frac{|v_n|}{\sqrt{v_n^2+v_t^2}} \exp\left(-\frac{m_i(v_n^2+v_t^2)}{2T_w}\right) \tag{5.11}$$

is the Knudsen cosine distribution (Knudsen 1916), and

$$\Gamma_0 := 2\pi \int_{-\infty}^{-B_z^{-1}(\partial\phi/\partial r)} \mathrm{d}v_\parallel \int_0^\infty \mathrm{d}v_\perp\, v_\perp \left|\frac{v_\parallel B_z}{B} + \frac{1}{B}\frac{\partial\phi}{\partial r}\right| f_i(r,0,v_\parallel,v_\perp,t) + \int_{-\infty}^\infty \mathrm{d}v_r \int_{-\infty}^0 \mathrm{d}v_z \int_{-\infty}^\infty \mathrm{d}v_\zeta\, |v_z| f_n(r,0,v_r,v_z,v_\zeta,t) \tag{5.12}$$

and

$$\Gamma_L := 2\pi \int_{-B_z^{-1}(\partial\phi/\partial r)}^\infty \mathrm{d}v_\parallel \int_0^\infty \mathrm{d}v_\perp\, v_\perp \left(\frac{v_\parallel B_z}{B} + \frac{1}{B}\frac{\partial\phi}{\partial r}\right) f_i(r,L_z,v_\parallel,v_\perp,t) + \int_{-\infty}^\infty \mathrm{d}v_r \int_0^\infty \mathrm{d}v_z \int_{-\infty}^\infty \mathrm{d}v_\zeta\, v_z f_n(r,L_z,v_r,v_z,v_\zeta,t) \tag{5.13}$$

are the fluxes of neutrals and ions towards the walls at $z=0$ and $z=L_z$.

6. 2D moment drift kinetics

Instead of solving for $f_s(r,z,v_\parallel,v_\perp,t)$ with $s=i,e$, we solve for

$$F_s(r,z,w_\parallel,w_\perp,t) := \frac{v_{ts}^3(r,z,t)}{n_s(r,z,t)} f_s\Big(r,z,u_{s\parallel}(r,z,t)+v_{ts}(r,z,t)w_\parallel, v_{ts}(r,z,t)w_\perp,t\Big), \tag{6.1}$$

where we have defined the normalized velocities

$$w_\parallel(r,z,v_\parallel,t) := \frac{v_\parallel - u_{s\parallel}(r,z,t)}{v_{ts}(r,z,t)} \tag{6.2}$$

and

$$w_\perp(r,z,v_\perp,t) := \frac{v_\perp}{v_{ts}(r,z,t)}, \tag{6.3}$$

the average parallel velocity

$$u_{s\parallel}(r,z,t) := \frac{2\pi}{n_s}\int_{-\infty}^\infty \mathrm{d}v_\parallel \int_0^\infty \mathrm{d}v_\perp\, v_\perp v_\parallel f_s(r,z,v_\parallel,v_\perp,t) \tag{6.4}$$

and the thermal speed

$$v_{ts}(r,z,t) := \sqrt{\frac{2T_s(r,z,t)}{m_s}}, \tag{6.5}$$

with

$$T_s(r,z,t) := \frac{2\pi}{n_s}\int_{-\infty}^\infty \mathrm{d}v_\parallel \int_0^\infty \mathrm{d}v_\perp\, v_\perp \frac{m_s[(v_\parallel - u_{s\parallel}(r,z,t))^2 + v_\perp^2]}{3} f_s(r,z,v_\parallel,v_\perp,t) \tag{6.6}$$

the temperature of species s. According to its definition, $F_s(r,z,w_\parallel,w_\perp,t)$ must satisfy the conditions

$$2\pi\int_{-\infty}^\infty \mathrm{d}w_\parallel \int_0^\infty \mathrm{d}w_\perp\, w_\perp F_s(r,z,w_\parallel,w_\perp,t) = 1, \tag{6.7}$$

$$2\pi\int_{-\infty}^\infty \mathrm{d}w_\parallel \int_0^\infty \mathrm{d}w_\perp\, w_\perp w_\parallel F_s(r,z,w_\parallel,w_\perp,t) = 0 \tag{6.8}$$

and

$$2\pi \int_{-\infty}^{\infty} \mathrm{d}w_{\parallel} \int_{0}^{\infty} \mathrm{d}w_{\perp}\, w_{\perp}(w_{\parallel}^2 + w_{\perp}^2) F_s(r, z, w_{\parallel}, w_{\perp}, t) = \frac{3}{2} \tag{6.9}$$

at every point (r, z) and time t.

Similarly, for neutrals, we solve for

$$F_n(r, z, \underbrace{w_r, w_z, w_\zeta}_{=\mathbf{w}}, t) := \frac{v_{tn}^3(r, z, t)}{n_n(r, z, t)} f_n\Big(r, z, \mathbf{u}_n(r, z, t) + v_{tn}(r, z, t)\mathbf{w}, t\Big), \tag{6.10}$$

where we have defined the neutral temperature

$$T_n(r, z, t) := \frac{1}{n_n} \int \frac{m_i |\mathbf{v} - \mathbf{u}_n(r, z, t)|^2}{3} f_n(r, z, \mathbf{v}, t)\, \mathrm{d}^3 v. \tag{6.11}$$

According to its definition, $F_n(r, z, \mathbf{w}, t)$ must satisfy the conditions

$$\int F_n(r, z, \mathbf{w}, t)\, \mathrm{d}^3 w = 1, \tag{6.12}$$

$$\int \mathbf{w} F_n(r, z, \mathbf{w}, t)\, \mathrm{d}^3 w = 0 \tag{6.13}$$

and

$$\int w^2 F_n(r, z, \mathbf{w}, t)\, \mathrm{d}^3 w = \frac{3}{2} \tag{6.14}$$

at every point (r, z) and time t.

6.1. *Ion equations*

The equations for n_i, $u_{i\parallel}$ and T_i are

$$\frac{\partial n_i}{\partial t} - \frac{\partial}{\partial r}\left(\frac{n_i}{B}\frac{\partial \phi}{\partial z}\right) + \frac{\partial}{\partial z}\left[n_i\left(\frac{u_{i\parallel} B_z}{B} + \frac{1}{B}\frac{\partial \phi}{\partial r}\right)\right] = n_n n_e R_{\mathrm{ion}} + \int S_i\, \mathrm{d}^3 v, \tag{6.15}$$

$$\begin{aligned} n_i m_i \left[\frac{\partial u_{i\parallel}}{\partial t} - \frac{1}{B}\frac{\partial \phi}{\partial z}\frac{\partial u_{i\parallel}}{\partial r} + \left(\frac{u_{i\parallel} B_z}{B} + \frac{1}{B}\frac{\partial \phi}{\partial r}\right)\frac{\partial u_{i\parallel}}{\partial z}\right] &= -\frac{B_z}{B}\frac{\partial p_{i\parallel}}{\partial z} - \frac{e n_i B_z}{B}\frac{\partial \phi}{\partial z} \\ &+ n_i m_i (n_n R_{in} + n_e R_{\mathrm{ion}})(u_{n\parallel} - u_{i\parallel}) + \int m_i (v_{\parallel} - u_{i\parallel}) S_i\, \mathrm{d}^3 v \end{aligned} \tag{6.16}$$

and

$$\begin{aligned} \frac{3}{2} n_i \left[\frac{\partial T_i}{\partial t} - \frac{1}{B}\frac{\partial \phi}{\partial z}\frac{\partial T_i}{\partial r} + \left(\frac{u_{i\parallel} B_z}{B} + \frac{1}{B}\frac{\partial \phi}{\partial r}\right)\frac{\partial T_i}{\partial z}\right] &= -\frac{B_z}{B}\frac{\partial q_{i\parallel}}{\partial z} - \frac{p_{i\parallel} B_z}{B}\frac{\partial u_{i\parallel}}{\partial z} \\ &+ \frac{3}{2} n_i (n_n R_{in} + n_e R_{\mathrm{ion}})(T_n - T_i) + \frac{1}{2} n_i m_i (n_n R_{in} + n_e R_{\mathrm{ion}})[(u_{n\parallel} - u_{i\parallel})^2 + u_{n\perp}^2] \\ &+ \frac{3 n_e m_e \nu_{ei}}{m_i}(T_e - T_i) + \int \left(\frac{1}{2} m_i |\mathbf{v} - u_{i\parallel}\hat{\mathbf{z}}|^2 - \frac{3}{2} T_i\right) S_i\, \mathrm{d}^3 v. \end{aligned} \tag{6.17}$$

Here,

$$\nu_{ei} := \frac{16\sqrt{\pi}}{3} \frac{e^4 n_i \ln \Lambda}{(4\pi\epsilon_0)^2 m_e^2 v_{te}^3} \tag{6.18}$$

is the electron-ion collision frequency as defined by Braginskii (Braginskii 1958), and we have defined the parallel pressure

$$p_{s\parallel}[F_s, n_s, v_{ts}](r, z, t) := 2\pi n_s m_s v_{ts}^2 \int_{-\infty}^{\infty} \mathrm{d}w_{\parallel} \int_{0}^{\infty} \mathrm{d}w_{\perp}\, w_{\perp} w_{\parallel}^2 F_s(r, z, w_{\parallel}, w_{\perp}, t) \tag{6.19}$$

and the parallel heat flux

$$q_{s\parallel}[F_s,n_s,v_{ts}](r,z,t):=\pi n_s m_s v_{ts}^3\int_{-\infty}^{\infty}\mathrm{d}w_\parallel\int_0^\infty \mathrm{d}w_\perp\, w_\perp w_\parallel (w_\parallel^2+w_\perp^2)F_s(r,z,w_\parallel,w_\perp,t) \tag{6.20}$$

for the charged species $s=i,e$.

The ion kinetic equation is

$$\frac{\partial F_i}{\partial t}+\dot{r}_i\frac{\partial F_i}{\partial r}+\dot{z}_i\frac{\partial F_i}{\partial z}+\dot{w}_{\parallel i}\frac{\partial F_i}{\partial w_\parallel}+\dot{w}_{\perp i}\frac{\partial F_i}{\partial w_\perp}=\dot{F}_i+\mathcal{C}_{ii}+\mathcal{C}_{in}+\mathcal{C}_{i,\mathrm{ion}}+\mathcal{S}_i. \tag{6.21}$$

Here, we have defined the coefficients

$$\dot{r}_i[\phi](r,z,t):=-\frac{1}{B}\frac{\partial\phi}{\partial z}, \tag{6.22}$$

$$\dot{z}_i[u_{i\parallel},v_{ti},\phi](r,z,w_\parallel,t):=\frac{u_{i\parallel}B_z}{B}+\frac{1}{B}\frac{\partial\phi}{\partial r}+\frac{v_{ti}B_z}{B}w_\parallel, \tag{6.23}$$

$$\begin{aligned}\dot{w}_{\parallel i}[F_i,n_i,u_{i\parallel},v_{ti}](r,z,w_\parallel,t):=&\frac{B_z}{n_i m_i v_{ti}B}\frac{\partial p_{i\parallel}}{\partial z}\\&+\frac{2w_\parallel B_z}{3n_i m_i v_{ti}^2 B}\left[\frac{\partial q_{i\parallel}}{\partial z}+\left(p_{i\parallel}-\frac{3}{2}n_i m_i v_{ti}^2\right)\frac{\partial u_{i\parallel}}{\partial z}\right]-\frac{w_\parallel^2 B_z}{B}\frac{\partial v_{ti}}{\partial z},\end{aligned} \tag{6.24}$$

$$\dot{w}_{\perp i}[F_i,n_i,u_{i\parallel},v_{ti}](r,z,w_\parallel,w_\perp,t):=\frac{2w_\perp B_z}{3n_i m_i v_{ti}^2 B}\left(\frac{\partial q_{i\parallel}}{\partial z}+p_{i\parallel}\frac{\partial u_{i\parallel}}{\partial z}\right)-\frac{w_\parallel w_\perp B_z}{B}\frac{\partial v_{ti}}{\partial z} \tag{6.25}$$

and

$$\begin{aligned}\dot{F}_i[F_i,n_i,u_{i\parallel},v_{ti}](r,z,w_\parallel,w_\perp,t):=&\frac{B_z}{B}\left[w_\parallel\left(3\frac{\partial v_{ti}}{\partial z}-\frac{v_{ti}}{n_i}\frac{\partial n_i}{\partial z}\right)\right.\\&\left.-\frac{2}{n_i m_i v_{ti}^2}\left(\frac{\partial q_{i\parallel}}{\partial z}+\left(p_{i\parallel}-\frac{1}{2}n_i m_i v_{ti}^2\right)\frac{\partial u_{i\parallel}}{\partial z}\right)\right]F_i.\end{aligned} \tag{6.26}$$

We have also defined a modified source $\mathcal{S}_i$ and several modified collision operators. The modified source for the charged species $s=i,e$ is given by

$$\begin{aligned}&\mathcal{S}_s[S_s,F_s,n_s,u_{s\parallel},v_{ts}](r,z,w_\parallel,w_\perp,t)\\&:=-\left[\frac{F_s}{n_s}\int S_s\,\mathrm{d}^3v-\frac{v_{ts}^3}{n_s}S_s(r,z,u_{s\parallel}+v_{ts}w_\parallel,v_{ts}w_\perp,t)\right]\\&\quad+\frac{\partial}{\partial w_\parallel}\left[F_s\left(\frac{1}{n_s v_{ts}}\int(v_\parallel-u_{s\parallel})S_s\,\mathrm{d}^3v+\frac{w_\parallel}{3n_s v_{ts}^2}\int\left(|\mathbf{v}-u_{s\parallel}\hat{\mathbf{z}}|^2-\frac{3}{2}v_{ts}^2\right)S_s\,\mathrm{d}^3v\right)\right]\\&\quad+\frac{1}{w_\perp}\frac{\partial}{\partial w_\perp}\left[\frac{w_\perp^2 F_s}{3n_s v_{ts}^2}\int\left(|\mathbf{v}-u_{s\parallel}\hat{\mathbf{z}}|^2-\frac{3}{2}v_{ts}^2\right)S_s\,\mathrm{d}^3v\right].\end{aligned} \tag{6.27}$$

Note that the differential terms in this modified source could have been included in the definitions of the coefficients $\dot{w}_{\parallel i}$, $\dot{w}_{\perp i}$ and $\dot{F}_i$, but we have decided to make them part of a modified source instead to separate the effect of the source clearly. We will do the same for collisions. This split should not be taken as a suggestion on how to implement these terms in a code. The modified collisions operators are described in Appendix A.

6.2. *Electron equations*

For the electrons, we use the expansion in m_e/m_i described in report 2047357-TN-05-01 M1.3. We first describe the electron fluid equations and how to use them.

- The electron continuity equation is

$$\frac{\partial n_e}{\partial t} - \frac{\partial}{\partial r}\left(\frac{n_e}{B}\frac{\partial \phi}{\partial z}\right) + \frac{\partial}{\partial z}\left[n_e\left(\frac{u_{e\parallel}B_z}{B} + \frac{1}{B}\frac{\partial \phi}{\partial r}\right)\right] = -n_e n_n R_{\text{ion}} + \int S_e \,\mathrm{d}^3 v. \quad (6.28)$$

Subtracting this equation from equation (6.15) and using quasineutrality, we obtain the current conservation equation

$$\frac{B_z}{B}\frac{\partial}{\partial z}\left[n_e\left(u_{i\parallel} - u_{e\parallel}\right)\right] = 0, \quad (6.29)$$

where we have used property (4.7). This equation can be used to calculate $u_{e\parallel}$ once $u_{e\parallel}$ is known at $z = 0$. We discuss how to obtain $u_{e\parallel}$ at $z = 0$ in the next bullet point.

- The electron parallel momentum equation simplifies to

$$0 = -\frac{B_z}{B}\frac{\partial p_{e\parallel}}{\partial z} + \frac{e n_e B_z}{B}\frac{\partial \phi}{\partial z} + F_{ei\parallel} + n_e m_e n_n R_{en}(u_{n\parallel} - u_{e\parallel}), \quad (6.30)$$

where

$$F_{ei\parallel}[F_e, n_e, n_i, u_{e\parallel}, u_{e\parallel}, v_{te}, v_{ti}](z,t) := -\frac{8\pi^2 e^4 n_e n_i \ln\Lambda}{(4\pi\epsilon_0)^2 m_e v_{te}^2}\int_{-\infty}^{\infty}\mathrm{d}w_\parallel \int_0^\infty \mathrm{d}w_\perp \frac{w_\perp (w_\parallel - (u_{i\parallel} - u_{e\parallel})/v_{te})F_e}{[(w_\parallel - (u_{i\parallel} - u_{e\parallel})/v_{te})^2 + w_\perp^2]^{3/2}} \quad (6.31)$$

is the friction force between electrons and ions. Equation (6.30) can be used to calculate the potential difference between $z = 0$ and any value of z, $\phi(r,z,t) - \phi(r,0,t)$. To completely determine the potential, we need to calculate $\phi(r,0,t)$. We do so with the current-potential relationships of the magnetic presheath and the Debye sheath, given in equations (5.5) and (5.8). We use two coupled nonlinear equations for the unknowns $\phi(r,0,t)$ and $\phi(r,L_z,t)$.

  - ◦ Integrating equation (6.29) between $z = 0$ and $z = L_z$, we obtain the condition $J_\parallel(r,L_z,t) - J_\parallel(r,0,t) = 0$. Since equations (5.5) and (5.8) give $J_\parallel(r,L_z,t)$ and $J_\parallel(r,0,t)$ as functions of $\phi(r,L_z,t) - \phi_w$ and $\phi(r,0,t)$, condition $J_\parallel(r,L_z,t) - J_\parallel(r,0,t) = 0$ is an equation for $\phi(r,L_z,t)$ and $\phi(r,0,t)$ (we assume the bias ϕ_w to be externally determined).
  - ◦ The other equation is the value of $\phi(r,L_z,t) - \phi(r,0,t)$ obtained by integrating equation (6.30) from $z = 0$ to $z = L_z$. Note that the value of $\phi(r,L_z,t) - \phi(r,0,t)$ depends on the unknown $u_{e\parallel}(r,0,t)$ (recall that $u_{e\parallel}$ can be determined everywhere from equation (6.29) for a given $u_{e\parallel}(r,0,t)$). The value $u_{e\parallel}(r,0,t)$ depends on $\phi(r,0,t)$ via equation (5.8) and so, in the end, equation (6.30) gives a relationship between $\phi(r,L_z,t) - \phi(r,0,t)$ and $\phi(r,0,t)$.

Once these two equations for $\phi(r,0,t)$ and $\phi(r,L_z,t)$ are solved, we can substitute the value of $\phi(r,0,t)$ in equation (5.8) to calculate $u_{e\parallel}(r,0,t)$, and then integrate equation (6.29) to find $u_{e\parallel}$ everywhere.

- The electron energy equation is

$$\frac{3}{2}n_e\left[\frac{\partial T_e}{\partial t}-\frac{1}{B}\frac{\partial\phi}{\partial z}\frac{\partial T_e}{\partial r}+\left(\frac{u_{e\parallel}B_z}{B}+\frac{1}{B}\frac{\partial\phi}{\partial r}\right)\frac{\partial T_e}{\partial z}\right]=-\frac{B_z}{B}\frac{\partial q_{e\parallel}}{\partial z}-\frac{p_{e\parallel}B_z}{B}\frac{\partial u_{e\parallel}}{\partial z}$$
$$-n_en_nR_{\rm ion}E_{\rm ion}+\frac{3n_em_e\nu_{ei}}{m_i}(T_i-T_e)+F_{ei\parallel}(u_{i\parallel}-u_{e\parallel})$$
$$+\frac{3n_em_en_nR_{en}}{m_i}(T_n-T_e)+n_em_en_nR_{en}[(u_{n\parallel}-u_{e\parallel})^2+u_{n\perp}^2]$$
$$+\int\left(\frac{1}{2}m_e|\mathbf{v}-u_{e\parallel}\hat{\mathbf{z}}|^2-\frac{3}{2}T_e\right)S_e\,\mathrm{d}^3v, \quad (6.32)$$

where $E_{\rm ion}$ is the ionization energy cost that includes in it radiation from excited states.

The kinetic equation for electrons is

$$\dot{z}_e\frac{\partial F_e}{\partial z}+\dot{w}_{\parallel e}\frac{\partial F_e}{\partial w_\parallel}+\dot{w}_{\perp e}\frac{\partial F_e}{\partial w_\perp}=\dot{F}_e+\mathcal{C}_{ee}+\mathcal{C}_{ei}+\mathcal{C}_{en}, \quad (6.33)$$

where

$$\dot{z}_e[F_e,v_{te}](z,w_\parallel,t):=v_{te}w_\parallel, \quad (6.34)$$

$$\dot{w}_{\parallel e}[F_e,u_{e\parallel},v_{te}](z,w_\parallel,t):=\frac{B_z}{n_em_ev_{te}B}\frac{\partial p_{e\parallel}}{\partial z}+\frac{2w_\parallel B_z}{3n_em_ev_{te}^2B}\frac{\partial q_{e\parallel}}{\partial z}-\frac{w_\parallel^2B_z}{B}\frac{\partial v_{te}}{\partial z}, \quad (6.35)$$

$$\dot{w}_{\perp e}[F_e,u_{e\parallel},v_{te}](z,w_\parallel,w_\perp,t):=\frac{2w_\perp B_z}{3n_em_ev_{te}^2B}\frac{\partial q_{e\parallel}}{\partial z}-\frac{w_\parallel w_\perp B_z}{B}\frac{\partial v_{te}}{\partial z} \quad (6.36)$$

and

$$\dot{F}_e[F_e,u_{e\parallel},v_{te}](z,w_\parallel,w_\perp,t):=\frac{B_z}{B}\left[w_\parallel\left(3\frac{\partial v_{te}}{\partial z}-\frac{v_{te}}{n_e}\frac{\partial n_e}{\partial z}\right)-\frac{2}{n_em_ev_{te}^2}\frac{\partial q_{e\parallel}}{\partial z}\right]F_e. \quad (6.37)$$

The modified collision operators $\mathcal{C}_{ee}$, $\mathcal{C}_{ei}$ and $\mathcal{C}_{en}$ are described in Appendix B.

6.3. *Neutral equations*

The fluid equations for the neutrals are

$$\frac{\partial n_n}{\partial t}+\nabla\cdot(n_n\mathbf{u}_n)=-n_nn_eR_{\rm ion}+\int S_n\,\mathrm{d}^3v, \quad (6.38)$$

$$n_nm_i\left(\frac{\partial\mathbf{u}_n}{\partial t}+\mathbf{u}_n\cdot\nabla\mathbf{u}_n\right)=-\nabla\cdot\mathbf{P}_n+n_nm_in_iR_{in}\left(u_{i\parallel}\hat{\boldsymbol{\zeta}}-\mathbf{u}_n\right)$$
$$+\int m_i(\mathbf{v}-\mathbf{u}_n)S_n\,\mathrm{d}^3v \quad (6.39)$$

and

$$\frac{3}{2}n_n\left(\frac{\partial T_n}{\partial t}+\mathbf{u}_n\cdot\nabla T_n\right)=-\nabla\cdot\mathbf{q}_n-\mathbf{P}_n:\nabla\mathbf{u}_n+\frac{3}{2}n_nn_iR_{in}(T_i-T_n)$$
$$+\frac{1}{2}n_nm_in_iR_{in}[(u_{n\parallel}-u_{i\parallel})^2+u_{n\perp}^2]+\frac{3n_em_en_nR_{en}}{m_i}(T_e-T_n)$$
$$+\int\left(\frac{1}{2}m_i|\mathbf{v}-\mathbf{u}_n|^2-\frac{3}{2}T_n\right)S_n\,\mathrm{d}^3v. \quad (6.40)$$

Here, we have defined the pressure tensor

$$\mathbf{P}_n[F_n, n_n, v_{tn}](r, z, t) := n_n m_i v_{tn}^2 \int \mathbf{w}\mathbf{w} F_n(r, z, \mathbf{w}, t)\, \mathrm{d}^3 w \tag{6.41}$$

and the heat flux

$$\mathbf{q}_n[F_n, n_n, v_{tn}](z, t) := \frac{1}{2} n_n m_i v_{tn}^3 \int w^2 \mathbf{w} F_n(r, z, \mathbf{w}, t)\, \mathrm{d}^3 w. \tag{6.42}$$

The neutral kinetic equation is

$$\frac{\partial F_n}{\partial t} + \dot{r}_n \frac{\partial F_n}{\partial r} + \dot{z}_n \frac{\partial F_n}{\partial z} + \dot{\mathbf{w}}_n \cdot \nabla_w F_n = \dot{F}_n + \mathcal{C}_{ni} + \mathcal{S}_n, \tag{6.43}$$

where we have defined the coefficients

$$\dot{r}_n[u_{nr}, v_{tn}](r, z, w_r, t) := u_{nr} + v_{tn} w_r, \tag{6.44}$$

$$\dot{z}_i[u_{nz}, v_{tn}](r, z, w_z, t) := u_{nz} + v_{tn} w_z, \tag{6.45}$$

$$\begin{aligned}\dot{\mathbf{w}}_n[F_n, n_n, \mathbf{u}_n, v_{tn}](r, z, \mathbf{w}, t) := {} & \frac{1}{n_n m_i v_{tn}} \nabla \cdot \mathbf{P}_n \\ & + \frac{2\mathbf{w}}{3 n_n m_i v_{tn}^2} \left(\nabla \cdot \mathbf{q}_n + \mathbf{P}_n : \nabla \mathbf{u}_n\right) - \mathbf{w} \cdot \nabla \mathbf{u}_n - \mathbf{w}\mathbf{w} \cdot \nabla v_{tn},\end{aligned} \tag{6.46}$$

The modified charge exchange collision operator $\mathcal{C}_{ni}$ is described in Appendix C. The modified source is

$$\begin{aligned}\mathcal{S}_n[S_n, F_n, n_n, \mathbf{u}_n, v_{tn}](r, z, \mathbf{w}, t) := {} & -\left[\frac{F_n}{n_n} \int S_n\, \mathrm{d}^3 v - \frac{v_{tn}^3}{n_n} S_s(r, z, \mathbf{u}_n + v_{tn}\mathbf{w}, t)\right] \\ & + \nabla_w \cdot \left[F_n \left(\frac{1}{n_n v_{tn}} \int (\mathbf{v} - \mathbf{u}_n) S_n\, \mathrm{d}^3 v + \frac{\mathbf{w}}{3 n_n v_{tn}^2} \int \left(|\mathbf{v} - \mathbf{u}_n|^2 - \frac{3}{2} v_{tn}^2\right) S_n\, \mathrm{d}^3 v\right)\right].\end{aligned} \tag{6.47}$$

6.4. *Boundary conditions*

These equations have to be solved with the boundary conditions in equations (5.1), (5.2), (5.6), (5.7), (5.9) and (5.10). For n_s, $u_{s\parallel}$, v_{ts} and F_s known at time t, we can construct f_s at $z = 0$ and $z = L_z$, and we can apply the wall boundary conditions to f_s. We can then use the resulting f_s to obtain n_s, $\mathbf{u}_s$, v_{ts} and F_s, closing the system of equations.

7. Discussion

The model that we propose is comprised of:

- the three fluid equations (6.15), (6.16) and (6.17) for ions that have to be solved in conjunction with the ion kinetic equation (6.21);
- the five fluid equations (6.38), (6.39) and (6.40) for neutrals that have to be solved in conjunction with the neutral kinetic equation (6.43);
- the two fluid equations (6.29) and (6.32) for electrons that have to be solved in conjunction with the electron kinetic equation (6.33); and
- the electron parallel momentum equation (6.30) for the potential.

The boundary conditions for this system of equations are described in section 5.

To test the model proposed in this report, we will first extend the existing 1D code based on adiabatic electrons to wall boundary conditions. We will then explore the effect

of adding electrons. For most physics of interest, it is sufficient to use simplified ion-ion and electron-electron collision operators, and for this reason we do not expect to implement a full Fokker-Planck collision operator.

Appendix A. Modified collision operators for the ion kinetic equation

The modified Fokker-Planck like-particle collision operator is

$$\begin{aligned}&\mathcal{C}_{ss}[F_s,n_s,v_{ts}](r,z,w_\parallel,w_\perp,t)\\&\quad:=\frac{2\pi e^4 n_s\ln\Lambda}{(4\pi\epsilon_0)^2 m_s^2 v_{ts}^3}\left\{\frac{\partial}{\partial w_\parallel}\left(\mathcal{D}_{\parallel\parallel}[F_s]\frac{\partial F_s}{\partial w_\parallel}+\mathcal{D}_{\parallel\perp}[F_s]\frac{\partial F_s}{\partial w_\perp}+\mathcal{P}_\parallel[F_s]F_s\right)\right.\\&\qquad\left.+\frac{1}{w_\perp}\frac{\partial}{\partial w_\perp}\left[w_\perp\left(\mathcal{D}_{\parallel\perp}[F_s]\frac{\partial F_s}{\partial w_\parallel}+\mathcal{D}_{\perp\perp}[F_s]\frac{\partial F_s}{\partial w_\perp}+\mathcal{P}_\perp[F_s]F_s\right)\right]\right\}.\end{aligned}\tag{A 1}$$

The coefficients needed for this collision operator are

$$\begin{aligned}\mathcal{D}_{\parallel\parallel}[F_s](r,z,w_\parallel,w_\perp,t):=4\int_{-\infty}^{\infty}\mathrm{d}w'_\parallel\int_0^\infty\mathrm{d}w'_\perp\,\frac{w'_\perp}{\sqrt{(w_\parallel-w'_\parallel)^2+(w_\perp+w'_\perp)^2}}\\\times\left(K(\kappa)-\frac{(w_\parallel-w'_\parallel)^2E(\kappa)}{(w_\parallel-w'_\parallel)^2+(w_\perp-w'_\perp)^2}\right)F_s(z,w'_\parallel,w'_\perp,t),\end{aligned}\tag{A 2}$$

$$\begin{aligned}\mathcal{D}_{\parallel\perp}[F_s](r,z,w_\parallel,w_\perp,t):=2\int_{-\infty}^{\infty}\mathrm{d}w'_\parallel\int_0^\infty\mathrm{d}w'_\perp\,\frac{w'_\perp(w_\parallel-w'_\parallel)}{w_\perp\sqrt{(w_\parallel-w'_\parallel)^2+(w_\perp+w'_\perp)^2}}\\\times\left(\frac{[(w_\parallel-w'_\parallel)^2-w_\perp^2+w'^2_\perp]E(\kappa)}{(w_\parallel-w'_\parallel)^2+(w_\perp-w'_\perp)^2}-K(\kappa)\right)F_s(z,w'_\parallel,w'_\perp,t),\end{aligned}\tag{A 3}$$

$$\begin{aligned}\mathcal{D}_{\perp\perp}[F_s](r,z,w_\parallel,w_\perp,t):=2\int_{-\infty}^{\infty}\mathrm{d}w'_\parallel\int_0^\infty\mathrm{d}w'_\perp\,\frac{w'_\perp}{w_\perp^2\sqrt{(w_\parallel-w'_\parallel)^2+(w_\perp+w'_\perp)^2}}\\\times\left\{2w_\perp\left[\frac{w_\perp(w_\parallel-w'_\parallel)^2}{(w_\parallel-w'_\parallel)^2+(w_\perp-w_\perp)^2}-w'_\perp\right]E(\kappa)\right.\\\left.+[(w_\parallel-w'_\parallel)^2+w_\perp^2+w'^2_\perp][K(\kappa)-E(\kappa)]\right\}F_s(z,w'_\parallel,w'_\perp,t),\end{aligned}\tag{A 4}$$

$$\begin{aligned}\mathcal{P}_\parallel[F_s](r,z,w_\parallel,w_\perp,t):=8\int_{-\infty}^{\infty}\mathrm{d}w'_\parallel\int_0^\infty\mathrm{d}w'_\perp\,\frac{w'_\perp(w_\parallel-w'_\parallel)}{\sqrt{(w_\parallel-w'_\parallel)^2+(w_\perp+w'_\perp)^2}}\\\times\left(\frac{K(\kappa)-E(\kappa)}{(w_\parallel-w'_\parallel)^2+(w_\perp+w'_\perp)^2}-\frac{E(\kappa)}{(w_\parallel-w'_\parallel)^2+(w_\perp-w'_\perp)^2}\right)F_s(z,w'_\parallel,w'_\perp,t)\end{aligned}\tag{A 5}$$

and

$$\mathcal{P}_\perp[F_s](r,z,w_\parallel,w_\perp,t) := 4\int_{-\infty}^{\infty}\mathrm{d}w'_\parallel\int_0^{\infty}\mathrm{d}w'_\perp\,\frac{w'_\perp}{w_\perp\sqrt{(w_\parallel-w'_\parallel)^2+(w_\perp+w'_\perp)^2}} \times\left(\frac{[(w_\parallel-w'_\parallel)^2-w_\perp^2+w'^2_\perp]E(\kappa)}{(w_\parallel-w'_\parallel)^2+(w_\perp-w'_\perp)^2}-K(\kappa)\right)F_s(z,w'_\parallel,w'_\perp,t). \quad (A\,6)$$

Here, $K(\kappa) := \int_0^{\pi/2}(1-\kappa^2\sin^2\alpha)^{-1/2}\,\mathrm{d}\alpha$ and $E(\kappa) := \int_0^{\pi/2}(1-\kappa^2\sin^2\alpha)^{1/2}\,\mathrm{d}\alpha$ are the elliptic integrals, and the function κ is

$$\kappa(w_\parallel,w_\perp,w'_\parallel,w'_\perp) := \sqrt{\frac{4w_\perp w'_\perp}{(w_\parallel-w'_\parallel)^2+(w_\perp+w'_\perp)^2}}. \quad (A\,7)$$

The modified charge exchange collision operator for the ion kinetic equation is

$$\begin{aligned}&\mathcal{C}_{in}[F_i,\langle F_n\rangle,n_n,u_{i\parallel},\mathbf{u}_n,v_{ti},v_{tn}](z,w_\parallel,w_\perp,t)\\ &\quad:= -n_nR_{in}\left[F_i-\frac{v_{ti}^3}{v_{tn}^3}\langle F_n\rangle\left(r,z,\frac{u_{i\parallel}-u_{n\parallel}}{v_{tn}}+\frac{v_{ti}}{v_{tn}}w_\parallel,\frac{v_{ti}}{v_{tn}}w_\perp,t\right)\right]\\ &\qquad+n_nR_{in}\frac{\partial}{\partial w_\parallel}\left[\left(\frac{u_{n\parallel}-u_{i\parallel}}{v_{ti}}+\frac{w_\parallel}{2}\left(\frac{v_{tn}^2}{v_{ti}^2}-1+\frac{2[(u_{n\parallel}-u_{i\parallel})^2+u_{n\perp}^2]}{3v_{ti}^2}\right)\right)F_i\right]\\ &\qquad+\frac{n_nR_{in}}{w_\perp}\frac{\partial}{\partial w_\perp}\left[\frac{w_\perp^2}{2}\left(\frac{v_{tn}^2}{v_{ti}^2}-1+\frac{2[(u_{n\parallel}-u_{i\parallel})^2+u_{n\perp}^2]}{3v_{ti}^2}\right)F_i\right], \quad (A\,8)\end{aligned}$$

where

$$\begin{aligned}&\langle F_n\rangle[F_n,\mathbf{u}_{n\perp}](r,z,w_\parallel,w_\perp,t)\\ &\qquad:=\frac{1}{2\pi}\int_0^{2\pi}F_n\left(r,z,w_\perp\cos\varphi-\frac{u_{nr}}{v_{tn}},w_\perp\sin\varphi-\frac{u_{nz}}{v_{tn}},w_\parallel,t\right)\mathrm{d}\varphi \quad (A\,9)\end{aligned}$$

is the gyroaverage of F_n.

Finally, the modified ionization collision operator for the ion kinetic equation is

$$\begin{aligned}&\mathcal{C}_{i,\mathrm{ion}}[\langle F_n\rangle,n_e,u_{i\parallel},\mathbf{u}_n,v_{ti},v_{tn}](r,z,w_\parallel,w_\perp,t)\\ &\quad:= -n_eR_{\mathrm{ion}}\left[F_i-\frac{v_{ti}^3}{v_{tn}^3}\langle F_n\rangle\left(r,z,\frac{u_{i\parallel}-u_{n\parallel}}{v_{tn}}+\frac{v_{ti}}{v_{tn}}w_\parallel,\frac{v_{ti}}{v_{tn}}w_\perp,t\right)\right]\\ &\qquad+n_eR_{\mathrm{ion}}\frac{\partial}{\partial w_\parallel}\left[\left(\frac{u_{n\parallel}-u_{i\parallel}}{v_{ti}}+\frac{w_\parallel}{2}\left(\frac{v_{tn}^2}{v_{ti}^2}-1+\frac{2[(u_{n\parallel}-u_{i\parallel})^2+u_{n\perp}^2]}{3v_{ti}^2}\right)\right)F_i\right]\\ &\qquad+\frac{n_eR_{\mathrm{ion}}}{w_\perp}\frac{\partial}{\partial w_\perp}\left[\frac{w_\perp^2}{2}\left(\frac{v_{tn}^2}{v_{ti}^2}-1+\frac{2[(u_{n\parallel}-u_{i\parallel})^2+u_{n\perp}^2]}{3v_{ti}^2}\right)F_i\right]. \quad (A\,10)\end{aligned}$$

Appendix B. Modified collision operators for the electron kinetic equation

The electron-electron collision operator is described in equation (A 1).

The modified ion-electron collision operator is

$$\begin{aligned}&\mathcal{C}_{ei}[F_e, n_i, u_{i\parallel}, u_{e\parallel}, v_{te}](r, z, w_\parallel, w_\perp, t)\\ &\quad:=\frac{2\pi e^4 n_i \ln\Lambda}{(4\pi\epsilon_0)^2 m_e^2 v_{te}^3}\left\{\frac{\partial}{\partial w_\parallel}\left[\mathcal{M}_{\parallel\parallel}\frac{\partial F_e}{\partial w_\parallel}+\mathcal{M}_{\parallel\perp}\frac{\partial F_e}{\partial w_\perp}+\left(1+\frac{2(u_{i\parallel}-u_{e\parallel})w_\parallel}{3v_{te}}\right)\mathcal{F}_\parallel F_e\right]\right.\\ &\qquad\left.+\frac{1}{w_\perp}\frac{\partial}{\partial w_\perp}\left[w_\perp\left(\mathcal{M}_{\parallel\perp}\frac{\partial F_e}{\partial w_\parallel}+\mathcal{M}_{\perp\perp}\frac{\partial F_e}{\partial w_\perp}+\frac{2(u_{i\parallel}-u_{e\parallel})w_\perp}{3v_{te}}\mathcal{F}_\parallel F_e\right)\right]\right\},\end{aligned}\tag{B 1}$$

where

$$\mathcal{M}_{\parallel\parallel}[u_{e\parallel}, v_{te}, u_{i\parallel}](r, z, w_\parallel, w_\perp, t) := \frac{w_\perp^2}{[(w_\parallel-(u_{i\parallel}-u_{e\parallel})/v_{te})^2+w_\perp^2]^{3/2}},\tag{B 2}$$

$$\mathcal{M}_{\parallel\perp}[u_{e\parallel}, v_{te}, u_{i\parallel}](r, z, w_\parallel, w_\perp, t) := -\frac{(w_\parallel-(u_{i\parallel}-u_{e\parallel})/v_{te})^2 w_\perp}{[(w_\parallel-(u_{i\parallel}-u_{e\parallel})/v_{te})^2+w_\perp^2]^{3/2}},\tag{B 3}$$

$$\mathcal{M}_{\perp\perp}[u_{e\parallel}, v_{te}, u_{i\parallel}](r, z, w_\parallel, w_\perp, t) := \frac{(w_\parallel-(u_{i\parallel}-u_{e\parallel})/v_{te})^2}{[(w_\parallel-(u_{i\parallel}-u_{e\parallel})/v_{te})^2+w_\perp^2]^{3/2}}\tag{B 4}$$

and

$$\begin{aligned}&\mathcal{F}_\parallel[F_e, u_{e\parallel}, v_{te}, u_{i\parallel}](r, z, t)\\ &\qquad:=-4\pi\int_{-\infty}^{\infty}\mathrm{d}w_\parallel\int_0^\infty \mathrm{d}w_\perp\,\frac{w_\perp[w_\parallel-(u_{i\parallel}-u_{e\parallel})/v_{te}]F_e(z, w_\parallel, w_\perp, t)}{[(w_\parallel-(u_{i\parallel}-u_{e\parallel})/v_{te})^2+w_\perp^2]^{3/2}}.\end{aligned}\tag{B 5}$$

The modified electron-neutral collision operator is

$$\begin{aligned}\mathcal{C}_{en}[F_e, n_n, \mathbf{u}_n, u_{e\parallel}, v_{te}](z, w_\parallel, w_\perp, t) := -n_n R_{en}&\left[F_e\right.\\ &\left.-\frac{1}{8\pi^2}\int_0^\pi \mathrm{d}\chi\int_0^{2\pi}\mathrm{d}\varphi\int_0^{2\pi}\mathrm{d}\varphi'\,\sin\chi F_e(z, \overline{w}_\parallel, \overline{w}_\perp, t)\right]\\ &+n_n R_{en}\frac{\partial}{\partial w_\parallel}\left[\left(1+\frac{2[(u_{n\parallel}-u_{e\parallel})^2+u_{n\perp}^2]w_\parallel}{3v_{te}^2}\right)F_e\right]\\ &+\frac{2n_n R_{en}[(u_{n\parallel}-u_{e\parallel})^2+u_{n\perp}^2]}{3v_{te}^2 w_\perp}\frac{\partial}{\partial w_\perp}\left(w_\perp^2 F_e\right),\end{aligned}\tag{B 6}$$

where

$$\overline{w}_\parallel[u_{e\parallel}, v_{te}, \mathbf{u}_n](r, z, w_\parallel, w_\perp, \chi, \varphi', t) := \frac{u_{n\parallel}-u_{e\parallel}}{v_{te}}+\overline{w}_{en}\cos\chi,\tag{B 7}$$

$$\overline{w}_\perp[u_{e\parallel}, v_{te}, u_{n\parallel}](r, z, w_\parallel, w_\perp, \chi, \varphi, \varphi' t) := \sqrt{\frac{u_{n\perp}^2}{v_{te}^2}+\overline{w}_{en}^2\sin^2\chi-\frac{2u_{n\perp}\overline{w}_{en}}{v_{te}}\sin\chi\cos\varphi}\tag{B 8}$$

and

$$\begin{aligned}&\overline{w}_{en}[u_{e\parallel}, v_{te}, \mathbf{u}_n](r, z, w_\parallel, w_\perp, \varphi', t)\\ &\qquad:=\sqrt{\left(w_\parallel+\frac{u_{e\parallel}-u_{n\parallel}}{v_{te}}\right)^2+w_\perp^2+\frac{u_{n\perp}^2}{v_{te}^2}-\frac{2u_{n\perp}w_\perp}{v_{te}}\cos\varphi'}.\end{aligned}\tag{B 9}$$

Appendix C. Modified collision operators for the neutral kinetic equation

The modified charge exchange collision operator for the neutral kinetic equation is

$$\begin{aligned}\mathcal{C}_{ni}[F_n, F_i, n_i, \mathbf{u}_n, u_{i\parallel}, v_{tn}, v_{ti}](r, z, w_r, w_z, w_\zeta, t)\\ := -n_i R_{in}\left[F_n - \frac{v_{tn}^3}{v_{ti}^3} F_i\left(r, z, \frac{u_{n\parallel} - u_{i\parallel}}{v_{ti}} + \frac{v_{tn}}{v_{ti}} w_\zeta, \frac{v_{tn}}{v_{ti}}\left|\mathbf{w}_\perp + \frac{\mathbf{u}_{n\perp}}{v_{tn}}\right|, t\right)\right]\\ + n_i R_{in} \nabla_w \cdot \left[\left(\frac{u_{i\parallel}\hat{\boldsymbol{\zeta}} - \mathbf{u}_n}{v_{tn}} + \frac{\mathbf{w}}{2}\left(\frac{v_{ti}^2}{v_{tn}^2} - 1 + \frac{2[(u_{n\parallel} - u_{i\parallel})^2 + u_{n\perp}^2]}{3v_{tn}^2}\right)\right) F_n\right],\end{aligned} \tag{C 1}$$

where

$$\left|\mathbf{w}_\perp + \frac{\mathbf{u}_{n\perp}}{v_{tn}}\right| \simeq \sqrt{\left(w_r + \frac{u_{nr}}{v_{tn}}\right)^2 + \left(w_z + \frac{u_{nz}}{v_{tn}}\right)^2}. \tag{C 2}$$

REFERENCES

Braginskii, S.I. 1958 Transport phenomena in a completely ionized two-temperature plasma. *Sov. Phys. JETP* **6**, 358.

Catto, P.J. 1994 A short mean-free path, coupled neutral-ion transport description of a tokamak edge plasma. *Phys. Plasmas* **1**, 1936.

Chodura, R. 1982 Plasma-wall transition in an oblique magnetic field. *Phys. Fluids* **25**, 1628.

Connor, J.W. 1977 An analytic solution for the distribution function of neutral particles in a Maxwellian plasma using the method of singular eigenfunctions. *Plasma Phys.* **19**, 853.

Geraldini, A. 2021 Large gyro-orbit model of ion velocity distribution in plasma near a wall in a grazing-angle magnetic field. *J. Plasma Phys.* **87**, 905870113.

Geraldini, A., Parra, F.I. & Militello, F. 2017 Gyrokinetic treatment of a grazing angle magnetic presheath. *Plasma Phys. Control. Fusion* **59**, 025015.

Geraldini, A., Parra, F.I. & Militello, F. 2018 Solution to a collisionless shallow-angle magnetic presheath with kinetic ions. *Plasma Phys. Control. Fusion* **60**, 125002.

Geraldini, A., Parra, F.I. & Militello, F. 2019 Dependence on ion temperature of shallow-angle magnetic presheaths with adiabatic electrons. *J. Plasma Phys.* **85**, 795850601.

Hazeltine, R.D. 1973 Recursive derivation of drift-kinetic equation. *Plasma Phys.* **15**, 77–80.

Hazeltine, R.D., Calvin, M.D., Valanju, P.M. & Solano, E.R. 1992 Analytical calculation of neutral transport and its effect on ions. *Nucl. Fusion* **32**, 3.

Helander, P., Krasheninnikov, S.I. & Catto, P.J. 1994 Fluid equations for a partially ionized plasma. *Phys. Plasmas* **1**, 3174.

Knudsen, M. 1916 Das Cosinusgesetz in der kinetischen Gastheorie. *Annal. Phys.* **353**, 1113.

Parker, S.E., Procassini, R.J. & Birdsall, C.K. 1993 A Suitable Boundary Condition for Bounded Plasma Simulation without Sheath Resolution. *J. Comput. Phys.* **104**, 41.

Pastukhov, V.P. 1974 Collisional losses of electrons from an adiabatic trap in a plasma with a positive potential. *Nucl. Fusion* **14**, 3.

Rosenbluth, M.N., MacDonald, W.M. & Judd, D.L. 1957 Fokker-Planck Equation for an Inverse-Square Force. *Phys. Rev.* **107**, 1.

2D drift kinetic model with periodic boundary conditions

Felix I. Parra, Michael Barnes and Michael Hardman

Rudolf Peierls Centre for Theoretical Physics, University of Oxford, Oxford OX1 3PU, UK

(This version is of 29 September 2021)

1. Introduction

In report 2047357-TN-07-02, we presented a 2D drift kinetic model for a helical magnetic field with wall boundary conditions. The wall boundary conditions made it possible to obtain the potential and the electron flow from the conservation of parallel current and the electron parallel momentum equation. With periodic boundary conditions, appropriate for closed flux surfaces, it will not be sufficient with conservation of parallel current, and we will have to include terms small in the expansion parameter that we use, the ion gyroradius over the characteristic width of the scrape-off layer (ρ_i/L_r).

In this report, we first remind the reader of the content in report 2047357-TN-07-02, and we then explain how to modify the current conservation equations for cases with periodic boundary conditions.

2. Magnetic field, geometry and orderings

We use the cylindrical coordinates $\{r, z, \zeta\}$ (see report 2047357-TN-07-02 for the direction of increase of ζ). We consider a magnetized plasma with one ion species with charge e and mass m_i, electrons with charge $-e$ and mass m_e, and one species of neutrals with mass

$$m_n = m_i. \tag{2.1}$$

The plasma is magnetized by the helical magnetic field

$$\mathbf{B}(r,\zeta) := B_z(r)\hat{\mathbf{z}} + B_\zeta(r)\hat{\boldsymbol{\zeta}}(\zeta), \tag{2.2}$$

where $\hat{\mathbf{z}}$ and $\hat{\boldsymbol{\zeta}}$ are the unit vectors in the direction of ∇z and $\nabla\zeta$. Note that the components B_z and B_ζ only depend on the radial position r.

We assume that the plasma only varies in r and z. We assume that the electric field produced by the plasma is electrostatic, $\mathbf{E} = -(\partial\phi/\partial r)\hat{\mathbf{r}} - (\partial\phi/\partial z)\hat{\mathbf{z}}$, where $\hat{\mathbf{r}}$ is the unit vector in the direction ∇r. The potential $\phi(r,z,t)$ depends on the coordinates r and z and on time t.

We impose periodic boundary conditions at $z = 0$ and $z = L_z$. In the radial direction, we consider the interval between $r = r_0$ and $r = r_0 + L_r$. The length L_r is determined by a balance between the fast parallel velocity of the particles along magnetic field lines and their slow drift across them. The characteristic length between the two walls along a magnetic field line is of order

$$L_\parallel \sim \frac{B}{B_z} L_z. \tag{2.3}$$

Thus, the typical time that it takes for an ion to move from wall to wall is $L_\parallel/v_{ti} \sim$

$(B/B_z)(L_z/v_{ti})$, where $v_{ti} := \sqrt{2T_i/m_i}$ is the ion thermal speed and T_i is the ion temperature. For a potential ϕ of the order of T_i/e, where e is the proton charge, the radial $\mathbf{E}\times\mathbf{B}$ drift is

$$v_{Er} := -\frac{B_\zeta}{B^2}\frac{\partial\phi}{\partial z} \sim \frac{\rho_i}{L_z} v_{ti}, \tag{2.4}$$

where $\rho_i := v_{ti}/\Omega_i$ is the characteristic ion gyroradius and $\Omega_i := eB/m_i$ is the ion gyrofrequency. Thus, the time it takes for an ion to cross the domain in the radial direction is $L_r/v_{Er} \sim L_r L_z/\rho_i v_{ti}$. By making this time of the same order as $L_\parallel/v_{ti}$, we solve for L_r to find

$$L_r \sim \frac{B}{B_z}\rho_i \tag{2.5}$$

To simplify the problem to a tractable drift kinetic form, we assume that ρ_i is much smaller than L_r. This implies that

$$\frac{\rho_i}{L_r} \sim \frac{B_z}{B} \sim \frac{B_z}{B_\zeta} \ll 1, \tag{2.6}$$

that is, we will limit our model to magnetic fields that are mostly azimuthal and have a very small vertical component. This is an approximation that is consistent with magnetic field geometry in conventional tokamaks and also in the edge of many shots in spherical tokamaks.

We also assume that $r_0 \sim L_z \gg L_r$. Since r_0 is the characteristic length of variation of the magnetic field $\mathbf{B}$, the magnetic field barely changes across the domain $[r_0, r_0 + L_r]$. Thus, within our ordering, we assume $\mathbf{B}$ to be uniform in the domain of interest.

We assume the time derivatives to be of the same order as the parallel and perpendicular time scales that we have discussed above,

$$\frac{\partial}{\partial t} \sim \frac{\rho_i}{L_r}\frac{v_{ti}}{L_z}. \tag{2.7}$$

Our orderings above rest on the assumption $\phi \sim T_i/e$. In the case with wall boundary conditions, the wall boundary conditions ensured that ϕ remained of this order. With periodic boundary conditions, the size of ϕ is controlled by the momentum input. The force per unit volume on the plasma due to external sources, neutral-plasma collisions or ionization must satisfy

$$|\mathbf{F}_{i,\mathrm{ext}\perp}|, |\mathbf{F}_{e,\mathrm{ext}\perp}|, |\mathbf{F}_{in\perp}|, |\mathbf{F}_{en\perp}|, |\mathbf{F}_{i,\mathrm{ion}\perp}|, |\mathbf{F}_{e,\mathrm{ion}\perp}| \lesssim \left(\frac{\rho_i}{L_r}\right)^2 \frac{p_i}{L_z}, \tag{2.8}$$

where p_i is the ion pressure. This estimate for the force per unit volume comes from making the force of the order of the perpendicular inertia, $\partial(n_i m_i \mathbf{u}_{i\perp})/\partial t$, where the perpendicular ion velocity $\mathbf{u}_{i\perp}$ is taken to be of order $(\rho_i/L_r)v_{ti}$ (see equation (4.7) below for a justification of this ordering for $\mathbf{u}_{i\perp}$; also note that this means that the perpendicular flow is much smaller than the parallel one, which we assume to be of the order of v_{ti}). Equation (2.8) might seem stringent, but the friction between ions and neutrals and electron and neutrals (due to elastic collisions or ionization) is small in the closed field line region of the tokamak because the neutral density is small, i.e. we can assume that

$$n_n R_{in} \sim n_n R_{en}\sqrt{\frac{m_e}{m_i}} \sim n_n R_{\mathrm{ion}} \lesssim \left(\frac{\rho_i}{L_r}\right)^2 \frac{v_{ti}}{L_z}, \tag{2.9}$$

where $n_n R_{in}$, $n_n R_{en}$ and $n_n R_{\mathrm{ion}}$ are the ion-neutral, electron-neutral and ionization collision frequencies.

3. Summary of report 2047357-TN-07-02

The model in report 2047357-TN-07-02 is comprised of:

- three fluid equations (conservation of particles, parallel momentum and energy) for ions that have to be solved in conjunction with an ion kinetic equation to determine the ion density $n_i = n_e$, the ion parallel velocity $u_{i\parallel}$, the ion temperature T_i and the normalized ion distribution function F_i;
- five fluid equations (conservation of particles, the three components of momentum and energy) for neutrals that have to be solved in conjunction with a neutral kinetic equation to determine the neutral density n_n, the three components of the neutral velocity $\mathbf{u}_n$, the neutral temperature T_n and the normalized neutral distribution function F_n;
- two fluid equations (conservation of parallel current,

$$\frac{B_z}{B}\frac{\partial}{\partial z}\left[n_i\left(u_{i\parallel}-u_{e\parallel}\right)\right]=0, \tag{3.1}$$

and conservation of energy) for electrons that have to be solved in conjunction with an electron kinetic equation to determine the electron parallel velocity $u_{e\parallel}$, the electron temperature T_e and the electron normalized distribution function F_e; and
- the electron parallel momentum equation,

$$0=-\frac{B_z}{B}\frac{\partial p_{e\parallel}}{\partial z}+\frac{en_eB_z}{B}\frac{\partial\phi}{\partial z}+F_{ei\parallel}+n_em_en_nR_{en}(u_{n\parallel}-u_{e\parallel}), \tag{3.2}$$

for the potential ϕ. Here, $F_{ei\parallel}$ is the collisional friction force between electrons and ions.

In report 2047357-TN-07-02, we proposed a method to solve equations (3.1) and (3.2) in conjunction with wall boundary conditions. Equation (3.1) can be integrated in z to obtain $u_{e\parallel}(r,z,t)-u_{e\parallel}(r,0,t)$ (recall that n_i and $u_{i\parallel}$ are time-advanced using ion equations). With this result, equation (3.2) can be integrated in z to obtain the difference $\phi(r,z,t)-\phi(r,0,t)$ as a function of the unknown $u_{e\parallel}(r,0,t)$ (recall that $p_{e\parallel}$ is determined by the electron energy equation and the electron kinetic equation, and that $F_{ei\parallel}$ depends on $u_{e\parallel}$). With wall boundary conditions, we could solve for both $u_{e\parallel}(r,0,t)$ and $\phi(r,0,t)$. Unfortunately, the same cannot be said for periodic boundary conditions. With periodic boundary conditions and these equations, it is possible to find an equation for $u_{e\parallel}(r,0,t)$, but not for $\phi(r,0,t)$. Indeed, dividing equation (3.2) by n_e, integrating in z and using the periodic boundary conditions for ϕ, we find the condition

$$0=\int_0^{L_z}\left[-\frac{B_z}{n_eB}\frac{\partial p_{e\parallel}}{\partial z}+\frac{F_{ei\parallel}}{n_e}+m_en_nR_{en}(u_{n\parallel}-u_{e\parallel})\right]\mathrm{d}z. \tag{3.3}$$

This condition is satisfied by choosing the correct value of $u_{e\parallel}(r,0,t)$. Within equations (3.1) and (3.2), there is no other similar condition for $\phi(r,0,t)$. To find such a condition, we need to modify equation (3.1) by keeping higher order terms in ρ_i/L_r.

4. Current conservation for periodic boundary conditions

Parra & Catto (2008) showed that gyrokinetic equations (and consequently the subsidiary limit of drift kinetics) require higher order terms in ρ_i/L_r in order to determine the component of the electric field perpendicular to the flux surfaces traced by the magnetic field when the magnetic field is axisymmetric. In this case, this means that one needs higher order terms to determine $\partial\phi/\partial r$.

The need for higher order terms can be demonstrated using moments of the full kinetic equation. Before we start taking moments, we explain what we mean by full kinetic distribution function and full kinetic equation in this report, and how they compare to

the drift kinetic distribution function and kinetic equation that we have used so far. Importantly, what follows does not apply to the neutral distribution function and kinetic equation as we have not reduced them using the drift kinetic approximation in previous reports.

We denote the ion and electron full distribution functions by $g_s(r, z, \mathbf{v}, t)$, where the velocity is given by

$$\mathbf{v} = v_\parallel \hat{\mathbf{b}} + \mathbf{v}_\perp = v_\parallel \hat{\mathbf{b}} + v_\perp (\cos\varphi\, \hat{\mathbf{r}} + \sin\varphi\, \hat{\mathbf{b}} \times \hat{\mathbf{r}}), \tag{4.1}$$

Here $v_\parallel$ is the velocity parallel to the magnetic field, $\hat{\mathbf{b}} := \mathbf{B}/B$ is the unit vector in the direction to the magnetic field, and the velocity perpendicular to the magnetic field $\mathbf{v}_\perp$ is described by its magnitude $v_\perp$ and its direction, given by the gyrophase φ. The full kinetic distribution functions for ions and electrons, g_i and g_e, satisfy the full kinetic equations

$$\frac{\partial g_i}{\partial t} + \nabla\cdot(\mathbf{v} g_i) + \nabla_v \cdot \left[\frac{e}{m_i}\left(-\nabla\phi + \mathbf{v}\times\mathbf{B}\right) g_i\right] = C_{ii} + C_{in} + C_{ie} + C_{i,\mathrm{ion}} + Q_i \tag{4.2}$$

and

$$\frac{\partial g_e}{\partial t} + \nabla\cdot(\mathbf{v} g_e) + \nabla_v \cdot \left[-\frac{e}{m_e}\left(-\nabla\phi + \mathbf{v}\times\mathbf{B}\right) g_e\right] = C_{ee} + C_{en} + C_{ei} + C_{e,\mathrm{ion}} + Q_e. \tag{4.3}$$

Note that we have included like-particle collisions, electron-ion collisions, collisions with neutrals and ionization collisions. The sources Q_e represent the particle, momentum and energy input into the plasma.

The drift kinetic ion and electron distribution functions f_i and f_e that we used in previous reports are gyroaverages of the full distribution functions,

$$f_s(r, z, v_\parallel, v_\perp, t) := \frac{1}{2\pi}\int_0^{2\pi} g_s(r, z, \mathbf{v}(v_\parallel, v_\perp, \varphi), t)\,\mathrm{d}\varphi. \tag{4.4}$$

(Correspondingly, the sources S_s that we used are the gyoraverage of the full sources Q_s.) For $\rho_i/L_r \ll 1$, the distribution functions g_s and f_s are almost identical, $g_s \simeq f_s$ (Hazeltine 1973). The difference between these distribution functions, of order $\rho_i/L_r \ll 1$, was negligible in the case with wall boundary conditions, but it will be important with periodic boundary conditions. Thus, we write

$$g_s = f_s + g_{s1} + \ldots, \tag{4.5}$$

where, neglecting the ion-neutral, electron-neutral and ionization collisions to lowest order (recall equation (2.9)),

$$g_{s1} = \sin\varphi\left(\frac{v_\perp}{\Omega_s}\frac{\partial f_s}{\partial r} - \frac{1}{B}\frac{\partial\phi}{\partial r}\frac{\partial f_s}{\partial v_\perp}\right) \sim \frac{\rho_s}{L_r} f_s. \tag{4.6}$$

Here $\Omega_s := Z_s e B/m_s$ is the gyrofrequency of species s, and Z_s is the charge number (1 for ions and -1 for electrons). Using equation (4.5), we can calculate the perpendicular average velocity of ions and electrons,

$$\mathbf{u}_{s\perp} := \frac{1}{n_s}\int \mathbf{v}_\perp g_s\,\mathrm{d}^3 v \simeq \frac{1}{n_s}\int \mathbf{v}_\perp g_{s1}\,\mathrm{d}^3 v = \hat{\mathbf{b}}\times\hat{\mathbf{r}}\left(\frac{1}{Z_s e n_s B}\frac{\partial p_{s\perp}}{\partial r} + \frac{1}{B}\frac{\partial\phi}{\partial r}\right) \sim \frac{\rho_i}{L_r} v_{ti}, \tag{4.7}$$

where $p_{s\perp} := \int (m_s v_\perp^2/2) f_s\,\mathrm{d}^3 v$ is the perpendicular pressure of species s. Note that since the average of $\mathbf{v}_\perp$ over the gyrophase vanishes, $\mathbf{u}_{s\perp}$ is only due to the small correction g_{s1}. Thus, $\mathbf{u}_{s\perp}$ is small. Note that this is a consequence of our assumption $\phi \sim T_i/e$. A larger ϕ would have led to a larger average velocity.

After this brief introduction to the full distribution functions g_s, we can use moments of these distribution functions to impose current conservation following the procedure proposed by Parra & Catto (2009). Current conservation can be written as

$$\nabla \cdot \left[en_i(u_{i\|} - u_{e\|})\hat{\mathbf{b}} \right] + \nabla \cdot \mathbf{J}_\perp = 0, \tag{4.8}$$

where $\mathbf{J}_\perp$ is the component of the current density perpendicular to the magnetic field. In report 2047357-TN-07-02 we could neglect the term $\nabla \cdot \mathbf{J}_\perp$ because it is small in $L_r/L_z \ll 1$. We cannot neglect it any longer, as we need it to determine $\phi(r, 0, t)$. Equation (4.8) can be written as

$$\frac{\partial}{\partial z}\left[\frac{en_iB_z}{B}(u_{i\|} - u_{e\|}) + \mathbf{J}_\perp \cdot \hat{\mathbf{z}} \right] + \frac{1}{r}\frac{\partial}{\partial r}\left(r\mathbf{J}_\perp \cdot \hat{\mathbf{r}}\right) = 0. \tag{4.9}$$

Due to the periodic boundary conditions, the large parallel current term can be eliminated by integrating in z,

$$\frac{\partial}{\partial r}\left(\int_0^{L_z} \mathbf{J}_\perp \cdot \hat{\mathbf{r}}\, \mathrm{d}z \right) = 0, \tag{4.10}$$

where we have also used the fact that $r \simeq r_0$ is almost constant. Condition (4.10) determines $\phi(r, 0, t)$.

Unfortunately, equation (4.7) is not enough to compute $\mathbf{J}_\perp \cdot \hat{\mathbf{r}}$ to the sufficiently high order needed to obtain $\phi(r, 0, t)$. The perpendicular current density can, however, be calculated to very high order by taking moments of the full kinetic equations for ions and electrons. Multiplying equations (4.2) and (4.3) by $m_s\mathbf{v}$ and integrating over velocity space, we find the ion and electron total momentum equations,

$$\frac{\partial}{\partial t}(n_im_i\mathbf{u}_i) + \nabla \cdot \left(\int m_i\mathbf{v}\mathbf{v}g_i\, \mathrm{d}^3v \right) = -en_i\nabla\phi + en_i\mathbf{u}_i \times \mathbf{B} + \mathbf{F}_{in} + \mathbf{F}_{ie} + \mathbf{F}_{i,\mathrm{ion}} + \mathbf{F}_{i,\mathrm{ext}} \tag{4.11}$$

and

$$\frac{\partial}{\partial t}(n_em_e\mathbf{u}_e) + \nabla \cdot \left(\int m_e\mathbf{v}\mathbf{v}g_e\, \mathrm{d}^3v \right) = en_e\nabla\phi - en_e\mathbf{u}_e \times \mathbf{B} + \mathbf{F}_{en} + \mathbf{F}_{ei} + \mathbf{F}_{e,\mathrm{ion}} + \mathbf{F}_{e,\mathrm{ext}}. \tag{4.12}$$

Here, $\mathbf{F}_\alpha := \int m_s\mathbf{v}C_\alpha\, \mathrm{d}^3v$ is the force due to the collision operator C_α, and $\mathbf{F}_{s,\mathrm{ext}} := \int m_s\mathbf{v}Q_s\, \mathrm{d}^3v$ is the external momentum input. Summing equations (4.11) and (4.12), using quasineutrality and $\mathbf{F}_{ie} + \mathbf{F}_{ei} = 0$, and neglecting the electron momentum compared to the ion momentum, we find

$$\mathbf{J} \times \mathbf{B} \simeq \nabla \cdot \left(\int m_i\mathbf{v}\mathbf{v}g_i\, \mathrm{d}^3v + \int m_e\mathbf{v}\mathbf{v}g_e\, \mathrm{d}^3v \right) + \frac{\partial}{\partial t}(n_im_i\mathbf{u}_i) - \mathbf{F}_{in} - \mathbf{F}_{i,\mathrm{ion}} - \mathbf{F}_{\mathrm{ext}}. \tag{4.13}$$

where we have defined the total external force $\mathbf{F}_{\mathrm{ext}} := \mathbf{F}_{i,\mathrm{ext}} + \mathbf{F}_{e,\mathrm{ext}}$. Multiplying equation (4.13) by $(\hat{\mathbf{r}} \times \hat{\mathbf{b}})/B$, we obtain the radial component of $\mathbf{J}_\perp$,

$$\begin{aligned}
\mathbf{J}_\perp \cdot \hat{\mathbf{r}} \simeq\ & -\frac{1}{B}\nabla \cdot \left(\int m_i\mathbf{v}\mathbf{v} \cdot (\hat{\mathbf{b}} \times \hat{\mathbf{r}})g_i\, \mathrm{d}^3v + \int m_e\mathbf{v} \cdot (\hat{\mathbf{b}} \times \hat{\mathbf{r}})g_e\, \mathrm{d}^3v \right) \\
& + \frac{1}{B}\int m_i\mathbf{v} \cdot \nabla\left(\hat{\mathbf{b}} \times \hat{\mathbf{r}}\right) \cdot \mathbf{v}g_i\, \mathrm{d}^3v + \frac{1}{B}\int m_e\mathbf{v} \cdot \nabla\left(\hat{\mathbf{b}} \times \hat{\mathbf{r}}\right) \cdot \mathbf{v}g_e\, \mathrm{d}^3v \\
& - \frac{\partial}{\partial t}\left[\frac{n_im_i}{B}\mathbf{u}_i \cdot (\hat{\mathbf{b}} \times \hat{\mathbf{r}}) \right] + \frac{1}{B}\mathbf{F}_{in} \cdot (\hat{\mathbf{b}} \times \hat{\mathbf{r}}) + \frac{1}{B}\mathbf{F}_{i,\mathrm{ion}} \cdot (\hat{\mathbf{b}} \times \hat{\mathbf{r}}) + \frac{1}{B}\mathbf{F}_{\mathrm{ext}} \cdot (\hat{\mathbf{b}} \times \hat{\mathbf{r}}),
\end{aligned} \tag{4.14}$$

where

$$\nabla\left(\hat{\mathbf{b}}\times\hat{\mathbf{r}}\right)=-\frac{B_\zeta^2}{B^2}\frac{\mathrm{d}}{\mathrm{d}r}\left(\frac{B_z}{B_\zeta}\right)\hat{\mathbf{r}}\hat{\mathbf{b}}-\frac{B_zB_\zeta}{rB^2}\hat{\mathbf{b}}\hat{\mathbf{r}}+\frac{B_z^2}{rB^2}(\hat{\mathbf{b}}\times\hat{\mathbf{r}})\hat{\mathbf{r}}\sim\frac{B_z}{r_0B}\sim\frac{\rho_i}{L_r}\frac{1}{L_z}. \tag{4.15}$$

The term with the time derivative in the right side of equation (4.14) sets the size of the equation. For $\partial/\partial t\sim\rho_i v_{ti}/L_rL_z$, using the fact that $|\mathbf{u}_{i\perp}|\sim(\rho_i/L_r)v_{ti}$, we find

$$\frac{\partial}{\partial t}\left[\frac{n_im_i}{B}\mathbf{u}_i\cdot(\hat{\mathbf{b}}\times\hat{\mathbf{r}})\right]\sim\left(\frac{\rho_i}{L_r}\right)^2\frac{p_i}{BL_z}. \tag{4.16}$$

This estimate justifies the ordering (2.8). Also, estimate (4.16) sets the size of the terms that we need to keep in the equation. For example, the integrals that contain $\nabla(\hat{\mathbf{b}}\times\hat{\mathbf{r}})$ are small because $\nabla(\hat{\mathbf{b}}\times\hat{\mathbf{r}})$ is itself small in ρ_i/L_r and the integrals over velocity are small by a factor of $(\rho_i/L_r)^2$, as can be checked using expression (4.6) for g_i and g_e. Thus, integrating over z, using equation (4.7) for $\mathbf{u}_{i\perp}$ and employing the approximation $r\simeq r_0$, we find

$$\begin{aligned}\int_0^{L_z}\mathbf{J}_\perp\cdot\hat{\mathbf{r}}\,\mathrm{d}z\simeq&-\frac{\partial}{\partial t}\left[\int_0^{L_z}\frac{n_im_i}{B^2}\left(\frac{\partial\phi}{\partial r}+\frac{1}{en_i}\frac{\partial p_{i\perp}}{\partial r}\right)\mathrm{d}z\right]\\&-\frac{1}{B}\frac{\partial}{\partial r}\left[\int_0^{L_z}\left(\int m_i\mathbf{v}\cdot\hat{\mathbf{r}}(\mathbf{v}\times\hat{\mathbf{b}})\cdot\hat{\mathbf{r}}\,g_i\,\mathrm{d}^3v+\int m_e\mathbf{v}\cdot\hat{\mathbf{r}}(\mathbf{v}\times\hat{\mathbf{b}})\cdot\hat{\mathbf{r}}\,g_e\,\mathrm{d}^3v\right)\mathrm{d}z\right]\\&+\int_0^{L_z}\left[\frac{1}{B}\mathbf{F}_{in}\cdot(\hat{\mathbf{b}}\times\hat{\mathbf{r}})+\frac{1}{B}\mathbf{F}_{i,\mathrm{ion}}\cdot(\hat{\mathbf{b}}\times\hat{\mathbf{r}})+\frac{1}{B}\mathbf{F}_{\mathrm{ext}}\cdot(\hat{\mathbf{b}}\times\hat{\mathbf{r}})\right]\mathrm{d}z.\end{aligned} \tag{4.17}$$

The velocity integrals in equation (4.17) can be calculated using a moment of equations (4.2) and (4.3). Multiplying equation (4.2) by $(m_i^2/4eB)[(\mathbf{v}\cdot\hat{\mathbf{r}})^2-((\mathbf{v}\times\hat{\mathbf{b}})\cdot\hat{\mathbf{r}})^2]$ and integrating in velocity space and z, we find

$$\begin{aligned}&\int_0^{L_z}\mathrm{d}z\int\mathrm{d}^3v\,m_i\mathbf{v}\cdot\hat{\mathbf{r}}(\mathbf{v}\times\hat{\mathbf{b}})\cdot\hat{\mathbf{r}}\,g_i\\&\quad\simeq\frac{1}{4\Omega_i}\frac{\partial}{\partial t}\left[\int_0^{L_z}\mathrm{d}z\int\mathrm{d}^3v\,m_i[(\mathbf{v}\cdot\hat{\mathbf{r}})^2-((\mathbf{v}\times\hat{\mathbf{b}})\cdot\hat{\mathbf{r}})^2]\,g_i\right]\\&\quad+\frac{1}{4\Omega_i}\frac{\partial}{\partial r}\left[\int_0^{L_z}\mathrm{d}z\int\mathrm{d}^3v\,m_i\mathbf{v}\cdot\hat{\mathbf{r}}[(\mathbf{v}\cdot\hat{\mathbf{r}})^2-((\mathbf{v}\times\hat{\mathbf{b}})\cdot\hat{\mathbf{r}})^2]\,g_i\right]\\&\quad-\int_0^{L_z}\frac{n_im_i}{2B^2}\left[\frac{\partial\phi}{\partial r}\left(\frac{\partial\phi}{\partial z}+\frac{1}{en_i}\frac{\partial p_{i\perp}}{\partial z}\right)+\frac{\partial\phi}{\partial z}\left(\frac{\partial\phi}{\partial r}+\frac{1}{en_i}\frac{\partial p_{i\perp}}{\partial r}\right)\right]\mathrm{d}z\\&\quad-\frac{1}{4\Omega_i}\int_0^{L_z}\mathrm{d}z\int\mathrm{d}^3v\,m_i[(\mathbf{v}\cdot\hat{\mathbf{r}})^2-((\mathbf{v}\times\hat{\mathbf{b}})\cdot\hat{\mathbf{r}})^2]C_{ii},\end{aligned} \tag{4.18}$$

where we have neglected most collision operators due to our assumption (2.9). Due to the integrals over the gyrophase, the terms with the time derivative and the ion-ion collision

operator vanish to the order of interest, leaving

$$\int_0^{L_z} \mathrm{d}z \int \mathrm{d}^3v\, m_i \mathbf{v}\cdot\hat{\mathbf{r}}(\mathbf{v}\times\hat{\mathbf{b}})\cdot\hat{\mathbf{r}}\, g_i$$
$$\simeq \frac{1}{4\Omega_i}\frac{\partial}{\partial r}\left[\int_0^{L_z}\mathrm{d}z\int \mathrm{d}^3v\, m_i\mathbf{v}\cdot\hat{\mathbf{r}}[(\mathbf{v}\cdot\hat{\mathbf{r}})^2-((\mathbf{v}\times\hat{\mathbf{b}})\cdot\hat{\mathbf{r}})^2]\, g_i\right]$$
$$-\int_0^{L_z}\frac{n_i m_i}{2B^2}\left[\frac{\partial\phi}{\partial r}\left(\frac{\partial\phi}{\partial z}+\frac{1}{en_i}\frac{\partial p_{i\perp}}{\partial z}\right)+\frac{\partial\phi}{\partial z}\left(\frac{\partial\phi}{\partial r}+\frac{1}{en_i}\frac{\partial p_{i\perp}}{\partial r}\right)\right]\mathrm{d}z. \tag{4.19}$$

There is still another integral over velocity to be calculated. We can use the moment $(m_i^2/3eB)[((\mathbf{v}\times\hat{\mathbf{b}})\cdot\hat{\mathbf{r}})^3+3(\mathbf{v}\cdot\hat{\mathbf{r}})^2(\mathbf{v}\times\hat{\mathbf{b}})\cdot\hat{\mathbf{r}}]$ of equation (4.2) to find

$$\int_0^{L_z}\mathrm{d}z\int\mathrm{d}^3v\, m_i\mathbf{v}\cdot\hat{\mathbf{r}}[(\mathbf{v}\cdot\hat{\mathbf{r}})^2-((\mathbf{v}\times\hat{\mathbf{b}})\cdot\hat{\mathbf{r}})^2]\, g_i \simeq -\int_0^{L_z}\frac{2p_{i\perp}}{B}\frac{\partial\phi}{\partial z}\,\mathrm{d}z. \tag{4.20}$$

With this result and employing integration by parts in z to write

$$\frac{\partial}{\partial r}\left[\int_0^{L_z}\frac{2p_{i\perp}}{B}\frac{\partial\phi}{\partial z}\,\mathrm{d}z\right]\simeq\int_0^{L_z}\frac{2}{B}\left(\frac{\partial p_{i\perp}}{\partial r}\frac{\partial\phi}{\partial z}+p_{i\perp}\frac{\partial^2\phi}{\partial r\partial z}\right)\mathrm{d}z$$
$$=\int_0^{L_z}\frac{2}{B}\left(\frac{\partial p_{i\perp}}{\partial r}\frac{\partial\phi}{\partial z}-\frac{\partial p_{i\perp}}{\partial z}\frac{\partial\phi}{\partial r}\right)\mathrm{d}z, \tag{4.21}$$

equation (4.19) simplifies to

$$\int_0^{L_z}\mathrm{d}z\int\mathrm{d}^3v\, m_i\mathbf{v}\cdot\hat{\mathbf{r}}(\mathbf{v}\times\hat{\mathbf{b}})\cdot\hat{\mathbf{r}}\, g_i=-\int_0^{L_z}\frac{n_i m_i}{B^2}\frac{\partial\phi}{\partial z}\left(\frac{\partial\phi}{\partial r}+\frac{1}{en_i}\frac{\partial p_{i\perp}}{\partial r}\right)\mathrm{d}z. \tag{4.22}$$

The electron integral in equation (4.17) can be calculated using the same procedure that has led to equation (4.22), and it turns out to be negligible due to the smallness of m_e/m_i.

Substituting equation (4.22) into equation (4.17) and then equation (4.17) into equation (4.10), and using the same simplified ion-neutral and ionization collision operators that we have used in previous reports,

$$C_{in}:=-R_{in}(n_n g_i-n_i f_n),\quad C_{i,\mathrm{ion}}:=n_e R_{\mathrm{ion}} f_n, \tag{4.23}$$

we find the final equation for $\phi(r,0,t)$,

$$\frac{\partial}{\partial r}\Bigg\{-\frac{\partial}{\partial t}\int_0^{L_z}\left[\frac{n_i m_i}{B^2}\left(\frac{\partial\phi}{\partial r}+\frac{1}{en_i}\frac{\partial p_{i\perp}}{\partial r}\right)\right]\mathrm{d}z$$
$$+\frac{1}{B}\frac{\partial}{\partial r}\left[\int_0^{L_z}\frac{n_i m_i}{B^2}\frac{\partial\phi}{\partial z}\left(\frac{\partial\phi}{\partial r}+\frac{1}{en_i}\frac{\partial p_{i\perp}}{\partial r}\right)\mathrm{d}z\right]$$
$$-\int_0^{L_z}\frac{n_i m_i n_n R_{in}}{B^2}\left(\frac{\partial\phi}{\partial r}+\frac{1}{en_i}\frac{\partial p_{i\perp}}{\partial r}\right)\mathrm{d}z$$
$$+\int_0^{L_z}\frac{n_i m_i n_n(R_{in}+R_{\mathrm{ion}})u_{nz}}{B}\,\mathrm{d}z+\int_0^{L_z}\frac{\mathbf{F}_{\mathrm{ext}}\cdot\hat{\mathbf{z}}}{B}\,\mathrm{d}z\Bigg\}=0. \tag{4.24}$$

Note that in several places we have used the approximation $\hat{\mathbf{b}}\times\hat{\mathbf{r}}\simeq\hat{\mathbf{z}}$.

Equation (4.24) is small by a factor of $(\rho_i/L_r)2$ compared to the parallel current term in the current conservation equation (4.8), of order $(\rho_i/L_r)(en_e v_{ti}/L_z)$. Thus, in principle,

to keep these terms we would need to keep terms up to order $(\rho_i/L_r)^3$ in this equation. Thankfully, we do not need to do that because we now have equation (4.24) in explicit form. We can add equation (4.24) to our set of equations in a consistent manner.

We finish by relating equation (4.24) to momentum conservation, a connection that we mentioned at the end of section 2. Equation (4.24) is a radial derivative of $\int_0^{L_z} \mathbf{J}_\perp \cdot \hat{\mathbf{r}}\, \mathrm{d}z$ (see equation (4.10)). Then, equation (4.24) can be integrated to show that $\int_0^{L_z} \mathbf{J}_\perp \cdot \hat{\mathbf{r}}\, \mathrm{d}z$ is a constant that we will call I_r, giving

$$\begin{aligned}\frac{\partial}{\partial t}\int_0^{L_z} n_i m_i \mathbf{u}_{i\perp}\cdot\hat{\mathbf{z}}\,\mathrm{d}z - \frac{\partial}{\partial r}\left(\int_0^{L_z}\frac{n_i m_i}{B}\frac{\partial\phi}{\partial z}\mathbf{u}_{i\perp}\cdot\hat{\mathbf{z}}\,\mathrm{d}z\right) = -I_r B \\ - \int_0^{L_z} n_i m_i n_n R_{in}(\mathbf{u}_{i\perp}\cdot\hat{\mathbf{z}} - u_{nz})\,\mathrm{d}z \\ + \int_0^{L_z} n_i m_i n_n R_{\mathrm{ion}} u_{nz}\,\mathrm{d}z + \int_0^{L_z}\mathbf{F}_{\mathrm{ext}}\cdot\hat{\mathbf{z}}\,\mathrm{d}z. \end{aligned} \tag{4.25}$$

Here we have used the $\hat{\mathbf{z}}$ projection of equation (4.7) to rewrite $\partial\phi/\partial r$ as a function of $\mathbf{u}_{i\perp}\cdot\hat{\mathbf{z}}$. Equation (4.25) is the perpendicular momentum balance in the z direction, and it includes the magnetic force due to the radial current I_r. This magnetic force is zero in tokamaks, where the radial current vanishes.

5. Moment drift kinetics

The moment drift kinetic formulation of the problem with periodic boundary conditions is thus the equations in report 2047357-TN-07-02 plus our new equation (4.24) for $\phi(r,0,t)$. The perpendicular pressure appearing in this equation can be calculated from the normalized distribution function using the formula

$$p_{s\perp}[n_s, v_{ts}, F_s](r,z) := \pi n_s m_s v_{ts}^2 \int_{-\infty}^{\infty}\mathrm{d}w_\parallel \int_0^\infty \mathrm{d}w_\perp\, w_\perp^3 F_s(r,z,w_\parallel,w_\perp,t). \tag{5.1}$$

6. Discussion

Note that the addition of equation (4.24) has only been possible because we evolve the densities of ions and electrons independently of their normalized distribution functions. Had we proposed to evolve the unnormalized ion and electron distribution functions, it would not have been possible to have an independent higher-order current conservation equation because it would not be consistent with the density that arises from the time evolution of the lowest order kinetic equations.

When implementing the equations proposed in this report, it is important to ensure that there is z-variation of density, temperature and flows. Otherwise, the equations become trivial. When connected to the open field line region (the topic of a future report), the z-variation will arise naturally due to the wall boundary conditions. In the absence of open field lines, one can use sources and sinks with that are not uniform in z (i.e. excess ionization in the region close to the divertor, where most neutrals are).

REFERENCES

Hazeltine, R.D. 1973 Recursive derivation of drift-kinetic equation. *Plasma Phys.* **15**, 77–80.

Parra, F.I. & Catto, P.J. 2008 Limitations of gyrokinetics on transport time scales. *Plasma Phys. Control. Fusion* **50**, 065014.

Parra, F.I. & Catto, P.J. 2009 Vorticity and intrinsic ambipolarity in turbulent tokamaks. *Plasma Phys. Control. Fusion* **51**, 095008.